STRUCTURAL ANALYSIS OF

THE BYGDIN AREA,

SOUTHERN NORWAY.

by JOHN R. HOSSACK, B.Sc.

Thesis presented for the Degree of DOCTOR OF PHILOSOPHY of the

UNIVERSITY OF EDINBURGH in the FACULTY OF SCIENCE.

1965.

CONTENTS

LIST OF FIGURES

LIST OF MAPS

(In pocket at the end of the thesis)

LIST OF TABLES

I. INTRODUCTION

1. LOCATION, TOPOGRAPHY AND EXPOSURE.

The area studied, which lies on the edge of the Jotunheim mountains, 190 km. northwest of Oslo in the county of Oppland, is situated at the eastern end of Lake Bygdin (alt. 1058 m.) and on the north and south shores of Lake Vinstri (alt. 1030 m.) to the east of Lake Bygdin (Fig. 1).

The western and northern parts of the area lie within the Upper Jotun Nappe, which is composed here of meta-igneous rocks. The part south of Lake Vinstri is occupied by meta-sedimentary Cambro-Ordovician rocks, which underlie the Upper Jotun Nappe.

The Jotun Nappe, north of Lake Vinstri, is dominantly granite which has weathered to give a rolling moorland topography, with poor exposure, reaching up to 1500 m. At the eastern end of Lake Bygdin however, the nappe is composed of gabbro which has weathered to a steep rocky mountainous area with good exposure. The highest part of the area is at 1600 m., but outside the area, the mountains rise to over 2300 m.

To the south of Lake Vinstri, the meta-sediments (including the Bygdin conglomerate) have formed a topography similar to that on the north side, but the exposure on the south side is excellent. The southern part of the area rises up to 1300 m.

In addition to Bygdin, a small area of 5 sq. km. was mapped near Synberg, which lies $2\frac{1}{2}$ km. south of the Bitihorn. The object was to determine the complete sequence of the Cambro-Ordovician rocks. At Synberg a complete section can be seen through the Cambro-Ordovician, down to the Pre-Cambrian basement which outcrops in the Beito window.

Access to the area is made by the N 225 road from Fagernes, 53 km. south of Bygdin. This road runs north-south through the western end of the area, passing between Lake Bygdin and Lake Vinstri and up over the Valdresflyi, the high moorland to the north of Vinstri. From this road, farther access can be gained by using two private toll roads, one of which runs along the north shore of Vinstri and the other from the N 225 at Haugen, north to the eastern end of Olevatn.

The area is covered by sheets 1617 IV (west end) and 1617 I (east end) of the New Military Map Series (Scale 1: 50,000) and geologically by Strand's Slidre Memoir and map (N.G.U.# no. 130). Aerial photographic coverage is provided by photographs produced by Widerøe's Flyveselskap A/S.

2. GEOLOGICAL SETTING AND HISTORY OF RESEARCH.

(a) Introduction

Before discussing the Bygdin area, the general geology of Southern Norway will be described (Fig. 1).

Most of Norway is composed of a northeast trending Caledonian Mountain chain resting on the Pre-Cambrian Baltic Shield which has been reworked in part by the Caledonian Orogeny. In the south of Norway part of this basement forms a Foreland to the Caledonian System. Between the Foreland and the core of the Caledonian chain, lies a complex marginal thrust zone. A section from Oslo, northwest through the Jotunheim Mountains will be described to illustrate the structure of the Caledonian system.

In the Oslo region and in the Hardangervidda to the west of Oslo, a thin sequence of fossiliferous autochthonous Cambro-Silurian sediments, up to 200 m. thick, overlies unconformably the Pre-Cambrian basement.

N.G.U. - Norges Geologiske Unersökelse.

Location and Geological map of Southern Norway

N

Pre-Cambrian reworked during
Caledonian Orogeny

Trondhjem
Synclinorium

"Quartzite" Nappe

Røssjøkollene

Bergen

Hardangervidda

Oslo

Pre—Cambrian
Foreland

O   50

km.

	Upper Jotun Nappe
	Valdres Sparagmite
	Lower Jotun Nappe
	"Quartzite" Nappes
	Autochthonous Cambro-Silurian Sediments
	Location of the Bygdin Area

Fig I
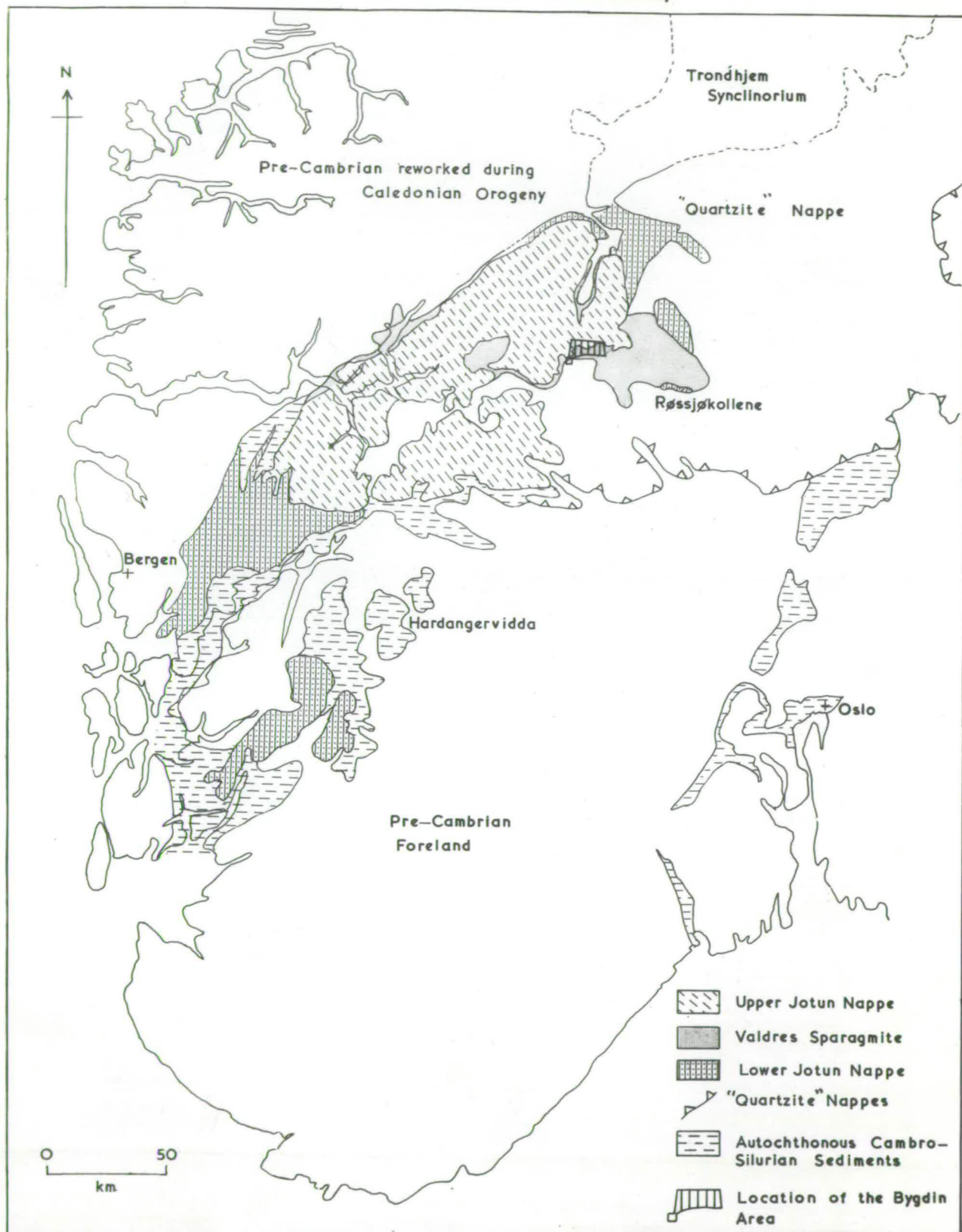
These sediments are the "Eastern" or miogeosynclinal Cambro-Silurian sediments deposited on the southeast Foreland of the Caledonian geosyncline.

When traced towards the northwest, these autochthonous "Eastern" sediments are overthrust by the lowest nappe of the marginal thrust zone. This nappe has Eo-Cambrian sparagmite (a Norwegian term for an arkosic sediment) at the base, and a cover of "Eastern" Cambro-Ordovician sediments. When this nappe is traced northeast into Sweden, it is found to have been over-ridden by higher nappes of Eo-Cambrian sparagmite and Cambro-Ordovician sediments. These nappes constitute the "Lower Quartzite Nappes" and show low grade greenschist facies metamorphism.

All of these nappes have been thrust towards the southeast along flat-lying thrust planes, over the non-metamorphic autochthonous sediments of the Oslo region. This thrusting has caused some folding of the Oslo rocks by décollement gliding along the junction with the Archaean basement.

Above the Lower Quartzite Nappes, lie the Lower and Upper Jotun Nappes, also thrust towards the southeast. These upper nappes are composed of Cambro-Ordovician sediments of the "Western" or eugeosynclinal type, and high grade crystalline rocks of amphibolite and granulite facies.

The Lower Jotun Nappe is composed of a crystalline basement with a relic cover of Cambro-Ordovician eugosynclinal sediments similar to those of the Trondheim Synclinorium.

Between the Lower and Upper Jotun Nappes lies a sequence of tectonic sediments, the Valdres Sparagmite, which has been derived from the Lower Nappe after or during its emplacement. The Sparagmite has later been over-:thrust and deformed by the Upper Jotun Nappe. The Upper Nappe is composed

entirely of charnockitic crystalline rocks of a unique type termed the Bergen-
Jotun kindred (Goldschmidt, 1916 b).

In the Bygdin area, the Lower Jotun Nappe is missing, and so the
Upper Jotun Nappe and the Valdres Sparagmite rest directly on the Cambro-
Ordovician sediments of the lowest "Quartzite" nappe.

Both Jotun Nappes lie in a northeast trending synclinal depression
termed the "Faltungsgraben" by Goldschmidt (1912). At the notheast end of
the Jotun Nappes, the eugosynclinal sediments of the Lower Nappe, open out
into the Trondheim Synclinorium. On the northwest side of the Jotunheim, the
Valdres Sparagmite reappears on the northwest limb of the "Faltungsgraben",
and here the Sparagmite overlies Cambro-Ordovician sediments which have
recently been shown by D. Cowan (personal communication) to be eugeosynclinal
and may in fact be part of the Lower Jotun Nappe and the Trondheim Synclinorium.

Below this eugeosynclinal sequence, lies the core of the Caledonian
mountain chain. This core seems to be composed dominantly of Pre-Cambrian
gneisses, reworked during the Caledonian Orogeny. The structure of this
core is largely unknown, although Muret (1960) has demonstrated a sequence
of four Alpine type nappes, rooted in Surnadal, with cores of basement gneiss
and envelopes of Eo-Cambrian and Cambro-Silurian rocks. These nappes, like
the thrust margin, have moved towards the southeast. Above these nappes lies
the Trondheim Synclinorium, which Strand (1961) has suggested might be
equivalent to the Lower Jotun Nappe.

Excellent summaries of the structure and petrology of the Norwegian
Calidonides are given by Holtedahl (1960) and Strand (1961).

(b) Introduction of the Nappe concept to the Jotunheim

The Jotun Nappes were included in a report on the Hardangervidda district by Brøgger (1893) and although the nappe concept had already been introduced to Scandinavia by the Swedish geologist A.E. Törnebohm, Brøgger failed to interpret the gneisses overlying Cambro-Silurian sediments as part of a nappe. He believed the contact to be a metamorphic boundary, and explained the increase in metamorphic grade upwards as a result of the intrusion of igneous rocks above the sediments which were later removed by erosion.

Bjørlykke (1902) described mechanical contacts, with mylonites, at the base of the crystalline massifs in the Hardangervidda, and along with Reush and Rekstad was ready to accept the nappe theory for that region (Strand, in Holtedahl, 1960, p.136). Then Bjørlykke (1905) described the geology of Central Southern Norway and showed that the crystalline massifs were situated above the Cambro-Ordovician sediments, or the Valdres Sparagmite, throughout the whole of the nappe region. But by this time he had rejected the nappe theory and accepted Brøgger's original hypothesis. He thought that the mechanical contacts at the base of the massifs only indicated small movements.

Goldschmidt (1916b) described the petrology of the crystalline rocks throughout the Jotun region, and grouped these rocks with similar rocks of the Bergen region into the "Bergen-Jotun kindred" all of which showed a supposed charnockitic stamp. He suggested that the Jotun rocks had moved into their present position along basal thrust planes, but were rooted in the "Faltungsgraben". (Goldschmidt, 1916a).

Holtedahl (1936, p.136) was the first to postulate a large transport distance for the Jotun Nappes. He suggested that the Jotun rocks were not rooted in the "Faltungsgraben" but in fact "floated" on a basal thrust plane

above the underlying sediments without showing signs of rooting anywhere.

Holtedahl's hypothesis has since been accepted by most Scandinavian geologists, although Oftedahl (1961) has tried to reintroduce Goldschmidt's hypothesis. However, since then, a gravity survey of the Jotun Nappes has been completed by Scott Smithson (1964). Smithson's results are ambiguous in that he can erect two models for the Jotun Nappes, depending on the two density contrasts used. With a density contrast of 0, 12 gm/cc, his results give a minimum thickness in the "Faltungsgraben" of 14 km., and with one of 0,20 gm/cc, a minimum thickness of 8 km. The first model suggests that the nappes may root in the "Faltungsgraben" and the second suggests that they do not. Smithson chooses the second model as the likeliest because it fits the geological data best. Even a minimum thickness of 8 km. is considerably greater than has previously been supposed.

(c) History of research in the Bygdin area.

The Bygdin conglomerate was included in a paper describing the conglomerates of the Valdres Sparagmite, by Goldschmidt (1916a). He figured the Bygdin conglomerate and included some measurements of deformed pebbles, as well as describing the petrology of the conglomerate and the Valdres Sparagmite. Goldschmidt also discussed the origin of the Jotun Nappes. This was followed by a description of the structural petrology of the Bygdin Conglomerate by Strand (1945), including microfabrics of the deformed pebbles. Near orthorhombic quartz girdles with northwest axes parallel to the pebble elongation and minor fold axes were described by Strand, as well as extreme variation in shape of the pebbles from rod shapes to flat pancake shapes.

Strand (1951) also published a memoir and a map of the Slidre area
(including Bygdin) and extended details of the Cambro-Ordovician stratigraphy
in the Valdres area (Strand, 1958). These are summarised in Table 1, where
the stratigraphy is correlated with the classic Oslo sequence, and with the
section mapped by the author in the Beito window near Bygdin.

Strand's work on the Bygdin conglomerate has often been used by
other workers to demonstrate the so-called "a"-lineation associated with
thrusting, which is formed parallel to the direction of movement of the
thrust (Anderson, 1948. Kvale, 1953).

Flinn (1959) has noted the geological similarities between North
East Shetlands and the Jotunheim, and also the comparable pebble deformation
in the Funzie conglomerate (Shetland) and the Bygdin conglomerate (Flinn,
1961). Both conglomerates show similar types of rod and cake deformation.

New work.

The object of research was to determine the relationship of the
elongated pebbles and the so-called cross-folds to the thrusting, and to
study the deformation of the Bygdin conglomerate. Before field work started,
base maps were constructed, with the help of Mr. R.P. Kirby of the Geography
Department at Edinburgh University, on the scale of 1:20,000 because the
existing Ordnance maps of the area were on too small a scale for detailed
structural mapping. Both the 1:50,000 Military Maps and aerial photographs
were used. At first, a Zeiss Stereotape A plotting machine was used but
unfortunately the vertical tilt of the aerial photographs was too large
to be able to provide accurate maps.

Finally the 1:50,000 maps were enlarged optically to 1:20,000, and a Zeiss Aerotopograph, combined with the aerial photographs used to correct the enlarged maps.

Field mapping was carried out during two summer field seasons, and the major structure and the structural history of the area determined, using the minor structures and modern structural techniques such as those used by Ramsay (1957a and b, 1960) and Turner and Weiss (1963).

The deformed pebbles in the Bygdin conglomerate were measured along joint faces to determine the amount and symmetry of strain throughout the conglomerate outcrop.

3. STRATIGRAPHY AND PETROGRAPHY

The stratigraphy and petrography will be considered in two parts.

(a)   The Upper Jotun Nappe

(b)   The Cambro-Ordovician Sediments

(a) The Upper Jotun Nappe

On the geological map of the area (Map I), the Upper Jotun Nappe is divided into two separate thrust sheets.

To the south of Lake Bygdin, towards the Bitihorn, including the peninsula at the east end of Lake Bygdin, the Upper Nappe is composed almost entirely of gabbroic rocks. The rest of the Jotun Nappe to the north and northeast of Bygdin, along the north side of Lake Vinstri, is composed dominantly of granite and intermediate igneous rocks. Between Lake Bygdin

and the Bitihorn, the gabbro and granitic sheets are separated by a thin wedge of Bygdin conglomerate, with both the granite and the conglomerate wedge dipping westwards underneath the gabbro sheet. The conglomerate may have been a thin wedge which has been caught up by the thrusting and squeezed in between two moving thrust sheets. This structure can be correlated with the Jotun thrust zone at Eidsbugaren at the west end of Lake Bygdin, where MacRitchie (personal communication) has found a granite sheet immediately above the basal thrust plane which has itself been over-:thrust by a gabbro sheet with a petrology similar to the Bitihorn gabbro.

(i) Gabbro sheet

The Bitihorn gabbros are coarse grained epigranular rocks with white or pink felspar and dark ferromagnesian minerals. In contrast to the granitic sheet, the gabbros show little sign of cataclasis induced by the Upper Jotun Thrust movements, except in the area above the thrust wedge of conglomerate, where the gabbro has been broken down to a fine grained well foliated phyllonite.

Most of the gabbros show well developed igneous textures, including some rhythmic layering of felspar and ferromagnesian minerals (Plate 11a), graded bedding, and in one case load casting of a dense ferromagnesian rich layer into a less dense felspar rich layer. Also in thin section, hornblende and spinel show well developed intercumulus textures suggesting crystal-:lization of a late liquid in the interstitial spaces between the cumulus phases.

The dominant assemblage is labradorite-clinopyroxene-orthopyroxene-hornblende, often with accessory quartz, apatite, and black spinel. The proportion of amphibole may vary considerably, with orthopyroxene being completely replaced in the assemblage by amphibole. In one case, the assemblage also contains some microperthite. Goldschmidt (1916b, p.40) gives a chemical analysis of a gabbro west of the Bitihorn, just outside the area mapped, to illustrate the composition of mangerite (a micro-perthite gabbroic rock common in the Bergen-Jotun suite). The gabbros grade into mangerite with increasing microperthite content. However, the amount of microperthite in any of the Bitihorn rocks mapped, does not justify classifying these as mangerites.

Goldschmidt (ibid, pp.35-38) also classified the Bergen Jotun gabbros as norites, but the Bitihorn gabbros have insufficient hypersthene to justify this classification, and are really hypersthene and hornblende gabbros.

On the west side of the Bitihorn massif, the gabbro has been intruded by ultra-basic ?dykes with an olivine-clinopyroxene-anthophyllite labradorite-biotite-green spinel core, and a clino-pyroxene-orthopyroxene margin. This intrusion seems to be similar to the ultra-basic dykes described by Battey (1960). The anthophyllite seems to be replacing olivine and probably crystallized during intrusion. The stability field of anthophyllite (Greenwood, 1963) suggests intrusion temperatures between $650^{\circ}C$ and $750^{\circ}C$.

The Bitihorn gabbros appear to have undergone a later phase of recrystallization. Many parts of the gabbro are cut by a later series of

anastomosing shear planes, and parts of the gabbro on the peninsula at the east end of Lake Bygdin are remobilized with xenoliths of gabbro with contorted igneous layering floating in a pegmatite matrix. This phase may be equivalent to the pre-thrusting remobilization phase at Eidsbugaren (Battey and MacRitchie, unpublished data).

(ii) Granite sheet.

This sheet is composed almost entirely of granitic and intermediate acidic igneous rocks. Unfortunately, most of these rocks have a strong cataclastic texture induced by the thrusting of the Jotun Nappe, which has destroyed much of the original texture of the rock. Hornblende and biotite granites are the dominant rocks, and most of the rocks contain microcline perthite and a plagoiclase which may range in composition from albite to oligoclase/andesine. The composition of many of these rocks is difficult to estimate because of the cataclastic texture and in fact many of the "intermediate" rocks have been classified only on their dark mineral content.

An analysis of a biotite granite from the Synshorn north of Bygdin, is given by Goldschmidt (1916b, p.52).

Just above the thrust plane at Bygdin and at various horizons throughout the granite sheet, the granitic rocks are cataclased to fine grained hornblende phyllonites.

One specimen of interest showed a quartz-mesoperthite-ortho-:pyroxene-clinopyroxene assemblage with an accessory amount of oligoclase, which suggests that this rock lies in the granulite facies. However, all other granitic rocks are of the amphibolite facies.

Age relationships of the igneous rocks can be determined, with the intermediate igneous rocks predating the granite. Plate 11b shows xenoliths of darker intermediate rock in a granite matrix.

North of Synshorn, four xenolith-like lenses of labradorite-hornblende amphibolite were found floating in the granite. These amphi-:bolites seem to be related to the hornblende gabbros of the Bitihorn and in fact the gabbro is intruded by granite on the peninsula at the east end of Lake Bygdin. A metadolerite dyke with a north north east trend was discovered intruded into granite at the east end of Lake Vinstri and similar dolerites with the same trend have been discovered at Eidsbugaren by Battey and MacRitchie (personal communication).

Piecing together these age relationships, the igneous history appears to be -

    i)   Gabbro crystallization and intrusion of ultra-basic dykes.

    ii)   ?Intermediate igneous rock crystallized.

    iii)   Intrusion of granite.

    iv)   Intrusion of dolerite dyke.

All the above rocks, including the dolerite dyke, show an overprinting of the greenschist facies metamorphism associated with the thrusting of the Upper Jotun Nappe, proving that the complete igneous history is pre-thrusting and probably of Pre-Cambrian age.

(b) The Cambro-Ordovician Sediments

The Cambro-Ordovician sequence erected by Strand (in Holtedahl, 1960, pl.8) for the Slidre area is given in Table I along with the writer's succession in the Beito window. Fossiliferous rocks up to Llandeilo age are present in Slidre below the Mellsenn Formation and the Valdres Sparagmite, but no fossils are present at Beito. The Mellsenn Formation in both areas seems to represent a passage group between the Cambro-Ordovician rocks and the Valdres Sparagmite (Strand, 1958).

The age and tectonic significance of the Valdres Sparagmite have been much discussed by Norwegian geologists. Goldschmidt (1916a) suggested that the Valdres Sparagmite was a flysch or molasse deposit derived after or during the emplacement of the Lower Jotun Nappe, and deformed by the later thrusting of the Upper Jotun Nappe.

Kulling (1961) suggested that in fact the Valdres Sparagmite represented a middle nappe of Eo-Cambrian Sparagmite between the Lower and Upper Jotun Nappes, on the basis of a supposed thrust plane between the Valdres Sparagmite and the Mellsenn Formation.

However, Strand (1951), who originally mapped the area for the Norwegian Survey, supports Goldschmidt's hypothesis and has replied to Kulling (Strand, 1958, 1962).

Essentially Goldschmidt's and Strand's views are as follows. At Røssjøkollene, 30 km. east of Mellene, South Slidre, a gabbro massif which represents the Lower Jotun Nappe, rests on a thrust plane above the Mellsenn Formation, and is itself covered by Valdres Sparagmite which overlaps the thrust plane on to the Mellsenn Formation. Much of the

TABLE 1

CAMBRO-SILURIAN SUCESSION IN SOUTH SLIDRE AND THE BEITO WINDOW.

South Slidre (after Strand, in Holtedahl, 1960.)	Bygdin and the Beito Window
?SILURIAN	
Valdres Sparagmite with conglomerate (1000 m.)	Valdres Sparagmite with conglomerate (360 m.)
Mellsenn Division { sandstone with sparagmite lenses / roofing slate / sandstone } (200 m.)	Mellsenn Division with [sandstone, quartzite, pelite, sparagmite.] (170 m.)
ORDOVICIAN	
Phyllite with [Dicellograptus, Diplograptus 3b-4a / Didymograptus, / Isograptus, / Phyllograptus.] , (200 m.)	Pelite (80 m.)
Shale with Archaeorthis christaniae 3a	Quartzite (160 m.)
Alum shales with fossils	
CAMBRIAN	
Shales, siltstones, sandstones (200 m.)	Semi-pelite (0-140 m.)
Eo-Cambrian Sparagmite	Pre-Cambrian gneiss

detritus of the Valdres Sparagmite (for example, the gabbro conglomerate in the lower parts of the Valdres Sparagmite at Røsjøkollene) can be shown to have been derived from the Lower Nappe and thus must have formed during or after the emplacement of the Lower Jotun Nappe.

To the northwest of Røsjøkollene (for example in the Bygdin area) the Valdres Sparagmite is itself deformed and overthrust by the Upper Jotun Nappe, and thus must be pre-Upper Nappe emplacement, Strand (1958) gives an age between the Upper Ordovician or Lower Silurian for the Valdres Sparagmite.

The Cambro-Ordovician sequence in the Beito window (Fig. 17) rests on Pre-Cambrian hornblende-gneisses and garnetiferous-quartzites. These gneisses have a steep foliation trending northwest while the overlying sediments have an east-west striking foliation with a shallow dip northwards. The contact which may or may not be an original unconformity, is not exposed anywhere in the area mapped, but the Pre-Cambrian just below the contact with the Cambrian has been retrograded to phyllonite with a foliation parallel to that in the Cambrian sediments. These phyllonites can be recognised as being derived from the Pre-Cambrian rocks because they contain relic garnets which are absent in the Cambro-Ordovician.

The Cambro-Ordovician pelites and semi-pelites are typical of those in Greenschist facies. They have a strong biotite strain slip cleavage with small lenses of strained quartz flattened in the strain slip cleavage. The quartzites which appear to be well sorted in the field, are surprisingly impure in thin section, with a high proportion of biotite,

felspar, and large porphyroclasts of mesoperthite. In the Mellsenn Division, sandstones, quartzites, and sparagmite alternate and apparently form a passage group grading up into sparagmite though this grading will be discussed in the structural section.

The Valdres Sparagmite is a typical meta-arkose with a quartz-microcline-albite/oligoclase groundmass, strongly deformed with the small quartz and felspars forming a strained partly recrystallized, mozaic. Biotite and muscovite form a foliation and much of the groundmass is flattened parallel to this foliation. Large rounded relic clastic grains of pethite and quartz can be found (Plate 9b), although these clastic grains are often shattered and broken (Fig. 3b). The clastic perthites are evident in hand specimen and may be confused with garnet, which is absent at Bygdin, but which occurs elsewhere in the Valdres Sparagmite (D. Wood, personal communication). Epidote, orthite and sphene have crystallized in the sparagmite as a result of the Greenschist facies metamorphism.

Tectonic evidence suggests that the sparagmite is highly deformed and thickened tectonically, although some relic sedimentary structures, are still evident (Plate 4b). The petrology of the Valdres Sparagmite is completely constant throughout the whole of the Bygdin area, showing no distinct alter-nation of bedding of differing composition.

The petrology of the matrix of the Bygdin conglomerate is exactly the same as that of the sparagmite, although the conglomerate may have a few spinel rich bands. Most of the pebbles are quartzite with under 5% microcline and chlorite, although a few epidosite and granitoid pebbles are present. The original texture in the pebbles has been completely destroyed

by cataclasis, although a few pebbles show some banding which is suggestive of relic bedding.

The contact of the Valdres Sparagmite with the conglomerate in the less deformed area at Olefjell is very irregular with much inter-tonguing of conglomerate and sparagmite. These complex facies changes which could also be early folds are to be expected in a piedmont or fluviatile depositional environment. postulated for the molassic Valdres Sparagmite.

II.   MINOR STRUCTURES

1. INTRODUCTION

At least four sets of minor structures were recognised, using interference relationships (e.g. refolding). If different sets of structures in an outcrop failed to interfere with one another, they were tentatively arranged in the movement sequence by comparing their style with structures of known age from other outcrops. The second set of minor structures are synchronous with the only set of major folds recognized in the area.

Three of the minor structure sets include foliations, axial plane cleavages, lineations, and minor fold axes. (Fig.2). The fourth set includes folds and tension gashes which are associated with joint formation.

The first foliation and axial plane cleavage (S1) generally has a west north west strike with a dip of 15° to 20° to the north north east. In some sub-areas, however, (Fig.2), S1 poles have a girdle pattern with a northwest plunging axis which represents refolding by the second movement phase. The first linear structures (B1) plunge at 20° to the northwest and southeast throughout most of the area, except in sub-area 10 where they plunge towards the east and northeast.

The second axial plane cleavage (S2) generally has a northwest strike with steep dips to the northeast and southwest. Second linear structures (B2) trend northwest with plunges of 20° to the northwest and southeast.

The third foliation (S3) displays a large range in orientation throughout most of the area, but S3-poles are distributed in north or north-:east trending girdle patterns which are a result of the conjugate symmetry of the third movement structures. Third linear structures (B3) have a wide range of trends, especially in sub-area 4 where they "box the compass".

The planar and linear structures of the fourth set generally trend northeast parallel to the cross-joints of the area.

A fold movement phase which pre-dates the minor structures discussed above, may be present in the Bitihorn gabbro. The poles of the igneous rhythmic layering of the gabbro have a point concentration pattern, breaking out into a girdle with a northeast plunging axis. (Fig.2, 1A). The girdle is rather diffuse, because in addition to the igneous layering, a post-igneous metamorphic layering reported by Battey and MacRitchie (unpublished data) from Eidsbugaren, may be included in the plot. This northeast folding has resulted in steep or inverted dips in the igneous layering of the gabbros (determined from inverted igneous graded bedding and load casts), but it does not fold the thrust plane (synchronous with B1) below the gabbro. Structurally the gently dipping thrust plane appears to cut across the steep layering of the gabbro and thus may be later than the northeast folding. It is suggested that the northeast folds are of Pre-Cambrian age.

2. MINOR STRUCTURES OF THE BYGDIN AREA. (MAP II)

(a) First movement phase (B1)

The first Caledonian movement phase at Bygdin consisted of large
scale thrusting of the Upper Jotun Nappe over the Cambro-Ordovician
sediments.   The thrusting induced cataclastic textures in the sediments
and the Jotun rocks, and formed the first foliation of the area (S1)
parallel to the thrust plane.   However, in two areas, S1 is cut by the
thrust plane, and the significance of this point will be discussed
later (p.40-41).

S1 in the granitic rocks of the nappe, is defined by a cataclastic
layering in which new biotites and muscovites have crystallised.   The
general effect of the B1 cataclasis has been to reduce massive ?igneous
granites to rocks with a gneissic texture in hand specimen. Regular and
irregular phyllonite bands (Plate 1) from a few centimetres to over one
metre thick, occur throughout the whole of the granite outcrop.   In
addition to the bands of phyllonite, small patches of "knots" of
phyllonite can be found (Fig.3 g and h). True mylonites are absent at
Bygdin because the strongly cataclastic rocks are too coarse to be defined
as mylonites. Lapworth (1885) defined a mylonite as a microscopic pressure
breccia with fluxion structure in which the interstitial paste is only
partly crystalline. Although the cataclastic rocks at Bygdin are completely
crystalline, they show no evidence of being recrystallized mylonites
(i.e. blastomylonites, Knopf, 1931, pp.10-14). Because of their phyllitic
appearance they are classified as phyllonites (ibid p.19). Hornblende-

Fig. 3. Minor structures of the First Movement Phase.

a) Phyllonite layers in Jotun Nappe rock folded about the S1 foliation.

b) Felspar porphyroclast elongated in S1.

c) Sparagmite band in conglomerate folded about S1.

d),e),f) Deformed pebbles folded about the S1 foliation.

g),h) Phyllonite "knots" in foliated granites of the Jotun Nappe.

Fig 3

Minor Structures of the First Movement Phase
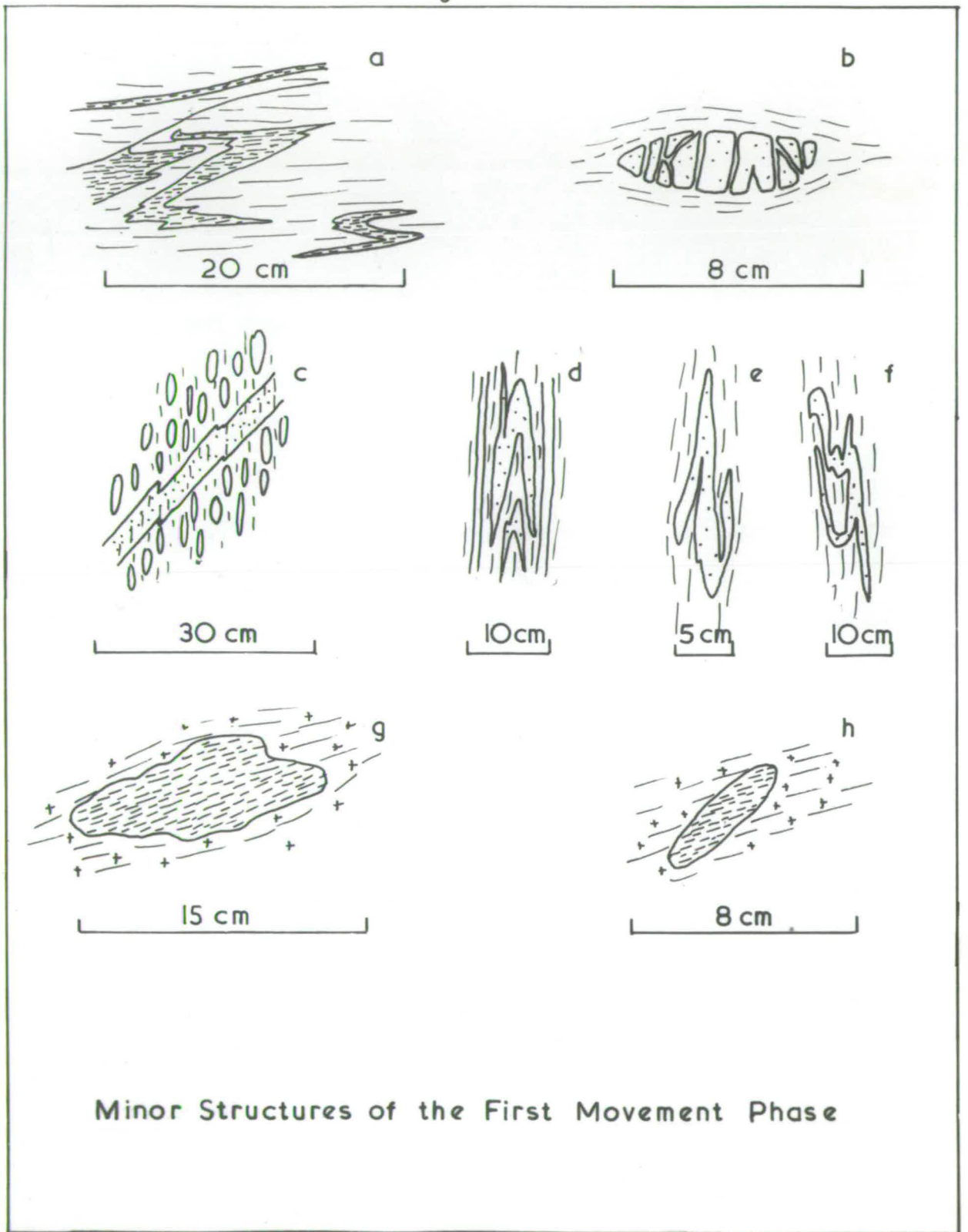
phyllonites are especially well developed just above the thrust plane near the Bygdih Hotel.

Most of the phyllonites have a fine hornblende-biotite cleavage parallel to the cataclastic banding, but in some cases this cleavage is absent or even oblique to the phylonitic shear bands. In addition, cataclastic and phyllonite layers can be found which are folded in a "similar" style, by B1 folds, about an S1 axial plane cleavage (Fig.3,a). This relationship is taken to indicate that the cataclasis generally was prior to the formation of the B1 folds and S1 foliation.

Only a small part of the Bitihorn gabbro has been altered to phyllonite. A thin sheet of gabbroic phyllonite, 10 metres thick, occurs just above the thrust plane 2 km. south of Bygdin.

In the non-conglomeratic sediments below the nappe, the biotite muscovite foliation (S1) is parallel to the cataclastic layering which is defined by alternating layers of differing composition and grain size. Some clastic textures are still evident in the sediments in hand and thin section e.g. large well rounded relic clastic grains of perthite and quartz which have been flattened and elongated in a northwest-southeast direction in S1 (Fig.3,b).

Most of the pebble deformation is ascribed to the first movement phase and the quartzite pebbles are flattened and elongated in S1 (Plate 2,a).

S1 throughout the area is a biotite-muscovite foliation, but in many of the igneous rocks, relic igneous hornblende has been orientated to form planar (S1) and linear (B1) fabrics.

Fig 4
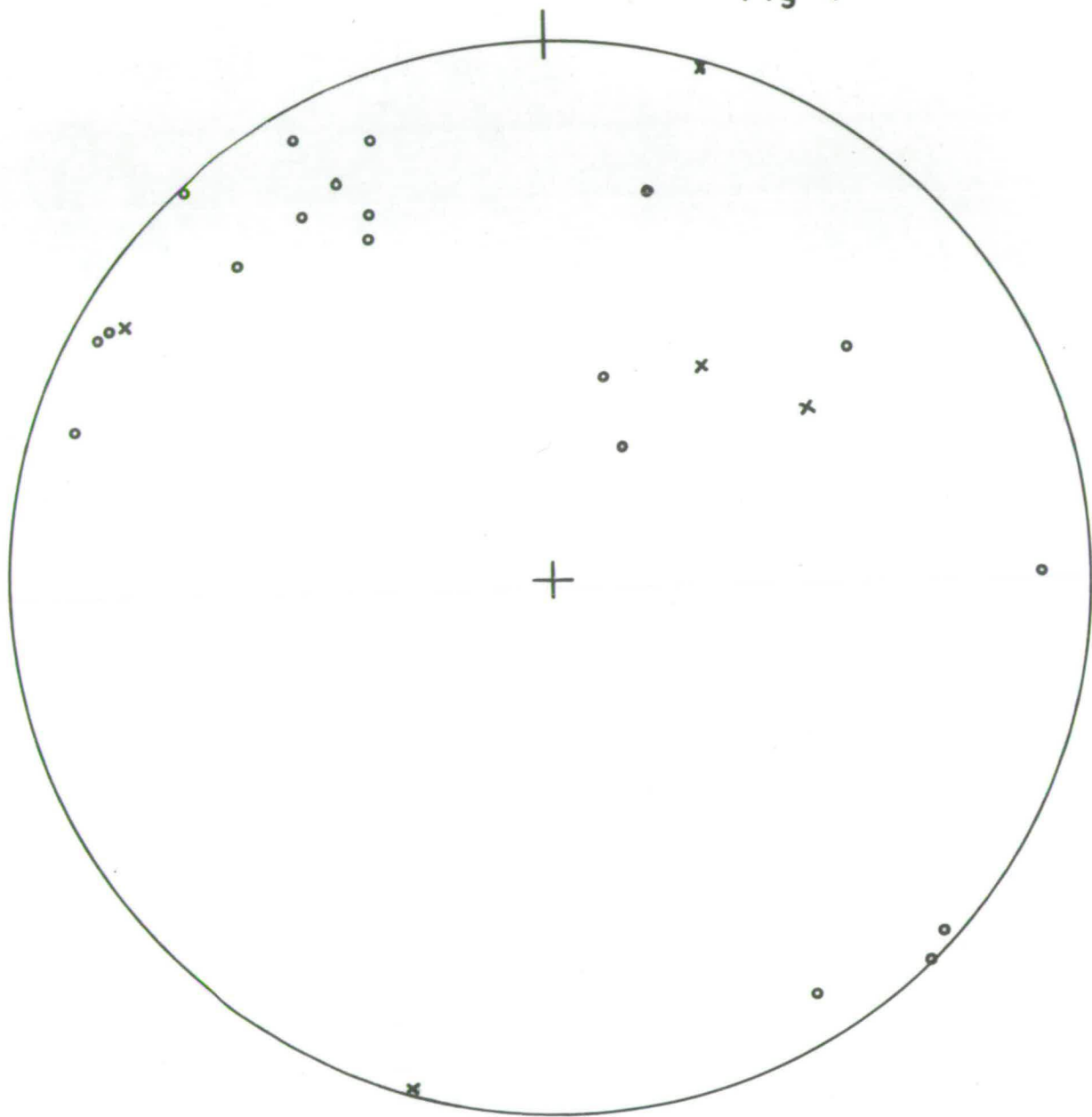
×   BI Folds in pebbles
○   BI Cleavage/Bedding intersection
          Lineation

Fig 5

S1

60 cm

S1

1 m
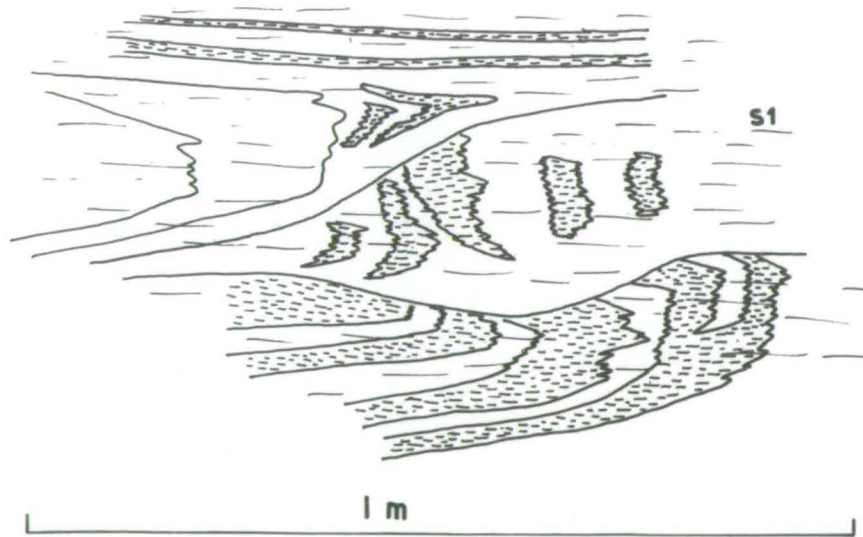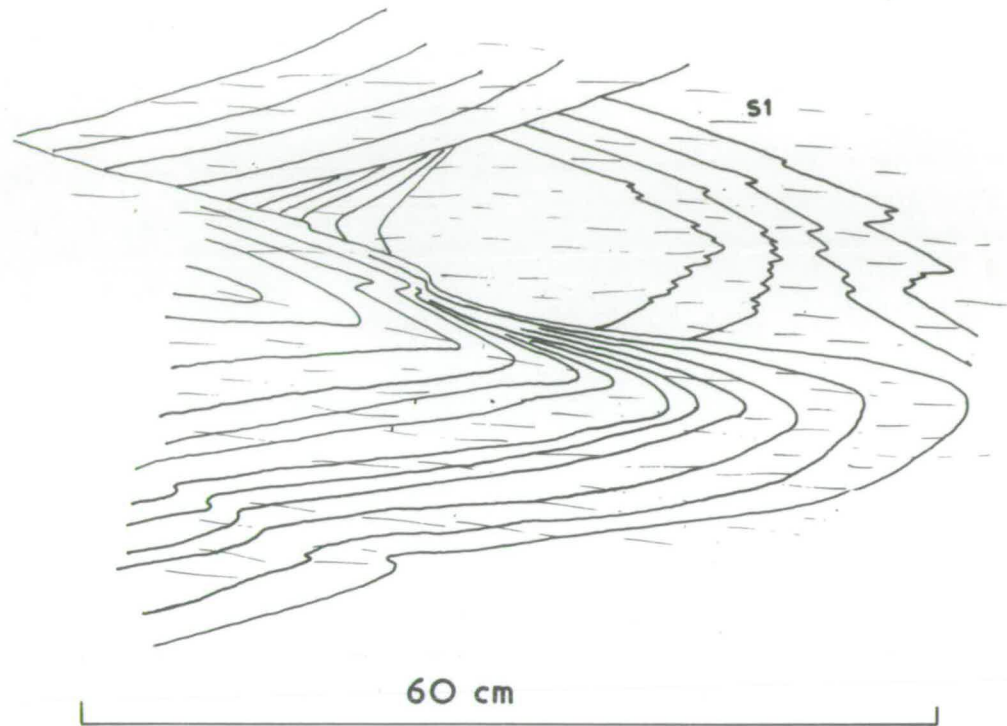
?B1 Folds in the Sparagmite

The B1 linear structures in the granite are due to the parallelism of elongate felspar or hornblende crystals. In some cases B1 is formed by "similar" folds which fold the cataclastic layering about S1, and by inter-sections of this layering with S1. In the gabbro on the peninsula at the east end of Lake Bygdin, only one B1 lineation was mapped, indicating the general resistance of the gabbro to the B1 deformation.

In the conglomerate, B1 linear structures are defined by elongate pebbles and a fine rodding lineation on the pebble surface exactly parallel to the longest pebble axis. In the cake pebbles, in which the longest pebble axis is not visible, the fine rodding on the pebble surface is assumed to define the trend and plunge of the longest axis of the cakes. However, the assumption that this fine rodding is of B1 age might be in error because a similar rodding on the pebble surfaces is parallel to the axes of the later B2 folds and B2 mica crinkle (Fig.7,f) and thus much of the rodding lineation might be of B2 age. However, the surface rodding can be found to be folded by B2 folds (Fig.7,e) and must therefore be at least partly of B1 age.

The conglomerate matrix is also lineated, with B1 being picked out by elongate felspars and micas. Cleavage/bedding intersection lineations are present, especially in thin sparagmite bands that indicate original bedding surfaces within the conglomerate (Fig.3,c). Most of these intersections are parallel to the regional B1 trend with shallow plunges to the northwest, but some plunge quite steeply to the northeast (Fig.4). These steep aberrant plunges could either be caused by rotation from the regional B1 trend (or vice versa) during the deformation (Flinn, 1962) or they were not active axes of buckling and therefore have no kinematic significance (Flinn, 1956, p.491).

Two types of B1 folds can be distinguished in the conglomerate. The first type is picked out by folded pebble-free sparagmite bands (Fig.3, c) and the second type by folded pebbles. The latter type is often difficult to distinguish from the folds in the pebbles due to the second movement phase. However, the first pebble folds are folded about S1 (Fig.3, d,e,f), whereas the second pebble folds always refold S1, the plane of pebble flattening (Plate 2, b). The first pebble folds must be the result of inhomogeneous deformation. Like the B1 cleavage/bedding intersection lineations, the B1 folds in the pebbles have the regional B1 northwest trend and the steep or shallow northeast trends (Fig.4).

B1 lineations in the Valdres Sparagmite are defined by elongate felspars and micas, and cleavage/bedding intersections with a northwest trend. Because of the remarkable compositional homogeneity of the sparagmite, folds of all ages are rare. However, B1 folds can be found in quartz veins folded about S1. In addition, examples of folded green and pink epidote and felspar rich bands (relic bedding?) are present. These folded bedding structures are either tectonic or sedimentary slump folds. Nearly all the folds in the sparagmite have an extremely plastic style (Plates 3 and 4, Fig.5) often with fold cores detached from their limbs. Sedimentary slumping may have continued into B1 tectonic folding without a break.

The sparagmite was deposited in the interval between the thrusting of the Lower and Upper Jotun Nappes (Strand, 1958) and was probably still unconsolidated when it was overthrust by the Upper Jotun Nappe. It is quite conceivable that sedimentary slumping and deposition continued just in front of the nappe during nappe emplacement and that both the sedimentary

Fig 6

BA3
T1
BA2
T3
BA3
BA1
T3
BA3
T3
T2

+

C1

C2
C3
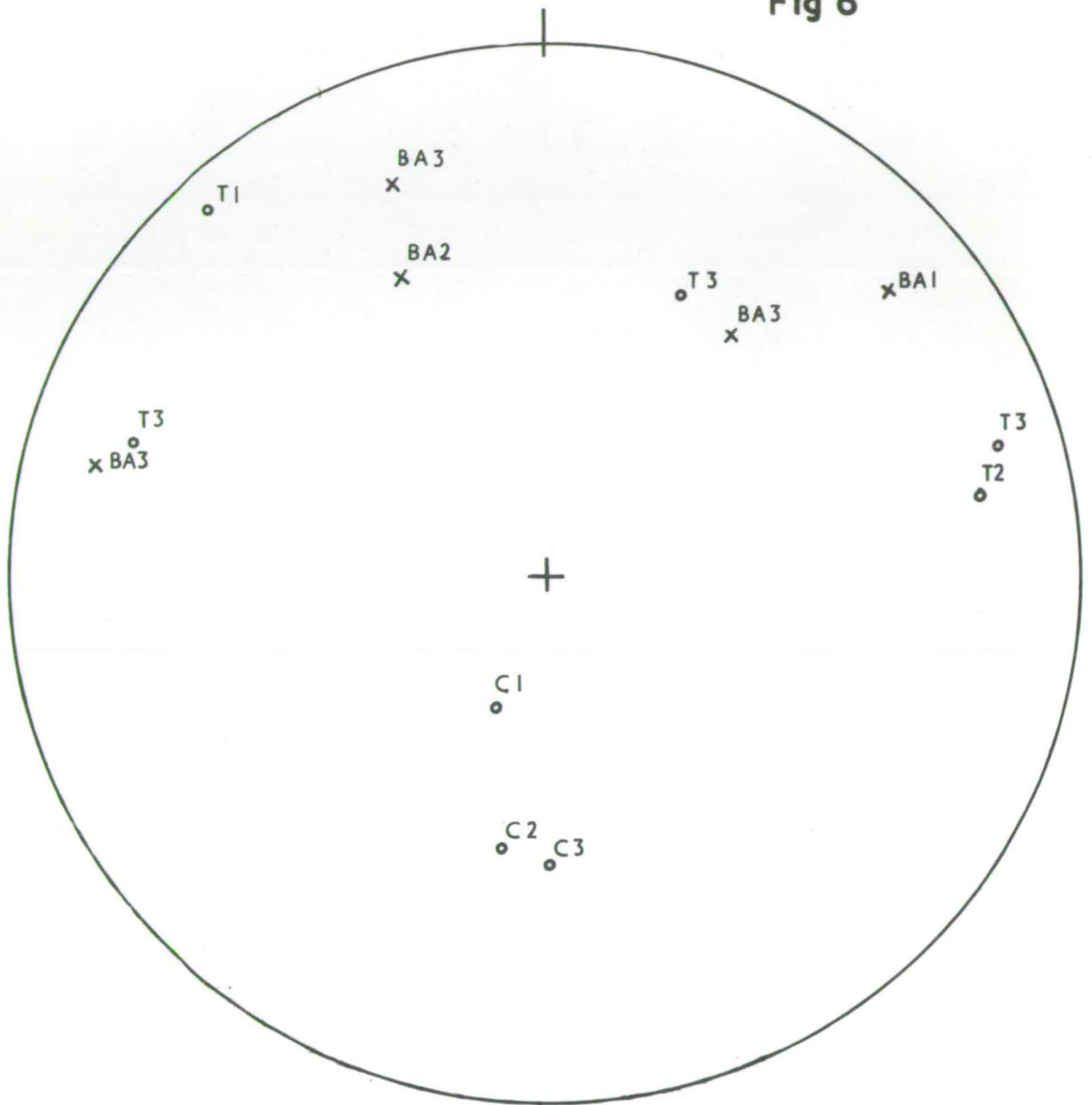
× BA1 Boudin Axes
○ T1 Tension Axes
○ C1 Compression Axes

Stereogram of BI Boudin Structures

slump folds and the B1 tectonic folds were impressed upon unconsolidated sediments. This would make a distinction difficult. Some of the folds are truncated by slide planes which are cut by the S1 cleavage (Fig.5, b) proving that the folding was pre-cleavage but this does not rule out tectonic action. The S1 foliation is parallel to the axial planes of all these folds.

B1 boudinage structures are present at three localities[x] in the nappe rocks and the sediments. They are thought to represent elongation strains of the first deformation. At two of the localities (B.A. 1 and 3) the boudins are flattened and elongated in S1 and were probably formed by a tension axis which lay normal to the boudin axis in S1 (though this is not necessarily true, c.f. Rast, 1956; Flinn, 1962). Application of the experimental results of Ramberg (1959) suggests that the compression axes for these two examples lay approximately normal to the boudin axis and S1.

At the other locality (B.A. 2) there are rhomboid boudins (Plate 5, a) and the tension and compression axes have been derived by bisecting the angles between the intersecting rhomboid planes.

Tension (T) and compression (C) axes are plotted for the three localities (Fig.6) and despite the paucity of data, it is interesting that all three examples are consistent with the kinematics of pebble deformation (p.79).

The rhomboid boudins discussed above (locality $2\frac{1}{2}$ km. east of Bygdin at 924998, sheet 1617 1) occur in a phyllonite shear band and indicate that boudinage occurred after cataclasis. B1 folding can also be shown to post-date the cataclasis and phyllonitization (p.26).

[x] B.A. 1   956908   1617 IV
B.A. 2   924998   1617 I
B.A. 3   016891   1617 IV

but the age relationships of the B1 folding and B1 boudinage are unknown.

Evidence of pegmatite injection synchronous with the B1 deformation has been found. A boudinaged phyllonite band with pegmatite injected into the spaces between the boudins was found at 949932 (Sheet 1617 1), $5\frac{1}{2}$ km. east of Bygdin. The pegmatite was obviously injected during a syn- or post-boudinage phase, but the pegmatite has undergone greenschist facies metamorphism which can be shown to be associated with the B1 phase (pp. 44-45). This pegmatite injection may be equivalent to the syn-thrusting pegmatite injection at Eidsbugaren (Battey and MacRitchie, unpublished data).

The detailed history of the B1 phase is as follows:

i) Thrusting of the Upper Jotun Nappe, with phyllonitization and cataclasis.

ii) Folding and boudinage of the phyllonite bands. S1 formation and ?pegmatite injection. ?Pebble deformation.

iii) Greenschist facies metamorphism (synchronous with ii ?).

(b) Second movement phase (B2).

The linear structures of the second movement phase (B2) are often difficult to distinguish from those of the first movement phase, because statistically the first and second linear structures are exactly parallel. However, the second folds can be proved to post-date the first

Fig. 7.   Minor structures of the Second Movement Phase.

a)   B1 fold in a quartz vein refolded by a B2
     minor fold with S2 axial plane cleavage.

b)   B1 fold in a deformed pebble refolded by a
     B2 minor fold.

c)   "Similar" B2 fold in the granite of the Jotun
     Nappe.

d)   B2 folds in a quartz vein with S2 axial plane
     cleavage.

e)   B2 concentric fold refolding a B1 rodding
     lineation.

f)   B2 concentric fold in the Jotun Nappe.

g)   Fine rodding lineation of a deformed pebble
     parallel to a B2 mica-crinkle lineation.

Fig 7
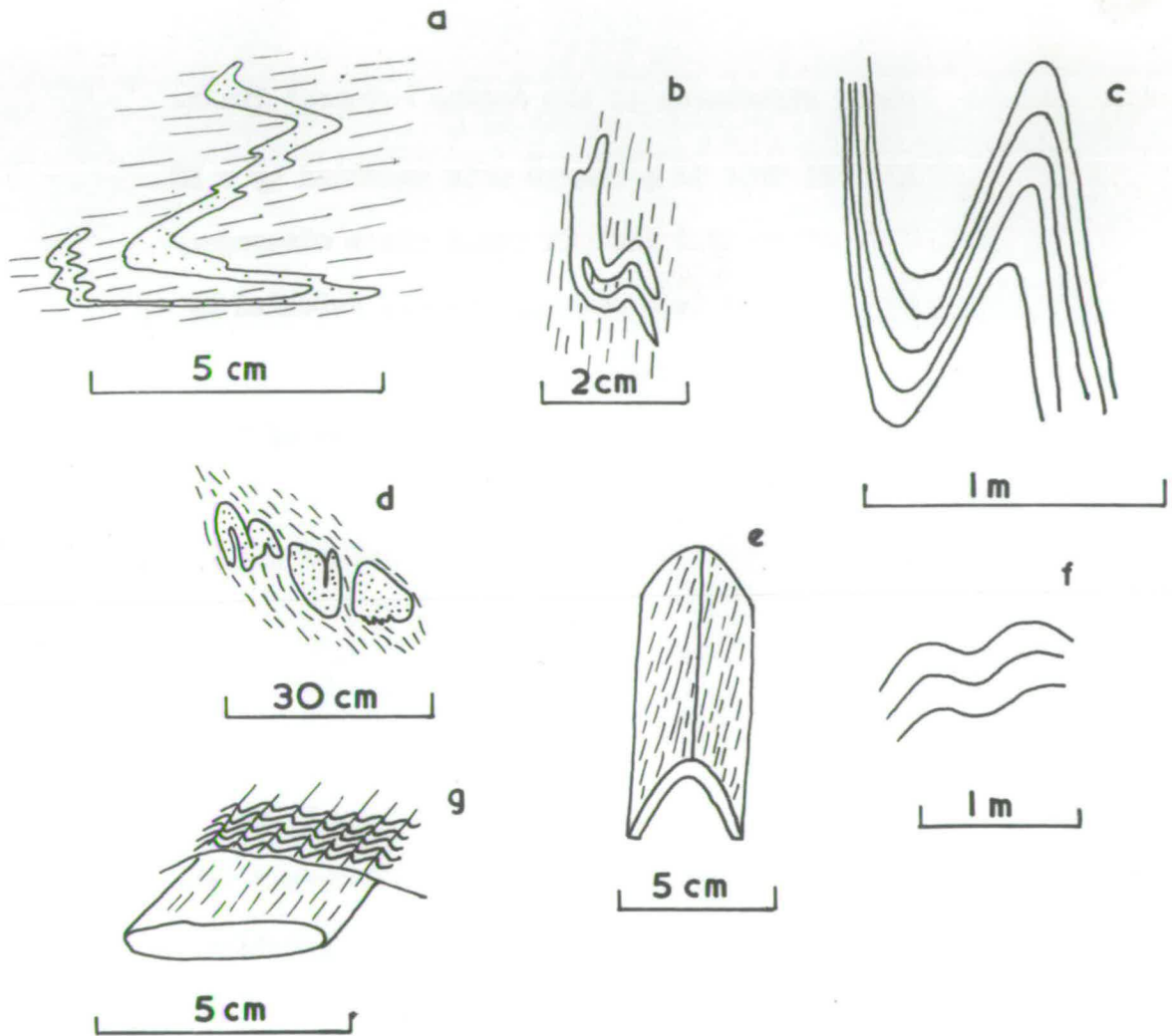
Structures of the Second Movement Phase

movement phase because they refold S1 (the plane of pebble flattening)
(Plate 6, Fig.7) and B1 folds (Plate 5, b).

The shape of the second folds ranges from gentle to isoclinal
(the terminology of Fleuty, 1964, is used throughout this thesis) and the
style from pure concentric to pure "similar" (Fig. 7), often with a strain
slip axial plane cleavage (Plate 6, b). That the latter are truly pure
"similar" folds was proved by applying the techniques of Ramsay (1962a)
(Fig.10). Both asymmetrical and symmetrical B2 folds are present, the
various shapes being related to the major structure (c.f. Chap. III).

The different styles of the B2 folds are not restricted to
any one rock type but occur throughout all rock types.

Recognition of the S2 strain slip axial plane cleavage is
important in strain measurment because unfolded ellipsoid pebbles can be
found lying flattened in S2 (Plate 6, b). These pebbles have either been
rotated as rigid bodies or have been plastically flattened in S2. In
addition the plane of pebble flattening can be rotated by B2 folding until
S1 is almost parallel to S2. Fortunately S2 cleavage formation is
restricted to the area covered by Map III and the core of antiform-h
(Fig.21).

The B2 fold axes and lineations are nearly always parallel
to the pebble elongation direction (B1) (Fig.7,f) and the fact that much
of the fine rodding lineation on the pebble surfaces may be of B2 age has
already been mentioned (p.21). However, B1 rodding lineation does
exist, because in two outcrops a fine B1 rodding is oblique to and folded

by B2 folds (Fig. 7,e). The divergence in trend of B1 and B2 is about 5°-10° and the significance of this divergence will be discussed below.

The majority of the second minor folds are restricted to the cake conglomerate and are rather rare in other rocks of the area.

One striking feature about the B2 structures is that in all the sub-areas (Fig.2), the B2 lineations are _always_ statistically parallel to the B1 lineations. On the mesoscopic scale only two examples of divergent B1 and B2 linear trends were found. This parallelism of B1 and B2 could be due to the following.

i) B1 and B2 are synchronous

ii) The B2 deformation has re-orientated B1 into parallelism with B2.

iii) B1 structures have controlled the orientation of the later B2 structures.

iv) The B2 stress field was parallel to that of B1.

i) B1 and B2 must be regarded as two separate phases because B2 folds refold the plane of pebble flattening and the mica foliation parallel to that plane. In addition, B2 folds refold an earlier B1 rodding lineation as discussed above. However, in spite of the fact that B1 and B2 can be regarded as two separate phases, B2 might have followed B1 without a time gap.

ii) Extensive rotation is unlikely because at Olefjell, B2 structures are absent but the B1 lineations still have the regional northwest trend. In addition the B2 folds which refold the B1 rodding lineation (Fig. 7,e) have a concentric style and when unrolled give the original trend of B1 as northwest-southeast. This suggests that prior to B2, the original trend of B1 was parallel to the present trend.

iii)   The B1 deformation may have imparted a "grain" to the rocks (c.f. the rod fabric) which controlled the orientation of the later B2 structures. However, the B1 fabrics do not control the orientation of the B3 structures (Plate 7, a) and the strain data (Chap. V) suggest that the dominant symmetry of the B1 deformation was one of flattening (i.e. planar fabrics dominant over linear fabrics, Flinn, 1965). True "grained" rocks are restricted to the rod conglomerates, which have a limited distribution. As a planar fabric cannot be expected to actively control the direction of a later deformation, this structural control seems unlikely.

iv)   The principal stress directions of the B2 phase might have been parallel to those of the B1 phase. This parallelism acting upon a B1 planar fabric, could conceivably produce two separate parallel linear fabrics. If the stress fields were parallel, however, the values of the stresses would have to change from the B1 to the B2 phase. For example, the maximum stress direction of the B1 phase would appear to have been vertical (c.f. Chap. VI) whereas that of the B2 phase (suggested by symmetry arguments) would appear to have been normal to this, i.e. in a northeast-southwest direction. If the stress axes of the two phases were parallel, the B1 deformation could have graded into the B2 deformation merely by a change in the values of the stresses.

Hypothesis iv) is accepted by the writer. In addition, the structural evidence described in ii) seems to indicate that the original trend of the B1 lineations (i.e. "stretching" lineations of pp.73-75) was parallel to the present trend.

Fig. 8.   Minor structures of the Third Movement Phase.

a)   Disharmonic B3 fold.

b)   Deformed B1 lineation on a planar pebble
                surface with an a3 lineation.

c)   B1 lineation deformed about an a3 lineation
                with a ?late stage B3 concentric fold.

d),e),f),g)   Conjugate B3 folds.

h)   Minor B3 fold with an S3 strain slip axial
                plane cleavage.

Fig 8

a   1 m

b   30 cm

c   15 cm

d   5 cm

e   15 cm

f   10 cm

g   5 cm

h   3 cm
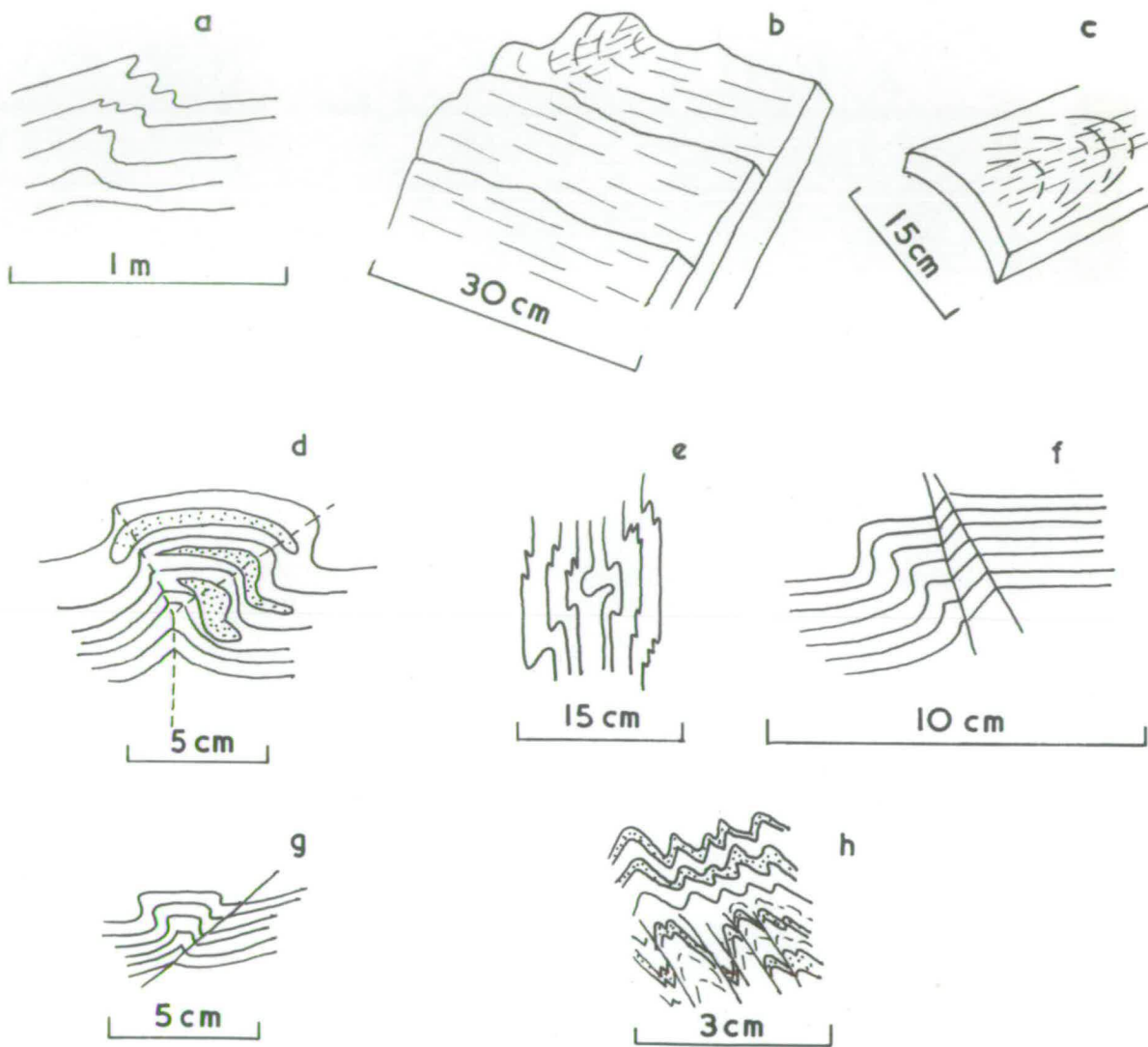
Structures of the Third Movement Phase

Fig 9

30 cm
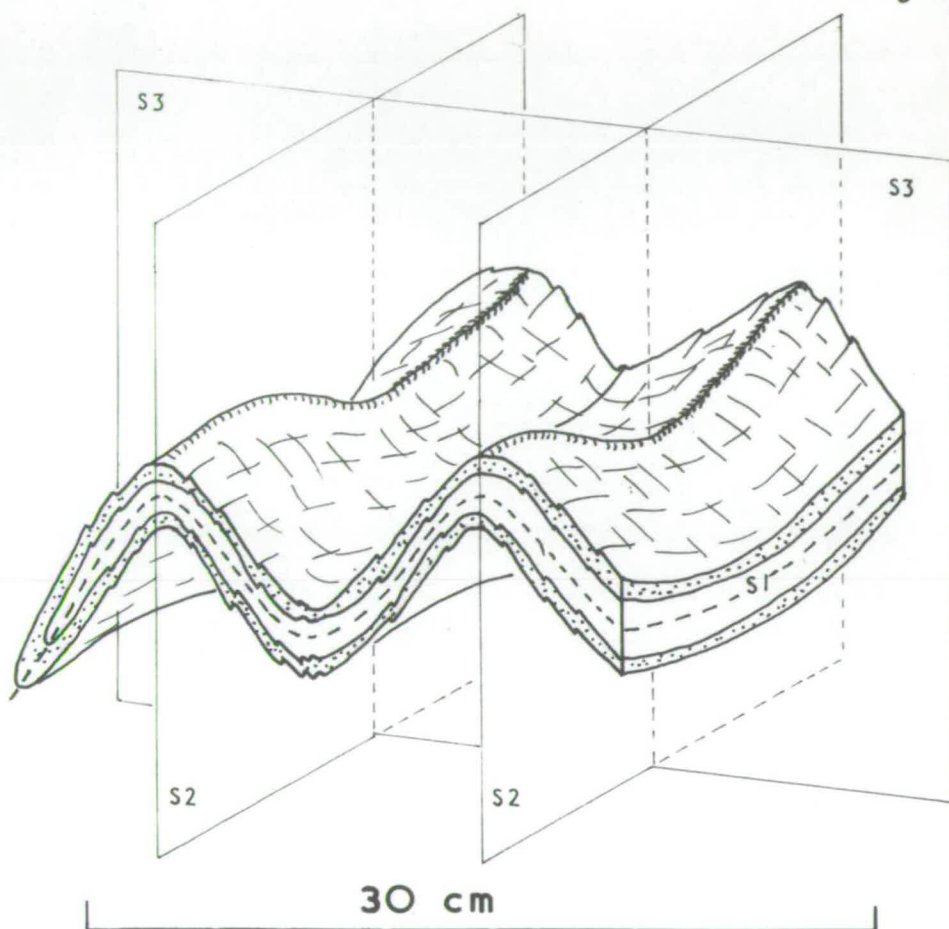
B3 fold refolding B1 and B2 folds
on the limb of antiform-f

Fig.10.   Thickness measurements from B2 and B3 folds.

      a)   B2 fold

      b)   B3 fold

Fig 10

QUARTZOFELSPATHIC LAYER

PHYLLONITE LAYER

SPARAGMITE

T

DISTANCE NORMAL TO AXIAL PLANE
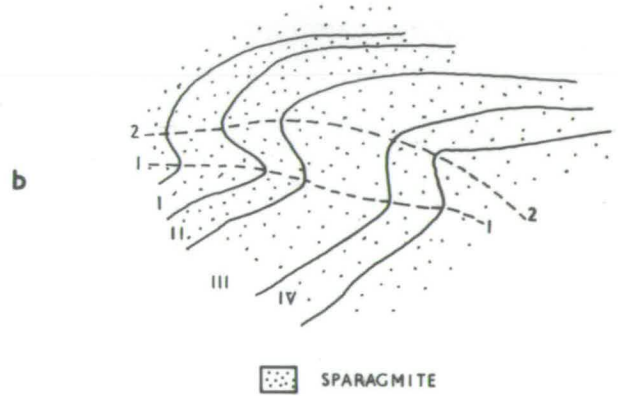
Thickness measurements from B2 and B3 folds

(c) Third movement phase (B3)

The third minor structures vary in symmetry from near perfect orthorhombic, through monoclinic, to triclinic, and vary in style from "similar" to concentric.   They also have a wide range of orientation which is a result of the conjugate symmetry of the third movement phase.   The third structures refold both B1 and B2 structures (Figs. 8 and 9).

The "similar" third folds are usually quite disharmonic (Plate 7 b) and may have a strain slip cleavage parallel to the axial plane (S3) (Fig. 8, h).   The "similar" style is indicated by graphs of T against distance normal to the axial plane (Ramsay, 1962a) which show maxima and minima at the axial planes (Fig.10).   Most B3 folds have this style and are usually asymmetric monoclinic folds.

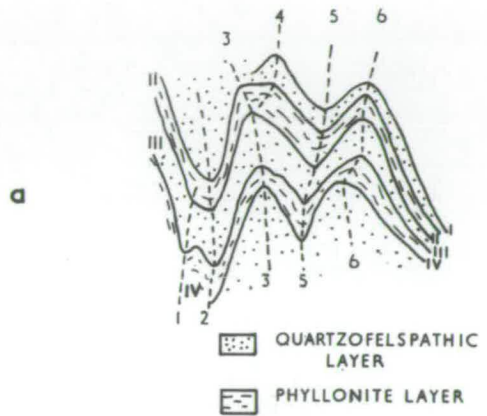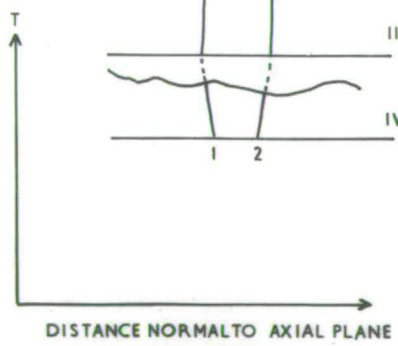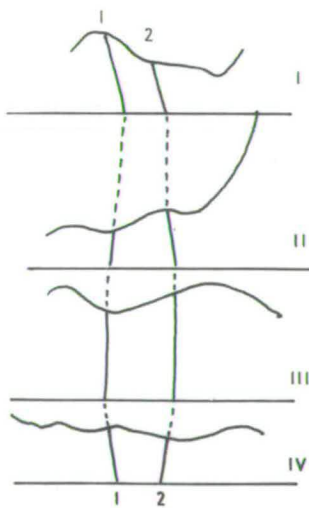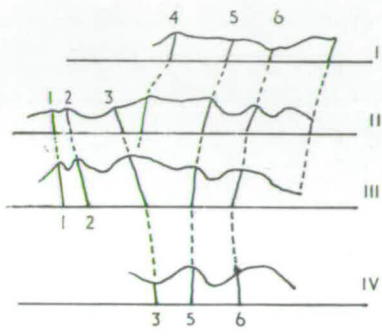A further indication of a "similar" component in the third deformation is shown by the patterns of deformed B1/B2 lineations developed in parts of the conglomerate.   The fine B1/B2 rodding lineation is deformed in a sine-wave pattern on a planar surface (i.e. the flattened pebble surface) (Fig.8, b).   This structure is analogous to the deformed lineation reported by Ramsay (1960, p.80) in Glenelg.   Ramsay (ibid p.90) suggested that if the movement direction which deforms a lineation, lies within the plane of the lineation, no folds will develop but the lineation will be deformed into a sine-wave pattern.   Any new lineation developed on the surface by the deforming movements will be parallel to the "a" direction. The B3 lineation in the above structure is thus probably a true "a"-lineation.

Fig II
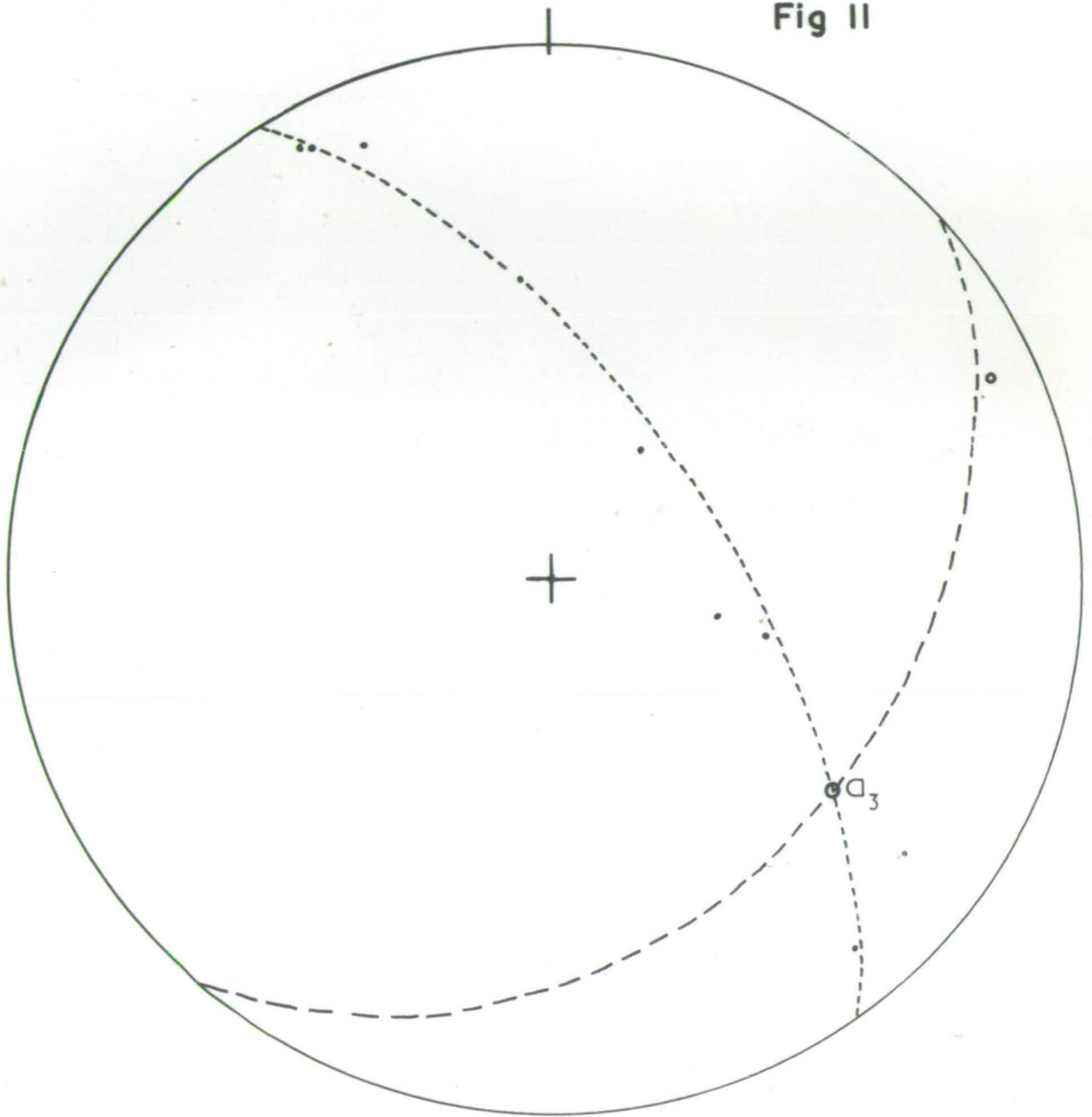
- • B1 lineation
- ⋰ Great circle trace of B1 lineation
- ° B3 fold axis
- \ B3 axial plane
- ○ a3 direction

B1 lineation deformed in a great circle pattern about a B3 fold

Fig. 12. $\underline{a}$3 directions and regional intermediate stress

axis of the Third Movement Phase.

Fig 12
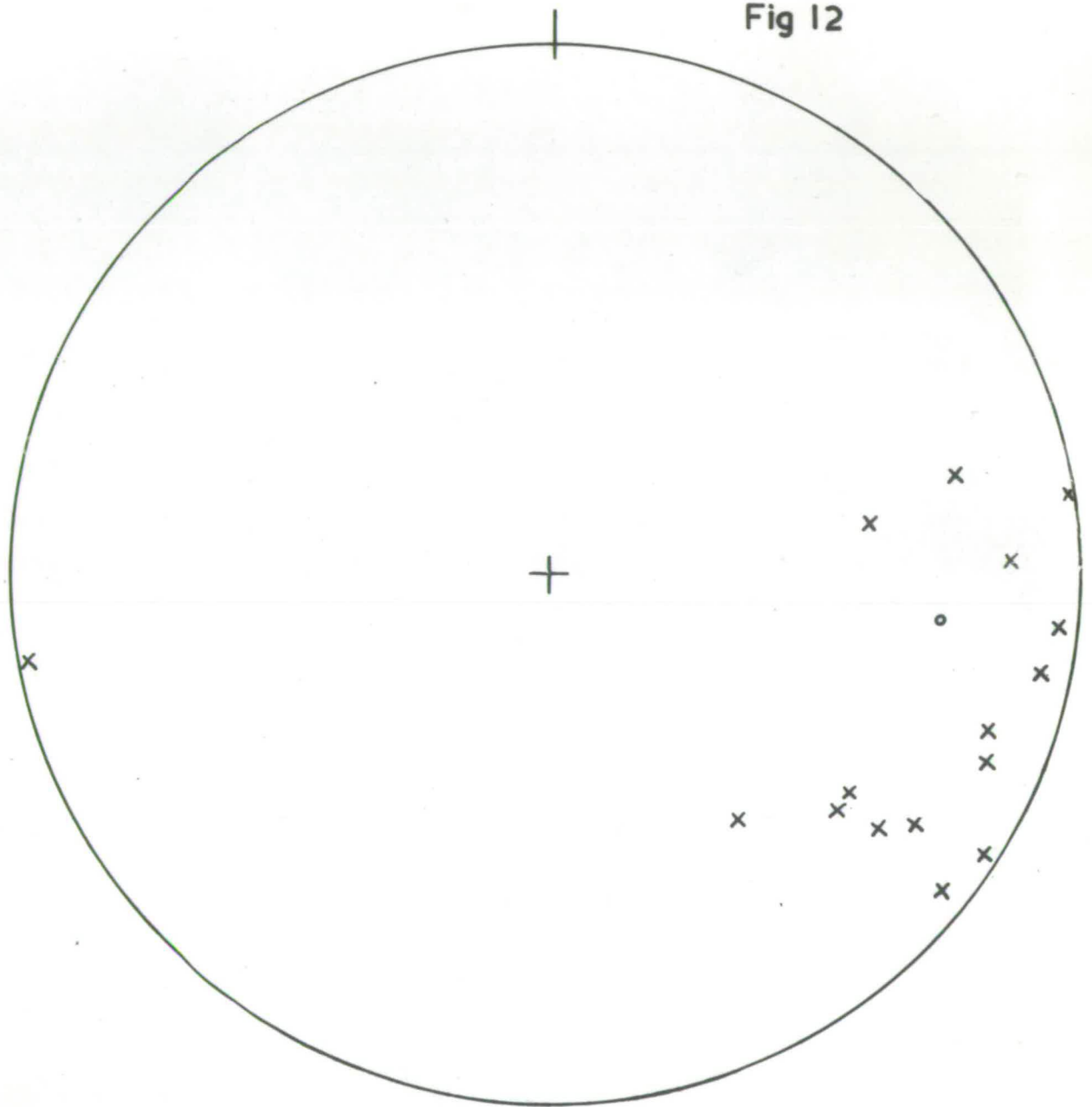
∘ S3 Girdle Axis
× a3 Axes

Some of the third "similar" folds described above deform B1 and B2 lineations about great circles (c.f. Fig.11). The "a" directions of these folds have been calculated (Ramsay, 1962a). In some outcrops B1 and B2 lineations were found deformed around B3 folds in which the angle between B1/B2 and B3 axis varies across the B3 axis, signifying that the deformation included a component other than that of concentric buckling. Because of the scale of these folds, the actual distribution of B1/B2 is unknown, but the approximate plane in which the B1 and B2 lies was measured *the B1/B2 lineation* in the field and the "a" axes calculated. Although this method is inaccurate, it probably gives some indication of the approximate movement directions within the B3 folds. All the measured "a"-lineations and "a"-directions calculated from deformed lineations are given in Fig.12. Almost all the "a_3" directions plunge between $0°$ and $45°$ to the east and southeast.

Some of the deformed sine-wave B1/B2 lineations lie in a slightly buckled surface with the axis of buckling parallel to the B3 lineation (Fig. 8,c). This buckling may be a late stage in the B3 deformation.

In the field, the third folds show an extreme variation in axial plane and fold axis orientation. This variation cannot be explained as being wholly due to the control of the orientation of B3 axes by already folded S1 surfaces, or by later refolding.

Much of the variation is thought to be due to the conjugate symmetry of B3. Many examples of conjugate folds were found throughout the area with axial trends parallel to neighbouring B3 folds, suggesting that at least some of the B3 folds have a conjugate symmetry. Many of these conjugate third folds have a "brittle" style comparable to those described

by Johnson (1956) in the Coulin Forest., Scotland (i.e. with a shear plane or kink band parallel to the axial plane) (Fig.3). This brittle style is only apparent because this style of deformation by kinking can be compared with "plastic" kink zones of deformed crystals (Johnson, 1964).

Only one third fold with perfect orthorhombic symmetry was found (Fig. 3,e), unfortunately in a fallen block. This fold has deformed an earlier lineation in a rather interesting manner. The angle between the deformed lineation and the B3 axis varies around the B3 fold axis. Unfortunately, because of the scale of the fold it was not possible to determine accurately whether the pattern of the deformed lineation lies on a small circle, great circle, or complex curve (Ramsay, in Johnson and Stewart, 1963). At least part of the deformation in this fold was accompanied by a "similar" component (i.e. a component which does not involve flexural slip). Nearly all conjugate folds described so far have been formed by flexural slip so a "similar" component in the deformation of the Bygdin conjugate folds raises some problems. The "similar" component could be a late stage plastic flattening imprinted on an already formed flexural slip fold. "Similar" B3 folds have already been described and may have formed at the same time as the conjugate folds. Thus the third deformation may have been complex with flexural slip folds forming in some areas while similar folds formed elsewhere.

The regional orientation of the S3 surfaces will be described to illustrate the conjugate symmetry of the B3 folds. Although most of the B3 folds do not have a conjugate symmetry on the mesoscopic scale, they have a conjugate symmetry on the macroscopic scale.

Fig 13

172 points
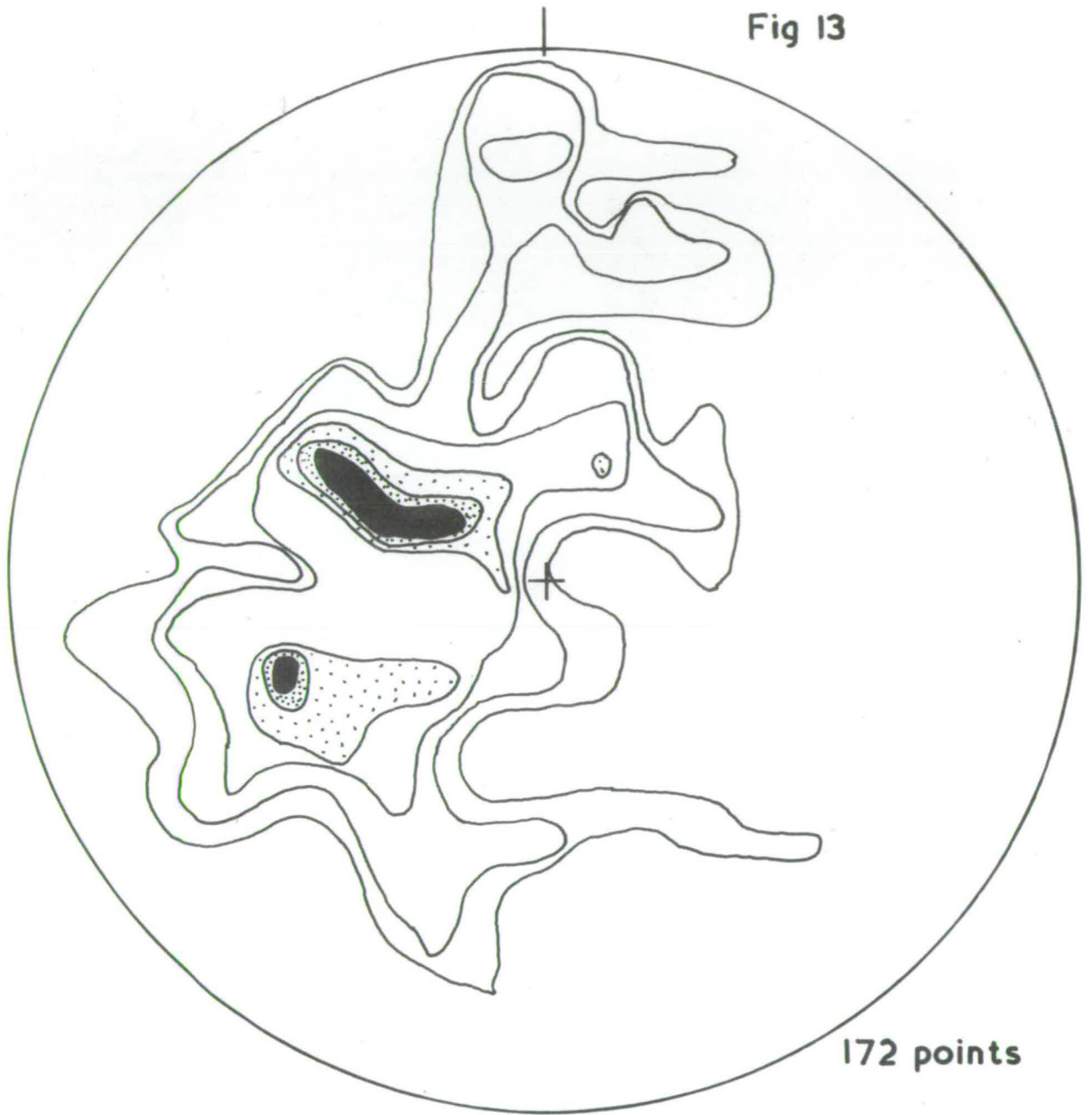
Stereogram of S3 poles from the whole
of the Bygdin area

Contours 1,2,3,4,5,6 %

Girdle distributions of S3-poles are apparent in sub-areas 3, 5 and 6 (Fig. 2) but are not so obvious in other sub-areas. The girdles are interpreted as reflecting the conjugate symmetry of B3 with the girdle axis representing the line of intersection of the conjugate axial planes. A composite plot of all S3-poles measured in the area (Fig.13) demonstrates a girdle distribution with the girdle axis plunging at 25° towards 98° east. In all sub-areas, the girdle axis or line of inter- :section of the S3 axial planes plunges through the S1 foliation. This asymmetry produces divergent S1/S3 intersections and accounts for the complex B3 axial distributions in all sub-areas. The geometric relationships of conjugate folds which are asymmetric to the foliation have already been described by Ramsay (1962b) and Louden (1963) and will not be described here.

An analysis of the third stress axes can be attempted using the symmetry of the B3 structures (Johnson, 1956; Ramsay, 1962b). The intermediate stress direction is assumed to lie along the line of inter- :section of the conjugate axial planes (and hence along the girdle axis). If this assumption is correct, the intermediate stress direction (σ_2) plunges at 25° towards 98° east. Now the maximum and minimum stress directions (σ_1 and σ_3 respectively) must lie normal to this and hence lie somewhere within the girdle of S3-poles.

In a simple conjugate fold with two intersecting axial planes, σ_1 and σ_3 will bisect the angles between the two axial planes. In the composite plot however (Fig.13) an almost complete girdle is present. A gap in the girdle occurs near the horizontal plane (representing a gap

Fig. 14. Calculation of the regional stress axes of the Third Movement Phase.

σ_2 is parallel to the line of intersection of the conjugate S3 axial planes and σ_1, σ_3 lie normal to this on the S3 pole girdle. σ_1 bisects the gap in the spread of the S3 axial planes and σ_3 lies normal to this.

Fig 14
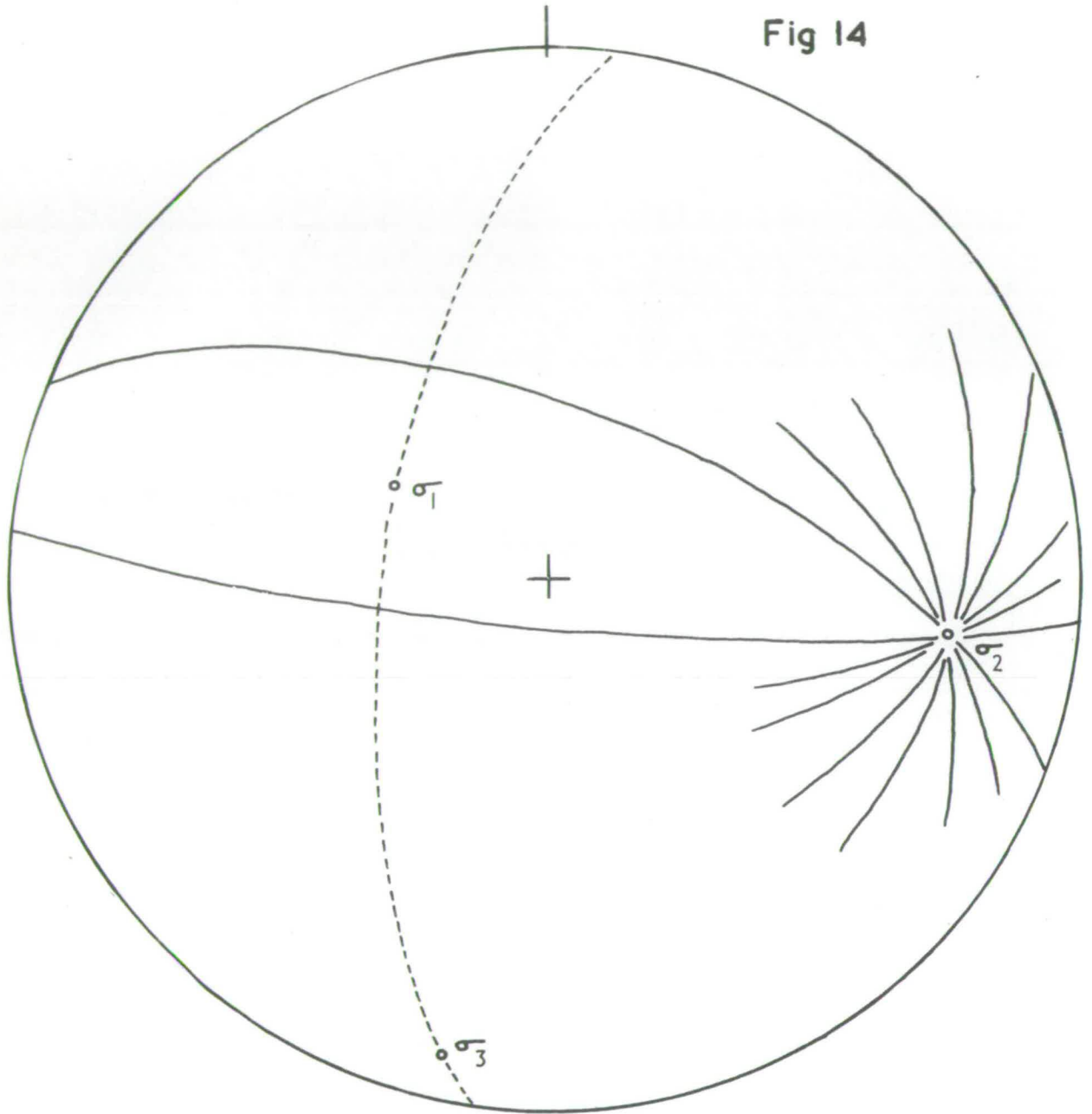
S3 pole girdle σ_3 Minimum stress axis

S3 planes

σ_1 Maximum stress axis σ_2 Intermediate stress axis

Fig 15
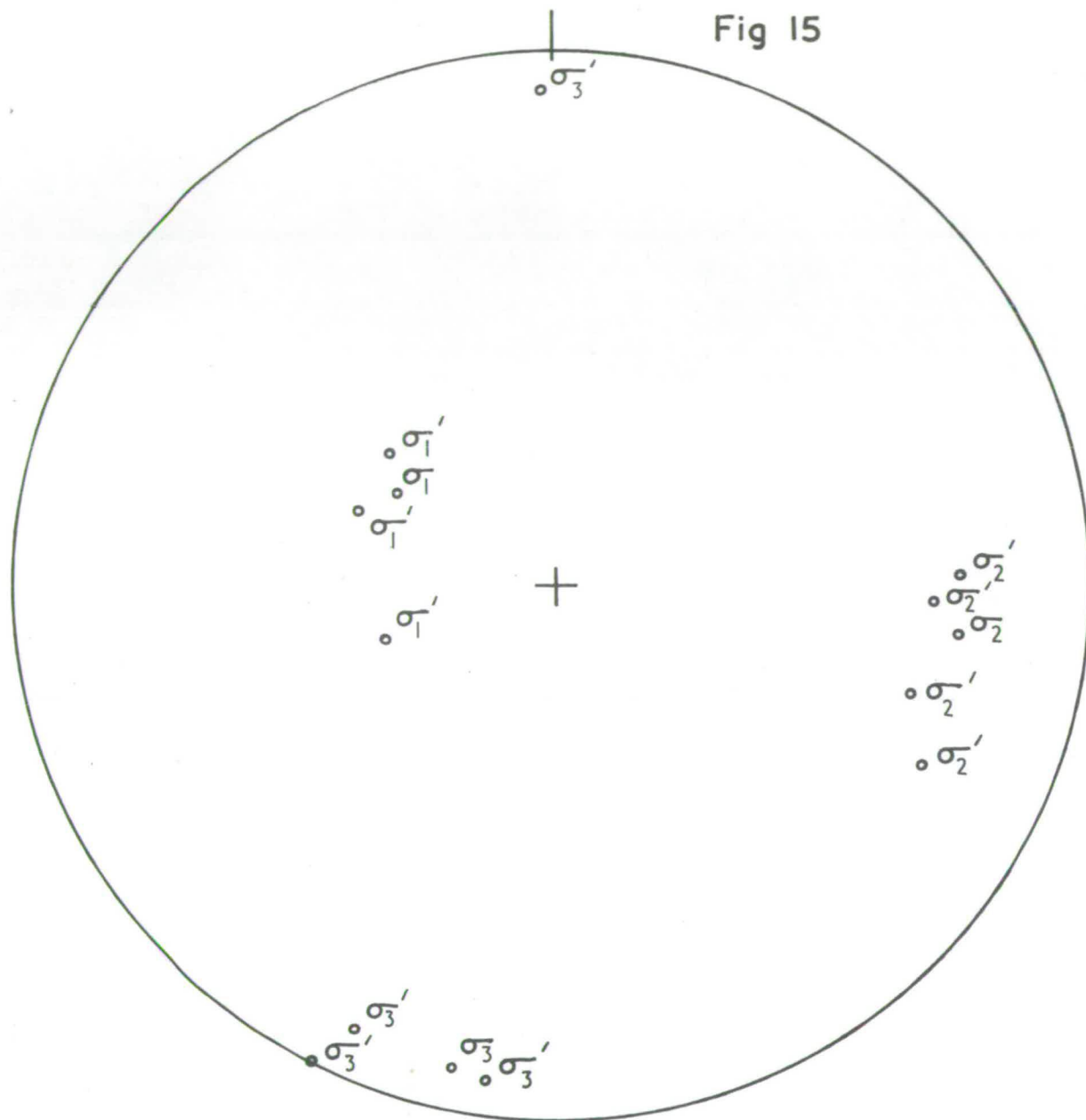
σ₁ Regional stress axes
σ₁' Sub-areal stress axes

Regional and sub-areal stress axes of the
Third Movement Phase

in the spread of axial planes near the vertical). The σ_1 axis must bisect the angle of the gap in the axial plane distribution (Fig. 14). σ_3 will then lie 90° from σ_1 on the S3 girdle.

σ_1 plunges at 62° towards 300° northwest, σ_3 at 8° towards 198° south, and σ_2 at 25° towards 98° east. In addition stress axes were calculated for each of the sub-areas with girdle distributions of S3-poles and are plotted along with the regional stress axes in Fig.15.

The third deformation was probably a three dimensional strain because the "a3" axes group around the regional σ_2 axis (Fig.12). In spite of the fact that the directions of some of the "a"-axes are only approximate because of the difficulty of accurate measurement, (p.29) and also an "a"-axis does not necessarily represent the only line of movement within a rock but one of many (e.g. in a three dimensional deformation), the grouping of "a"-axes about σ_2 demonstrates that at least some of the movement took place along the intermediate stress direction.

(d) Fourth movement phase (B4)

This is the final movement phase in the area to imprint minor structures, all of which have a brittle style and seem to be intimately associated with joint formation.

A joint analysis has been done by Strand (1945) and will not be repeated here. Strand recognised three joint sets with the dominant set trending northeast-southwest approximately normal to the B1 and B2 linear structures. The northeast cross joints are often represented by two conjugate joint sets intersecting in a small angle. The other

Fig 16
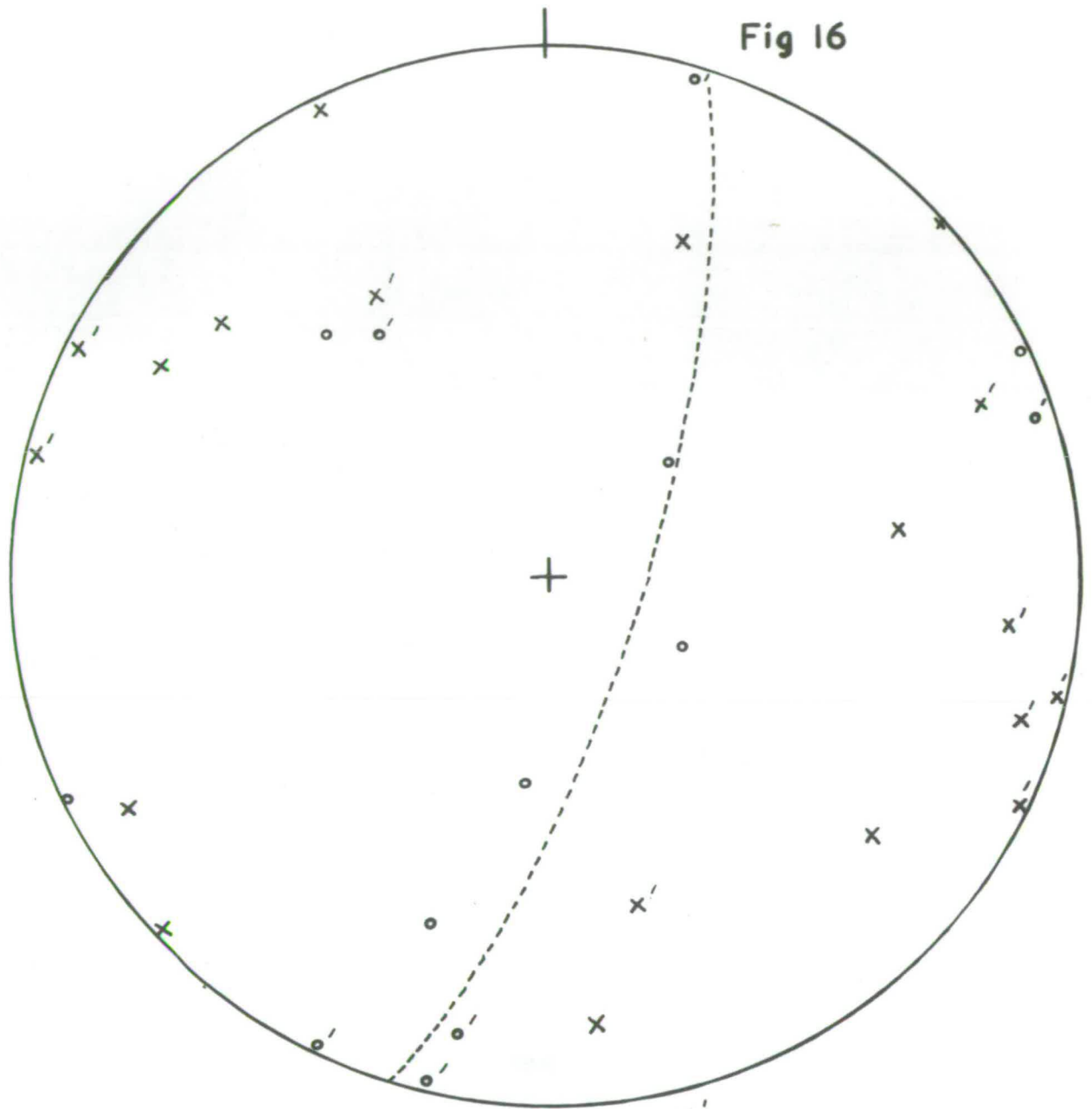
× Poles of axial planes and
   kink zones
○ Movement directions
╲ Trace of cross joints

×'
○' Dextral

×
○ Sinistral

Stereogram of the movement directions of the
Fourth Movement Phase

two sets of joints trend north-south and west north west-east south east.

Because all the joints cut through the structures of the first three movement phases, they are regarded as being later.

Small joint drag folds can be found associated with the cross joints and because of the symmetry of the cross joints, the joint drag folds may have a conjugate symmetry. The joint drag folds can also be found where joints are absent (Plate 8, b).

Other structures of the fourth phase include quartz or chlorite filled tension gashes which may or may not occur with the joint drag folds (Plate 8, a). Both dextral and sinistral tension gashes are present.

These B_4 minor structures show little preferred orientation but a plot of the possible movement directions of the minor structures have a significant distribution. Assuming a simple shear deformation for the tension gashes, shear directions in the kink-zones have been calculated assuming that the shear directions are normal to the line of intersection of the tension gashes with the kink-zone. Shear directions for both the dextral and sinistral tension gashes plot in a northeast great circle (Fig.16) which is parallel to the trace of the northeast cross joints. This indicates movement along the northeast cross joints but the direction does not appear to have been constant.
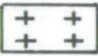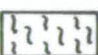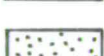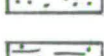
3. MINOR STRUCTURES OF THE SYNBERG AREA (FIG.17).

The Synberg area, 2½ km. south of the Bitihorn, was mapped to determine the structural history of the rocks lower down in the

Fig 17

Geological and Structural map of the Synberg area

Fig 18

- · B I lineations
- ° Poles of SI foliation
- × Poles of bedding

Stereogram of the minor structures of the
First Movement Phase
at Synberg

Cambro-Ordovician sequence than the rocks at Bygdin. A complete section
of Cambro-Ordovician sediments (Table 1) is exposed in the area, down to
the Pre-Cambrian basement upon which they rest (Beito-Window). The
structural history of the Synberg area seems to be comparable with that
at Bygdin.

(a) First movement (B1)

The first foliation (S1) has a similar trend to the first
foliation at Bygdin (Fig. 18). S1 has a strike of 280° northwest with a
dip of 10° to the northeast. Surprisingly, S1 at Synberg is a strain
slip cleavage (Plate 9, a) and this raises the possibility of a pre-S1
foliation occurring at Synberg.

The B1 lineations (which include cleavage/bedding inter-
:sections, mineral elongations, and mica-crinkle lineations) show a large
variation in trend (Fig. 17 and 18) with trends varying from 60° north-
east to 150° southeast.

An important problem at Synberg is whether or not the B1
phase can be correlated with B1 of Bygdin. The key to any correlation is
the nature of the contact between the Lower Cambro-Ordovician sediments
(up to the Mellsenn Division) and the Valdres Sparagmite. The junction
plane has three possible origins.

i) The junction is a normal sedimentary contact, with the
Mellsenn Division as a passage group between the phyllite and quartzite
facies of the Lower Cambro-Ordovician rocks and the arkosic facies of

of the Valdres Sparagmite (Strand, 1958). If the section is a complete
sedimentary sequence from Lower Cambrian to Valdres Sparagmite, there
can be no minor tectonic structures in the phyllites and quartzites which
pre-date the deposition of the Valdres Sparagmite.

ii) The Lower Cambro-Ordovician sediments may have been
overthrust and deformed by the Lower Jotun Nappe, with the Nappe being
eroded away at a later date and the Valdres Sparagmite deposited on
top of already deformed Cambro-Ordovician sediments. This relationship
is present at Røssjøkollene (c.f. pp. 13-14) which shows that at
least to the east of Bygdin the Lower Jotun Nappe at one time extended
further south than Bygdin and may have covered the Bygdin area. This
relationship would imply possible tectonic structures in the Cambro-
Ordovician sediments which pre-date the first deformation of the Valdres
Sparagmite.

iii) The junction between the Valdres Sparagmite and the
Mellsenn Division may be a thrust plane. Kulling (1961) has suggested
that the Valdres Sparagmite represents a middle nappe between the
Lower and Upper Jotun Nappes, and that the Valdres Sparagmite is not
of Cambro-Ordovician age but is in fact Eo-Cambrian Sparagmite. This
hypothesis could imply that tectonic structures may be present in both
the rocks below the Mellsenn Division and the Valdres Sparagmite
that pre-date those produced by the thrusting of the Upper Jotun
Nappe.

The evidence of the nature of this contact at Synberg
is difficult to interpret as the junction is exposed in only one outcrop,

midway up an inaccessible cliff-face. The junction appears to be a normal sedimentary contact (c.f. i) above) with alternations of thin sparagmite and phyllite bands passing up into Valdres Sparagmite proper. If this is indeed a sedimentary contact, there cannot be any tectonic structures which pre-date the Sparagmite deposition, anywhere in the sedimentary succession. The first tectonic structures of the area will probably be present in both the Valdres Sparagmite and the sediments below the Mellsenn Division.

In fact the first strain slip cleavage of the Lower sediments seems to pass up, without any change in orientation, into the Sl foliation of the Sparagmite. However, an Sl strain slip cleavage is absent in the rocks above the Mellsenn Division (Plate 9b). In addition the Bl lineations of Synberg can be traced up into the Bl lineation of the Valdres Sparagmite. The Bl axes in the Upper Phyllite Division have a general east-west trend; they swing round into a northwest trend in the Mellsenn Division and this continues up into the northwest trending Bl lineation in the Valdres Sparagmite. On this evidence the writer would suggest that the Bl phase at Synberg is equivalent to the Bl phase at Bygdin.

If, however, Sl strain slip at Synberg is correlated with Sl at Bygdin, what is the significance of the muscovites and biotites which are strained by Sl at Synberg?

The writer would suggest that the muscovites and biotites crystallized along ?bedding planes during an earlier phase of Bl and were strained by a later Bl phase. If, however, the nature of the junction between the Valdres Sparagmite and the Mellsenn Division has been

Fig. 19
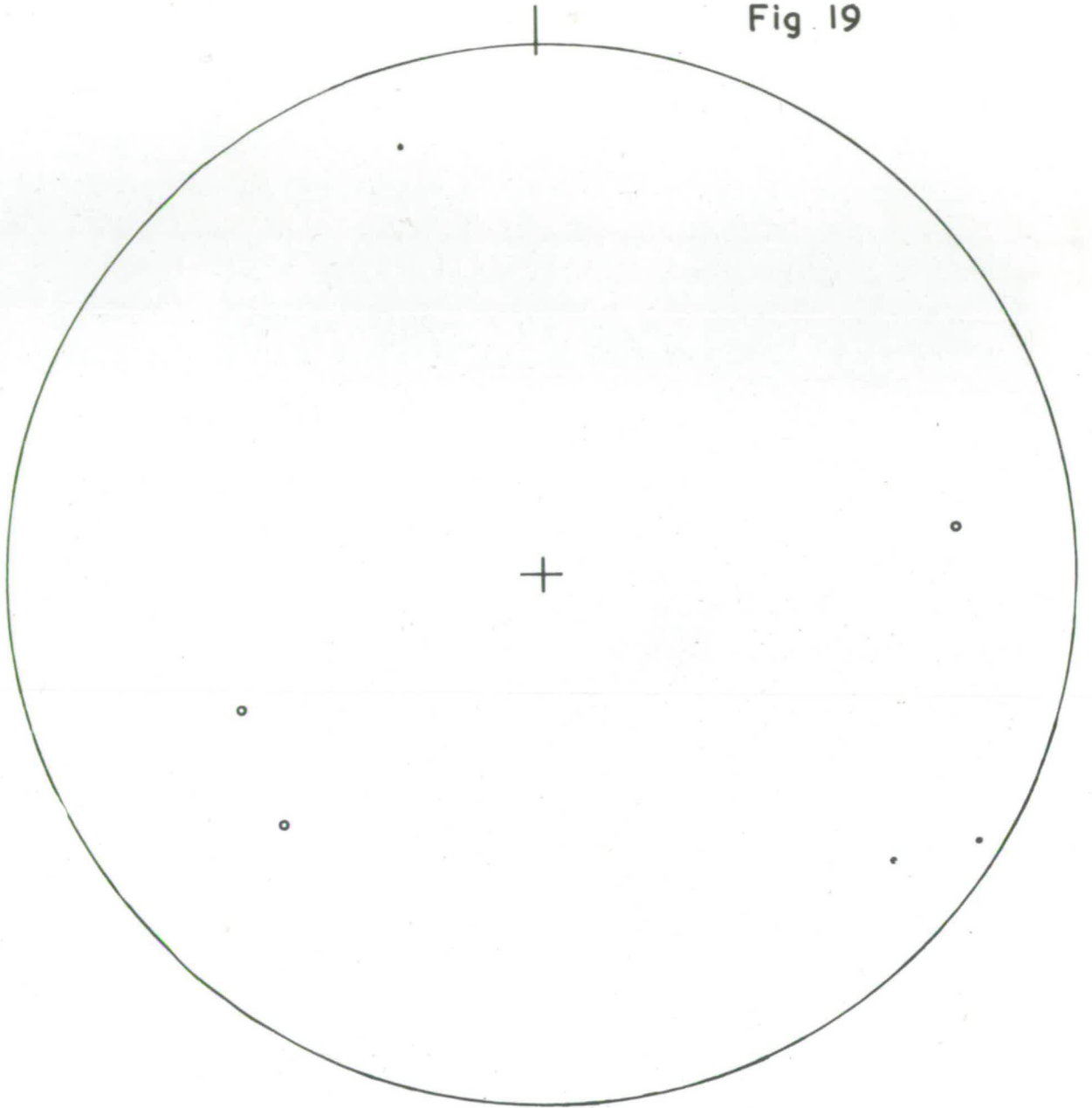
· Fold axis
° Poles to the axial plane

Stereogram of the minor structures of the
Second Movement Phase at Synberg

Fig 20
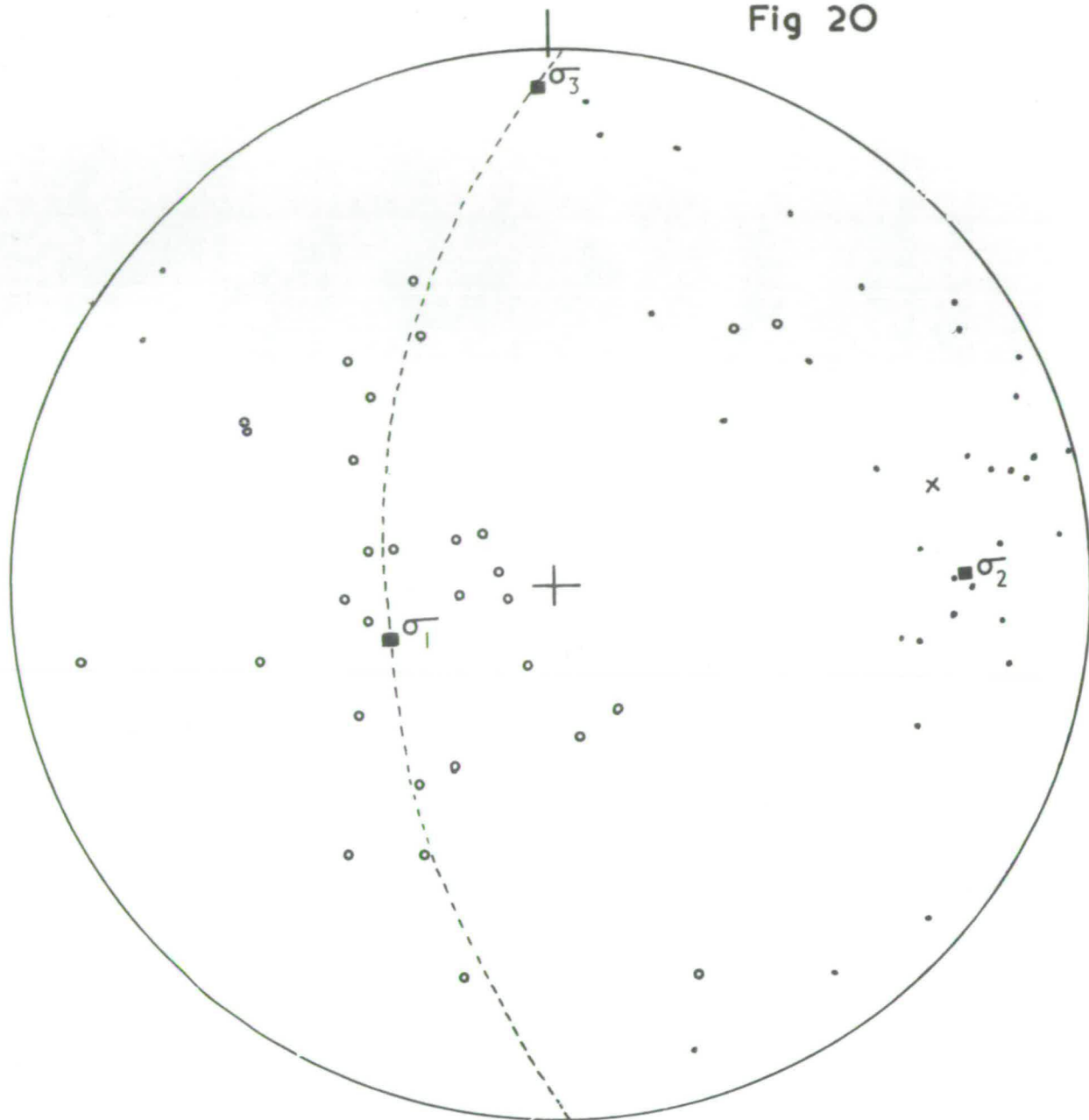
- Fold axes
- Poles to axial planes

S3 pole girdle
Stress axes

Stereogram of the minor structures of the Third
Movement Phase at Synberg

misinterpreted, the micas could have crystallized during a pre-B1 movement phase (e.g. during the thrusting of the Lower Jotun Nappe).

(b) Second movement phase (B2).

Only three folds of this movement phase were mapped at Synberg (Fig. 19). They are tentatively correlated with B2 at Bygdin because of a similarity of style to the B2 folds of Bygdin.

(c) Third movement phase (B3).

The B3 folds at Synberg have a comparable style, symmetry and orientation (with axes varying in trend from north-south to southeast-northwest to the B3 folds at Bygdin. S3-poles are spread into a girdle distribution with a girdle axis plunging at 25° to the east (Fig.20). This girdle pattern suggests that the Synberg B3 folds have a regional conjugate symmetry and are in fact equivalent to the B3 folds at Bygdin. A stress analysis of B3 gives the same result as that for Bygdin and are plotted with the Bygdin stress axes in Fig.15.

Fig 21

B2 Antiform

B2 Synform

Axial plane traces of the B2 major folds in
the Bygdin area
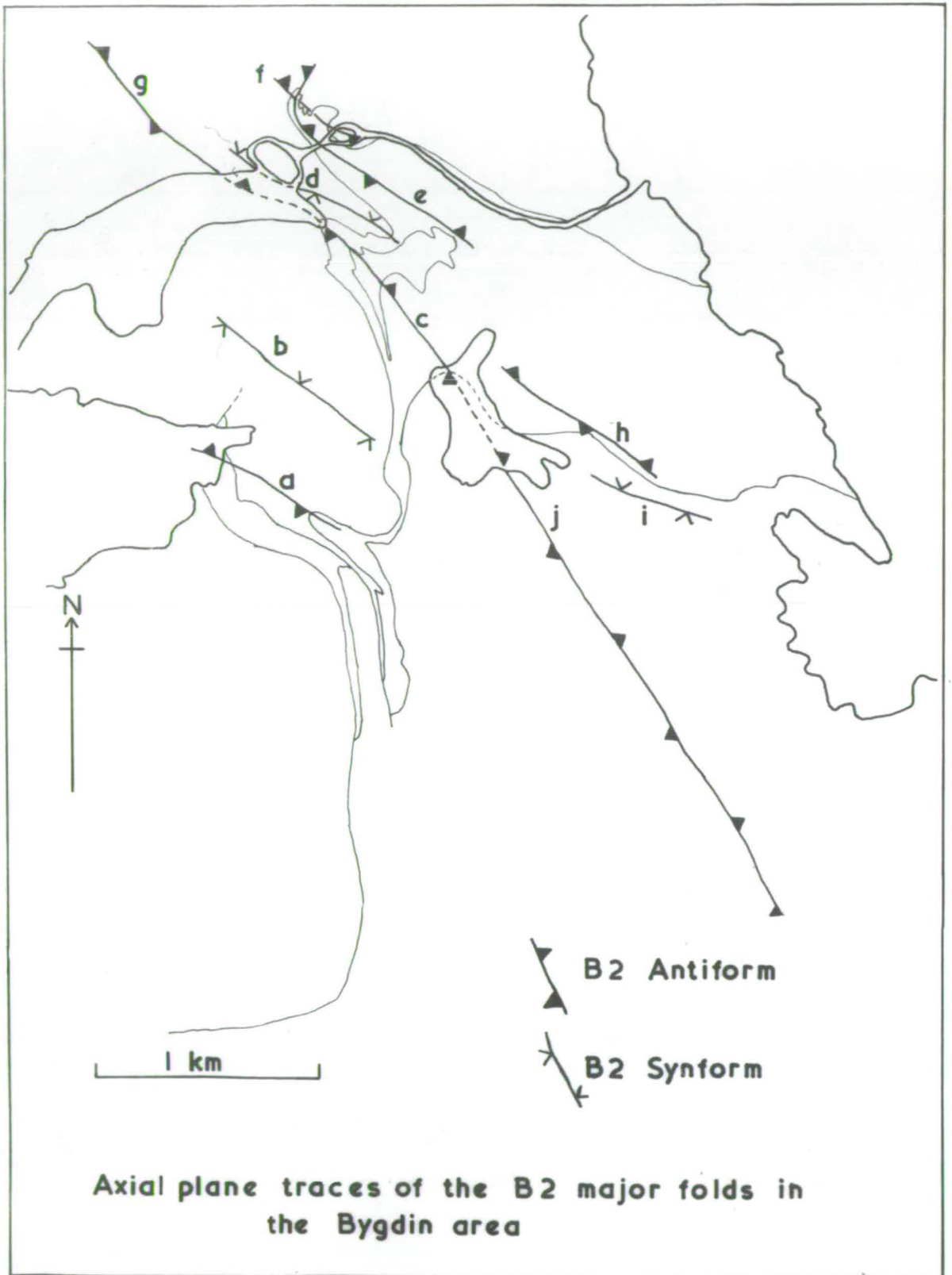
III.   MAJOR STRUCTURE

1.   INTRODUCTION

The only major structures recognised at Bygdin were formed during the first and second movement periods.   The major structure of the first movement period is the basal thrust zone of the Upper Jotun Nappe.   The major structures of the second movement period are northwest trending antiforms and synforms (Fig.21).

2.   BASAL THRUST ZONE

In the extreme southwest of the area (Map I) the thrust zone is defined by a clean cut thrust at the base of the gabbro.   Here the thrust has a northeast strike (at 059°) with a dip varying between 14° and 47° to the northwest.   The change in trend of the thrust trace, from east-west to north-south in crags just southeast of the Bitihorn summit is purely a result of topography.   Phyllonitic rocks are absent below the Bitihorn where instead the rocks only show slight crushing.   Most of the original igneous textures of the gabbro are retained to within a few metres of the thrust plane.

$1\frac{1}{2}$ km. north of the Bitihorn, the thrust plane at the base of the gabbro transgresses to a higher structural level and a second thrust plane continues north to define the basal thrust zone of the Jotun Nappe. A basal phyllonitized gabbro outcrops where the thrust plane at the base of the gabbro transgresses upwards. This is a fine grained foliated rock which can be traced upwards from the thrust for 10 metres and gradually passes into less cataclased gabbro. At the transgression, the trace

of the thrust plane swings round to a northwest trend due to refolding by antiform-a (Map II).   The thrust zone on the southwest limb of this antiform is composed of a series of thrust wedges which dip westwards below the gabbro. The structural sequence below the gabbro is -

    i)   Conglomerate wedge closing towards the north.

    ii) Granite sheet wedging out towards the south.

    iii) Conglomerate and sparagmite.

The granite and gabbro probably form two separate thrust sheets (p. 9) separated by the conglomerate wedge.   The conglomerate wedge pinches out on the peninsula at the east end of Lake Bygdin.   The contact between the granite and gabbro to the north of this is not exposed but is probably a thrust zone.

The thrust at the base of the granite sheet (unit ii) can be traced north towards Bygdin defining the basal thrust zone of the Jotun Nappe. Near the Bygdin Hotel, the thrust is folded about major antiforms of the second movement phase (Map III).   This folding has produced steep or inverted dips in the thrust plane.   On the northeast limb of the antiforms, the thrust plane trace continues southeast into Lake Vinstri.   The strike here is northwest with steep dips of 60° to 70° to the northeast.

A basal zone of phyllonite is present in the granite just above the thrust plane, and can be traced from the thin granite wedge on the west limb of antiform-a, round the antiforms at Bygdin towards Lake Vinstri. The phyllonites vary in thickness from one metre in the core of antiform-a to 100 metres at Bygdin.   In addition to the basal phyllonite zone,

extensive phyllonite horizons are exposed up to 400 metres above the thrust plane to the north and northeast of Bygdin (Map I).

Five thin slices of cake-conglomerate occur within the nappe to the north and northeast of Bygdin. Three slices lie between 5 and 20 metres above the thrust plane in the nose of the antiformal structures at Bygdin (Map III).   The other two slices are structurally about 300 metres above the basal thrust plane on the northeast limb of the antiforms. They are regarded as slices picked up during thrusting rather than fold cores, because the structural data do not indicate closures.

The thrust plane trace reappears on the north side of Lake Vinstri on the Barnesodden peninsula and is only exposed in one outcrop to the northeast of the peninsula.

Throughout the whole area, the conglomerate and sparagmite just below the thrust plane have not been cataclased to mylonitic rocks. Although deformed, the sediments still retain their identity.

In the thrust zone near the Bygdin Hotel some intermixing of conglomerate and igneous rocks has taken place.   Thin bands of blue hornblende phyllonite (derived from igneous rocks) up to 10 cm. thick, can be found within the conglomerate near the thrust plane. (Plate 10, b). In addition, within the phyllonite above the thrust plane small fragments of deformed conglomerate pebbles can be found (Plate 10, a). As recognised by Flinn (1961), the thrust near the Bygdin Hotel is not clean cut, but is defined by a lithological break rather than an obvious tectonic break.

Exposures where the thrust plane truncates the S1 foliation have already been mentioned (p. 19).   In several outcrops on the Bitihorn

gabbro

T ——— T

conglomerate

VERTICAL
SECTION

10 m
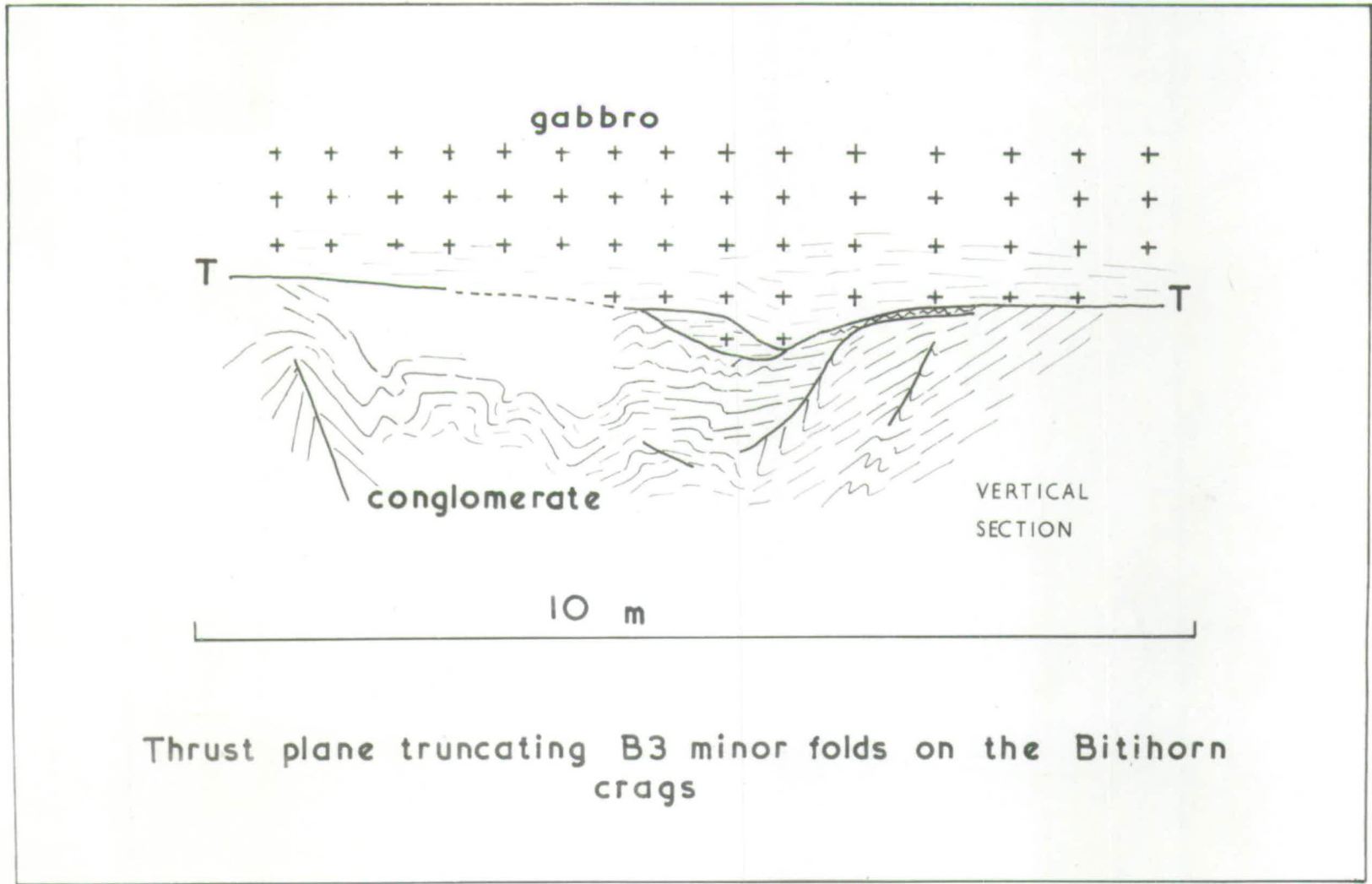
Thrust plane truncating B3 minor folds on the Bitihorn
crags

Fig 22

TABLE 2

Fold	Axis trend/plunge	Axial plane strike/dip	Dip of SW limb	Dip of NE limb	Remarks
Antiform-a	310°/12° NW	305°/68° NE	60°-80° to SW	20° to NE	Asymmetric, disharmonic. Refolds thrust plane and minor B2 folds.
Synform-b	310°/10° NW	300°/60° NE	20° to NE	40°-50° to SW	Disharmonic, no minor folds.
Antiform-c	310°/10° NW	305°/80° NE	20° to SW	20° to NE	Symmetrical. Folds thrust plane. Minor folds on both limbs. Part of the Bygdin Antiform.
Synform-d	315°/20° NW	303°/75° NE	20° to NE	75° to NE	Disharmonic. NE limb inverted. Refolds thrust plane. Minor folds on both limbs.
Antiform-e	314°/12° NW	310°/70° NE	Both limbs dip at 70° to NE		Asymmetric. SW limb inverted. Disharmonic. Folds thrust plane on major and minor scale.
Antiform-f	310°-315°/ 15°-18° NW	310°-315°/ 50° NE	70° to NE	40° to NE	Disharmonic. Asymmetric. SW limb inverted. Refolds Antiform-e.
Antiform-g	320°/40° NW	330°/75° SW	30°-40° to SW	40°-50° to NE	Disharmonic. No minor folds. Part of the Bygdin Antiform.
Antiform-h	319°/8° NW (S. part)	320°/85° NE (S.part)	20°-30° to SW	20°-30° to NE	Symmetrical in the south but overturned at the northern end. Minor folds on SW limb.
		320°/65° SW (N.part)	30° to SW	90°	
Synform-i	326°/18° NW	330°/75° SW	30° to NE	20° to SW	Open warp. No minor folds.
Antiform-j	328°/14° NW	330°/85° SW	15°-20° to NNW	20°-30° to NE	Disharmonic. Very open in the lower structural levels. Part of the Bygdin Antiform.

DESCRIPTION OF THE MAJOR SECOND FOLDS OF THE BYGDIN AREA

crags, the thrust plane was found to truncate B3 folds (Fig.22). This indicates
that the Bitihorn gabbro has undergone a post-B3 phase of thrusting. This
late movement could be a result of readjustment along the thrust plane
during a late phase of the third movement period. This rejuvenation is
similar to that reported by Christie (1963) in the Moine Thrust zone.
However, kakirites or secondary mylonites are absent on the Bitihorn.

3. MAJOR SECOND FOLDS

Ten major B2 folds are recognised in the area. The axial plane
traces of the folds (a-j, Fig.21) have been determined using changes in
the shape of B2 minor folds and by major swings in the strike and dip of
S1. Three of the antiforms (g, c and j) are part of one large antiform
(the Bygdin Antiform) but have been separated for the purposes of description.
These major folds are described in Table 2.

Apart from the Bygdin Antiform, the folds can be followed for a
short distance only. The Bygdin Antiform is quite disharmonic when traced
from the lower structural level in the south of the area towards Bygdin.
The antiform in sub-area 4 is quite open with dips of 15°-30° on each limb.
However, in the area of traces c and g, the limbs dip more steeply with dips
of up to 80°. All other major folds in the Bygdin area are major parasitic
folds (de Sitter, 1958) on the limbs of the Bygdin Antiform.

The refolding of antiform-e by antiform-f will now be discussed.
(Map III). The trace of e can be followed northwest from the small tarns
to the northeast of Stavtjern, passing northeast of the Bygdin Hotel.
On the northeast limb of e, just north of the Bygdin Hotel, the thrust

plane is folded about parasitic folds of antiform-e. The shape of these folds is consistent with the geometry of e. The trace then swings northeast to cross the trace of antiform-f. This refolding of e by f causes antiform-e to change from an upwards-closing fold (in the lower structural levels) to a side-ways closing fold (as it crosses the core of f).

Antiform-f is excellently exposed on the island in the outlet stream of Lake Bygdin and has a style and orientation similar to the B2 folds. In addition, the parasitic folds on the limb of antiform-f are refolded by minor B3 folds (Fig.9). It is tentatively suggested that antiform-f is of B2 age and that it has refolded antiform-e during a later phase of the second movements. The causes of this refolding may be similar to those discussed by Wynne-Edwards (1963, pp. 810-811). Wynne-Edwards suggested that refolding produced during a single movement phase could be broughtabout by unsteady flow in the rocks. This unsteady flow could be the result of varying strain rates in a direction parallel to the axial plane or by a change in the direction of flow. In the first case, if an anticline advanced at a greater rate than the adjacent syncline, the unsteady flow would be relieved by material crossing the flow planes (parallel to the axial planes). Folds adjacent to the anticline might then curl over the anticline into the syncline to produce refolded folds (ibid p.807).

In the second type, fluctuations in the flow direction might cause the flow direction to become oblique to the axial planes causing refolding (ibid, p.809).

The refolding of B2 minor folds by antiform-f gives the partial girdle of plotted S2-poles for sub-area 3. (Fig.2).

Refolding of second minor folds by a later major second fold is also present in antiform–a. The poles of minor S2 planes are distributed in a girdle with an axis parallel to the axis of antiform–a. This refolding is probably analogous to the refolding in antiform–f.

No major folds are recognised to the east of Bygdin. The Vinstri area is not folded on the major scale and has a regional dip of 20°–30° to the northeast. Girdle distributions developing from point concentrations of S1 poles in sub-areas 5, 6, 9 and 10 (Fig.2) are a result of B2 minor folds.

In addition no major folds are recognized in the Synberg area.

Major third folds are absent in the area. However a plunge culmination of B1 and B2 axial structures exists in the conglomerate 1 km. southeast of Bygdin. To the north of the culmination, B1 and B2 axes plunge northwest and to the south the axes plunge southeast. This culmination has a north or northeast trend which suggests that the culmination may be a result of the third movement phase.

IV. METAMORPHIC HISTORY

The metamorphic history will only be described briefly to indicate the metamorphic effects of the movement phases at Bygdin. Strand (1945) and Flinn (1961) have already described briefly the constructive and destructive effects of the large scale thrusting of the Upper Jotun Nappe.

The effect of thrusting on the igneous rocks of the nappe was largely destructive, with phyllonitic and schistose rocks being derived from ?massive igneous rocks. The amphibolite facies of the granitic rocks has been partly retrograded to greenschist facies but the granulite facies of the gabbro is largely untouched. The greenschist metamorphism is defined by the growth of muscovite and biotite in the S1 foliation. In addition, porphyroblasts of epidote and sphene have crystallized. The hornblendes of the granites have been partly or completely decolourized suggesting that they have recrystallized to an amphibole of the Tremolite-Actinolite series.

The metamorphic effect on the sediments was largely constructive with the unmetamorphosed sediments being upgraded to greenschist facies. Biotites and muscovites have crystallized in the S1 foliation and prophyro-:blasts of epidote and sphene have formed. This metamorphism extends right down into the rocks of the Synberg section but appears to decrease in grade downwards as the only new minerals in the Lower Cambro-Ordovician sediments are biotites, muscovites and chlorites.

The greenschist metamorphism can be shown to pre-date the second movement phase as epidotes are bent and broken in B2 fold hinges.

Both the B2 and B3 movement phases were accompanied by the recrystallization of biotite and muscovite in the S2 and S3 foliations, but these are restricted and are obviously of a lower grade than the main greenschist facies metamorphism.

Fig 23

Location map of the pebble stations at Bygdin

Location map of the pebble stations at Olefjell   Fig 24
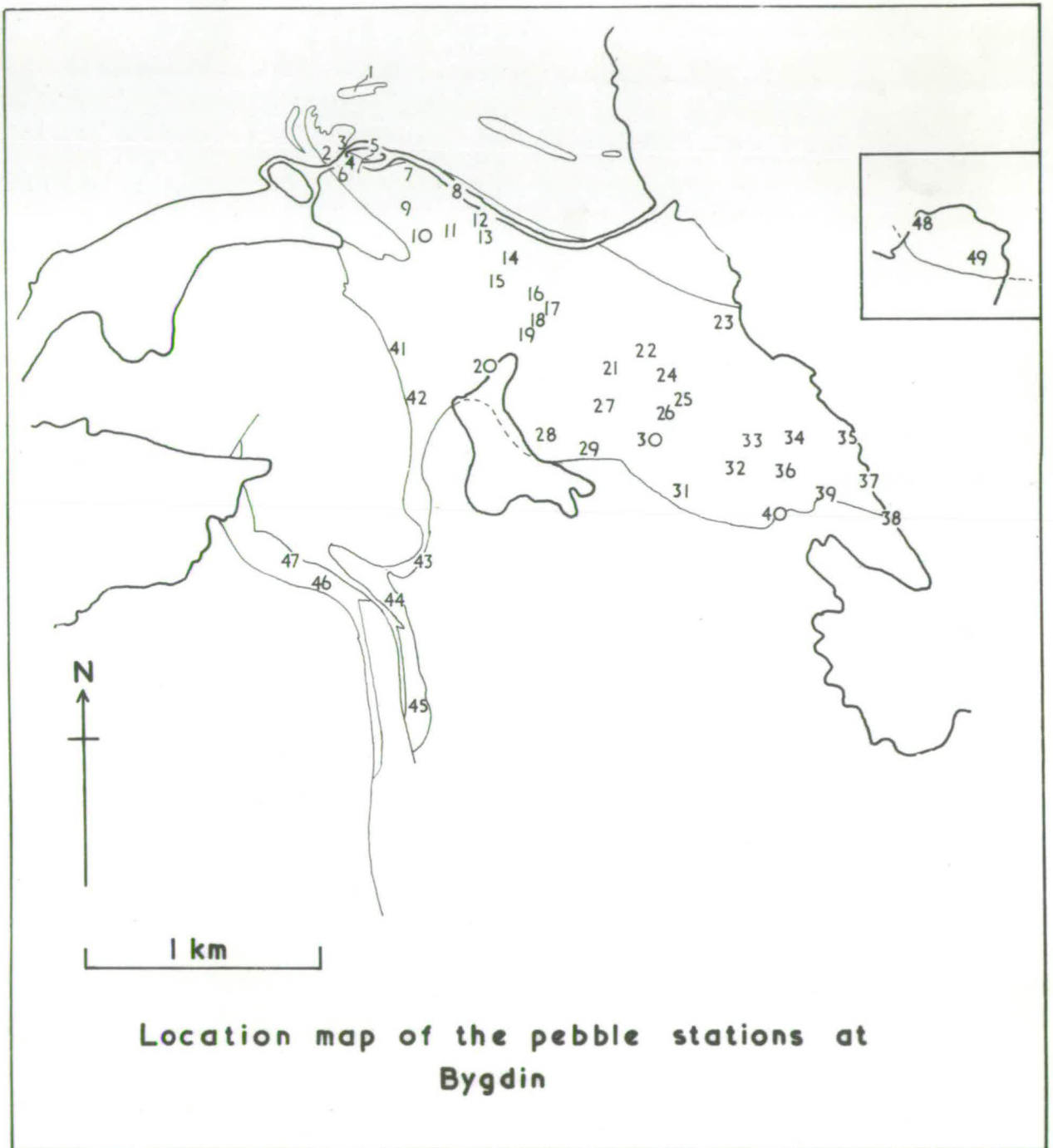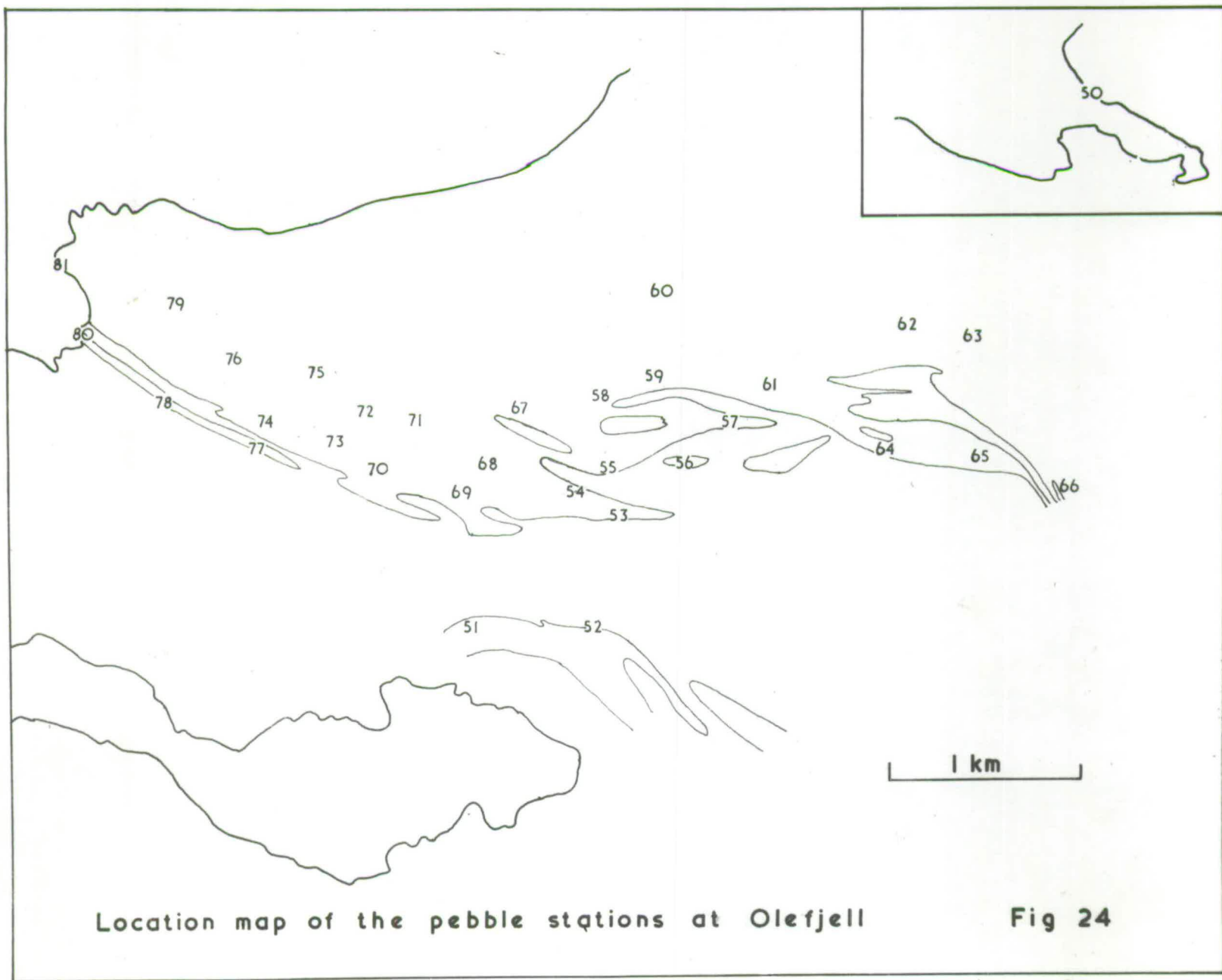
V. PEBBLE DEFORMATION

1. METHODS OF MEASUREMENT

Deformed pebbles were measured at 81 localities (or stations) in the conglomerate (Figs. 23 and 24). Because the pebbles could not be extracted, the axial ratios were measured along joint planes. Fortunately, joints approximately parallel to the principal planes of the pebble ellipsoids can be found at most localities. However, this method does not allow the three principal axes to be measured in any one pebble.

At each station 30 axial ratios were measured in each of two joint planes (c.f. Flinn, 1956) which were generally parallel to the XY and XZ sections of the pebble ellipsoids (Axial terminology of Flinn, 1962, used in this thesis). In some stations, however, measurements could only be made in the XY and YZ sections. A total of 60 measurements per station was possible in 72 stations. In the rest of the stations only a smaller sample number could be measured.

Measurements were taken only at stations where later folds are absent to try and eliminate the influence of later strains on the shape of the pebbles. This influence will be discussed later (pp. 57-60). In outcrops with folded pebbles, a visual estimation of pebble shape was used to construct maps displaying the distribution of pebble shapes (Figs. 33, 34 and 35).

2. STRAIN CALCULATIONS

The arithmetic average of the axial ratios in each of the two joint planes at a station was calculated and the axis common to both planes reduced to unity. The two axial ratios were then combined to give the

three axial ratios of the station.   Strain parameters based on these ratios
are given in Appendix A.

In the strain calculations, the initial shape of the pebbles was
assumed to be a perfect sphere and volume loss during deformation was
neglected.   Possible errors arising from these assumptions are discussed
later.

The three principal strains (corresponding to those along the
X, Y and Z ellipsoid axes) were first calculated in the <u>Conventional Strain</u>
<u>Unit</u> ($\in$).

$$\in = \frac{1 - l_o}{l_o}$$

where l = length after strain

l_o = length before strain

(Nadai, 1950, p. 70)

With the advice of Dr. T.C. Hsu of the Mechanical Engineering Dept.
at Edinburgh University, the Conventional Strain Units were converted to
logarithmic strain units, <u>Natural Strain</u> ($\overline{\in}$).

$$\overline{\in} = \log_e (1 + \in) = \ln (1 + \in) \qquad \text{(Nadai, 1950, pp.73-74)}$$

From the three principal natural strains at each station
($\overline{\in}_1, \overline{\in}_2, \overline{\in}_3$), strain parameters determining the <u>amount</u> and <u>symmetry</u> of strain
were calculated.

They are -

      a) Natural octahedral unit shear ($\overline{\in}_S$)

      b) Lode's Unit (v)

(a) Natural octahedral unit shear (ϵ_S)

This is a measure of the amount of shear along an octahedral plane, where the axes of the regular octahedron are parallel to the principal strains. The unit shear along this octahedral plane is an absolute measure of the <u>amount</u> of distortional strain in any deformation of any symmetry and can be used to compare the amount of distortional strain in the rod and cake conglomerates.

$$\bar{\varepsilon}_S = \frac{1}{\sqrt{3}} \sqrt{(\bar{\varepsilon}_1 - \bar{\varepsilon}_2)^2 + (\bar{\varepsilon}_2 - \bar{\varepsilon}_3)^2 + (\bar{\varepsilon}_3 - \bar{\varepsilon}_1)^2}$$ (Nadai, 1963, pp.44-47).

Nadai (1963, p.47) gives a different constant (2/3) to that used by the writer. This, however, does not affect the comparative use of this measurement.

An important property of $\bar{\varepsilon}_S$ is that it is directly proportional to the amount of work (ω) applied in the distortional component of strain.

$$\omega = \frac{3}{2} \int_0^{\bar{\varepsilon}_S} \tau_o \, d\bar{\varepsilon}_S$$

τ_o - octahedral shearing stress.

$d\bar{\varepsilon}_S$ - incremental octahedral unit shear.

(Nadai, 1963, p.47).

Theoretically, strains with equal $\bar{\varepsilon}_S$ values have had the same amount of mechanical energy expended in the distortional deformation, provided the simplest path possible is taken in the deformation (Nadai, 1963,

footnote to p.73). $\bar{\mathcal{E}}_S$ does not give any indication of the amount of rotational strain in the deformation.

(b) Lode's unit (v)

This is a measure of the symmetry of strain and is equivalent to Flinn's k-value (Flinn, 1962, p.388).

$$\nu = \frac{2\bar{\mathcal{E}}_2 - \bar{\mathcal{E}}_1 - \bar{\mathcal{E}}_3}{\bar{\mathcal{E}}_1 - \bar{\mathcal{E}}_3}$$

(Lode, 1926, p.932).

V-values range from -1,0 (pure tension) to +1,0 (pure flattening).

pure tension $(k = \infty)$	pure shear $(k = 1)$	pure compression $(k = 0)$
v = -1,0	v = 0	v = +1,0

However, unlike Flinn's k-value, v in a simple deformation of the type discussed by Ramsay (1964), does not change in value during the deformation. During a progressive deformation, each incremental stage in the deformation can be represented as a point on the deformation plot (Flinn, 1962, p.336). The locus of points represents the deformation path. Ramsay (1964) has shown that deformation paths representing the simplest types of deformation are curves of the type $a = b^{\log a' / \log b'}$. Now Flinn's symmetry measurement, k, is defined essentially by the slope of the line from the origin of the deformation plot through any one point on the deformation path. Thus on

Fig. 25. Geometry and derivation of the strain plane.

a) Orthogonal system of $\bar{\epsilon}$ axes which are projected parallel to the space diagonal (OP) on to the plane $\bar{\epsilon}_1 + \bar{\epsilon}_2 + \bar{\epsilon}_3 = 0$.

b) The projected strain plane with coplanar axes of pure tension (T), pure compression (C), and pure or simple shear (S).

Fig 25
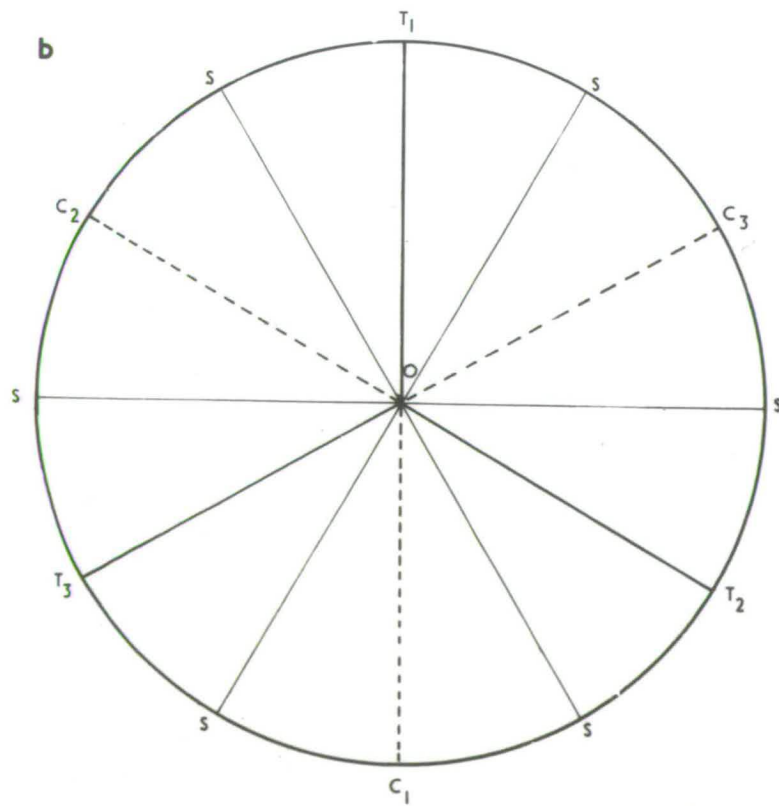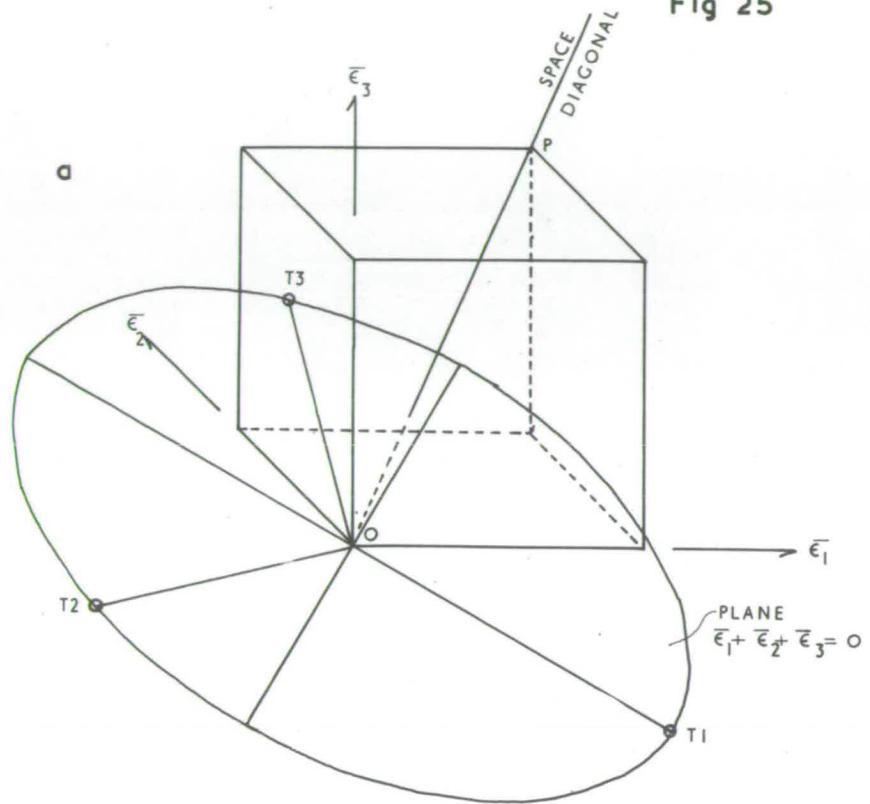
on a curved deformation path, $\underline{k}$ must change in value along the deformation path.

However, on a logarithmic plot, Ramsay's deformation paths plot as straight lines and thus $\underline{v}$, because it is based on a logarithmic strain unit, does not change in value during deformation. In a progressive deformation in which the stresses do not change in value or orientation and the minimum amount of work is applied in the deformation, $\underline{v}$ will determine the symmetry of the incremental strain ellipsoid (i.e. the constant ellipsoid which is added on at each incremental stage in the deformation) rather than the symmetry of the ellipsoids which result from the addition of the incremental strain ellipsoid. In geological strains, however, where the above conditions do not necessarily hold (and where the incremental strain ellipsoid may not have a constant shape throughout the deformation), the use of $\underline{v}$ to denote strain symmetry will not have any advantage over Flinn's $\underline{k}$-value.

3. PLOTTING OF DATA

States of strain may be plotted in a three dimensional space defined by orthogonal axes of $\bar{\mathcal{E}}_1$, $\bar{\mathcal{E}}_2$, and $\bar{\mathcal{E}}_3$ (Fig.25). In practice, this three dimensional space is projected on to the plane $\bar{\mathcal{E}}_1 + \bar{\mathcal{E}}_2 + \bar{\mathcal{E}}_3 = 0$ and is termed the strain plane (Nadai, 1963, pp.70-76). This strain plane lies normal to the space diagonal (OP) of the three dimensional space (where $\bar{\mathcal{E}}_1 = \bar{\mathcal{E}}_2 = \bar{\mathcal{E}}_3$) and cuts the diagonal at the origin (Fig.25). Sequences of simple tension, compression, and of pure shear are

Fig. 26.   The strain plane and the deformation plot.

a) The strain plane with coordinates

$\bar{\epsilon}_1, \bar{\epsilon}_2, \bar{\epsilon}_3$.
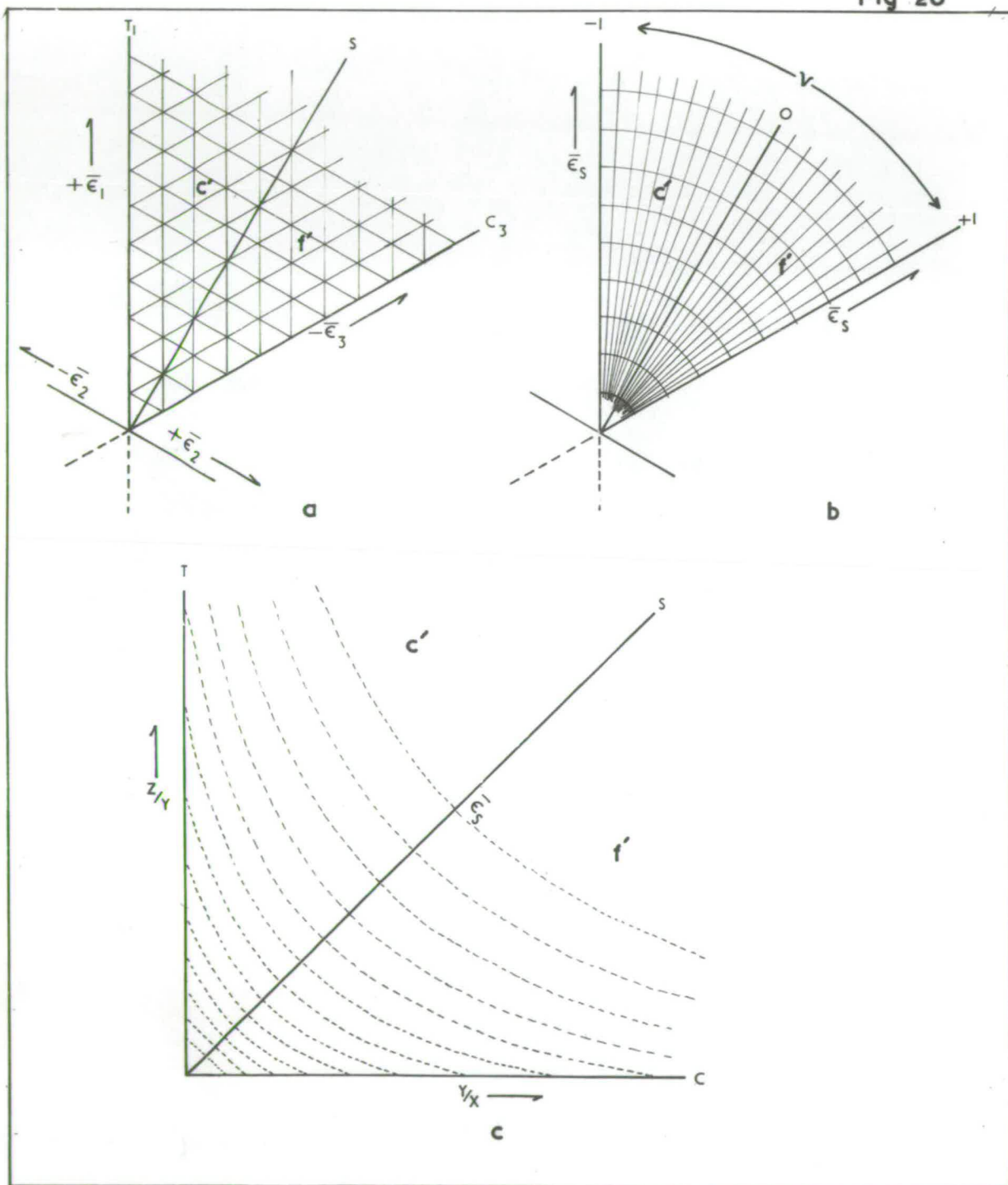
b) The strain plane with coordinates

$\bar{\epsilon}_S, \upsilon$.

c) Flinn's deformation plot with lines

of equal distortional strain $(\bar{\epsilon}_S)$.

f Field of flattening

c Field of constriction

Fig 26

a

b

c

represented in this strain plain by 6 coplanar straight rays making equal angles
with each other (Fig.25). A deformation path representing one of the above
types of deformation will start at the origin and follow one of the 6 coplanar
rays. States of strain with symmetries intermediate to the above types will
plot as points between the 6 rays.

For geological strains, only one 60° segment is required to plot
all types of strain if it is assumed that $\overline{\epsilon}_1 > \overline{\epsilon}_2 > \overline{\epsilon}_3$. Two methods of
plotting geological strains on the strain plane can be used. For the first
type, a petrological triangular diagram may be used with the origin of the
plot at one of the apices of the triangle (Fig.26). States of strain are
represented by the coordinates $\overline{\epsilon}_1, \overline{\epsilon}_2, \overline{\epsilon}_3$.

In the second type, at 60° segment of a polar diagram may be used
(Fig.26). States of strain are represented by the coordinates $\overline{\epsilon}_S, \upsilon$, (which
are of course based on $\overline{\epsilon}_1, \overline{\epsilon}_2, \overline{\epsilon}_3$). The locus of points of equal υ-values
are straight lines radiating from the origin, and the locus of points of equal
$\overline{\epsilon}_S$-values are concentric circles centred on the origin. A single state of
strain will plot at the same point in both diagrams.

The strain plane is completely analogous to Flinn's deformation
plot (Flinn, 1962, pp. 336-338) as the fields of flattening and constriction
lie on either side of the line of pure shear. The strain plane rather than
the deformation plot is used because the simplest deformation paths plot as
straight lines on the strain plane. Curved deformation paths will result
if the stresses change in value or orientation during the deformation. In
addition, the deformation plot is distorted with respect to the amount of
distortional strain. Points of equal $\overline{\epsilon}_S$ do not lie equidistant from the
origin like points on the strain plane (Fig.26) but lie on hyperbolae (Fig.26,c).

WRT what coordinates?

A projection diagram similar to the strain plane can be constructed to represent states of stress (Nadai, 1963, pp. 71-72). This is the stress plane in which a three dimensional space represented by orthogonal stress axes $(\sigma_1, \sigma_2, \sigma_3)$ is projected on to the plane $\sigma_1 + \sigma_2 + \sigma_3 = 0$. As all points along the space diagonal have $\sigma_1 = \sigma_2 = \sigma_3$ (i.e. a state of hydrostatic stress), the projection of points on to the stress plane parallel to the space diagonal effectively removes the hydrostatic component of stress. All points on the stress plane represent the deviatoric component of stress $(\sigma_1', \sigma_2', \sigma_3')$.

4. FACTORS INFLUENCING THE SHAPE OF STRAINED PEBBLES.

The measured axial ratios of deformed pebbles do not give the true value of the strain in the pebbles, because the final shape is influenced by factors other than that of strain (Higgins, 1964). The ratios are influenced by -

(a) Errors of measurement.

(b) Variation of pebble composition.

(c) Variations of the original shape of the pebbles and orientation to the stress axes.

(d) Volume loss during deformation.

(e) Effect of repeated deformation.

(a) Errors of measurement

Pebble axial ratios were measured as accurately as possible with callipers. On the advice of Flinn, 30 ratios were measured in each of two

Fig. 27.   Deformed pebbles lying in the S1 foliation at
           Olefjell.

           The Z axes of the pebbles have a variation in
           orientation but the fine B1 rodding lineation
           (which may be parallel to the Z axis of the
           strain ellipsoid) has a constant orientation.

Fig 27

15 cm

15 cm
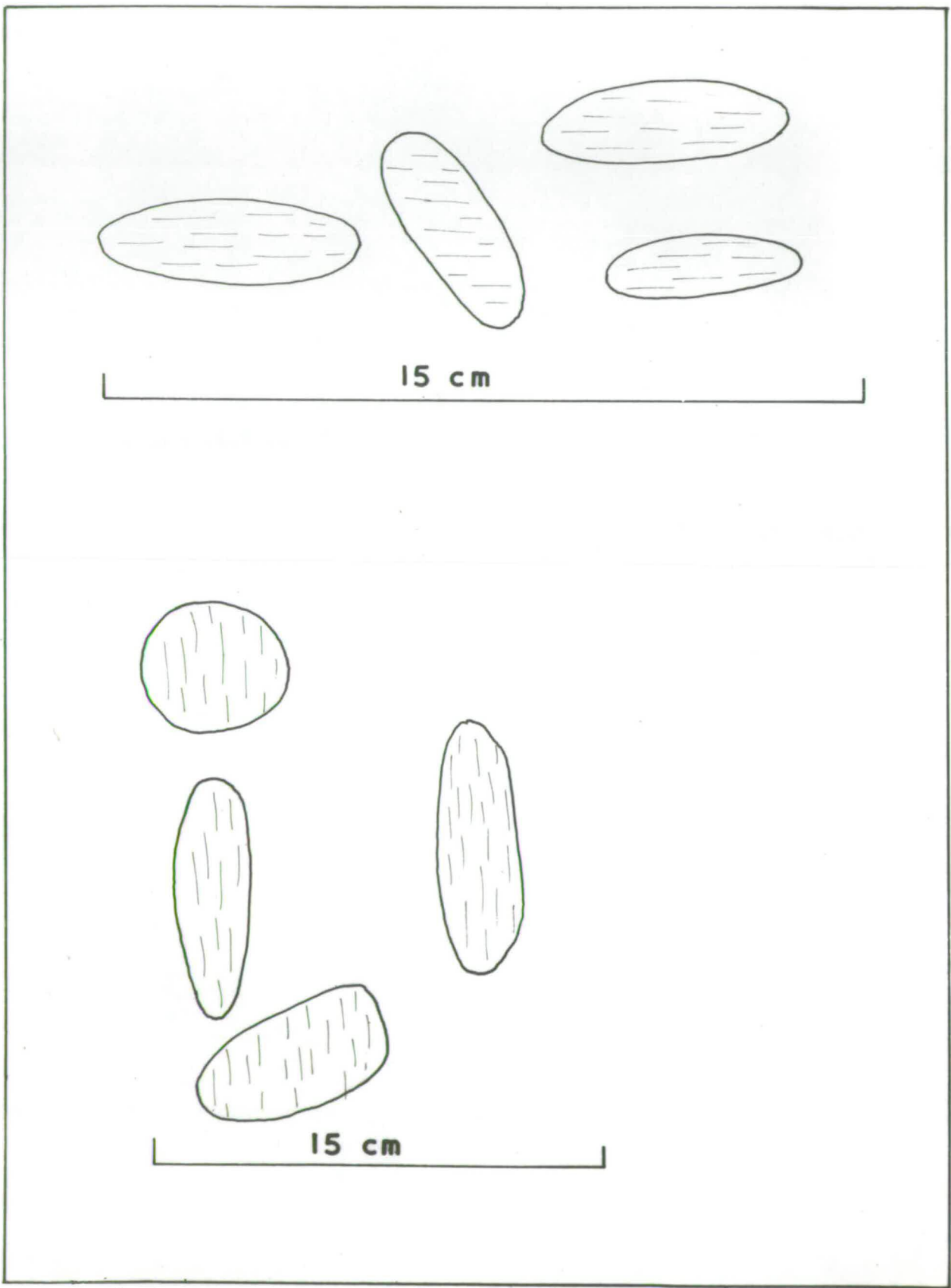
Fig. 28   Superposition of a strain on an ellipsoid
           pebble where the stress axes are not parallel
           to the pebble axes.

           The Z axis of the pebble after deformation is
           parallel to neither the Z axis of the initial
           pebble shape nor the Z axis of the true strain
           ellipsoid.

Fig 28

ϵ_3

ϵ_1

ϵ_3

ϵ_1

Pebble before deformation

True strain ϵ_1 +100 %
ϵ_3 −50 %

Apparent strain in the pebble after deformation
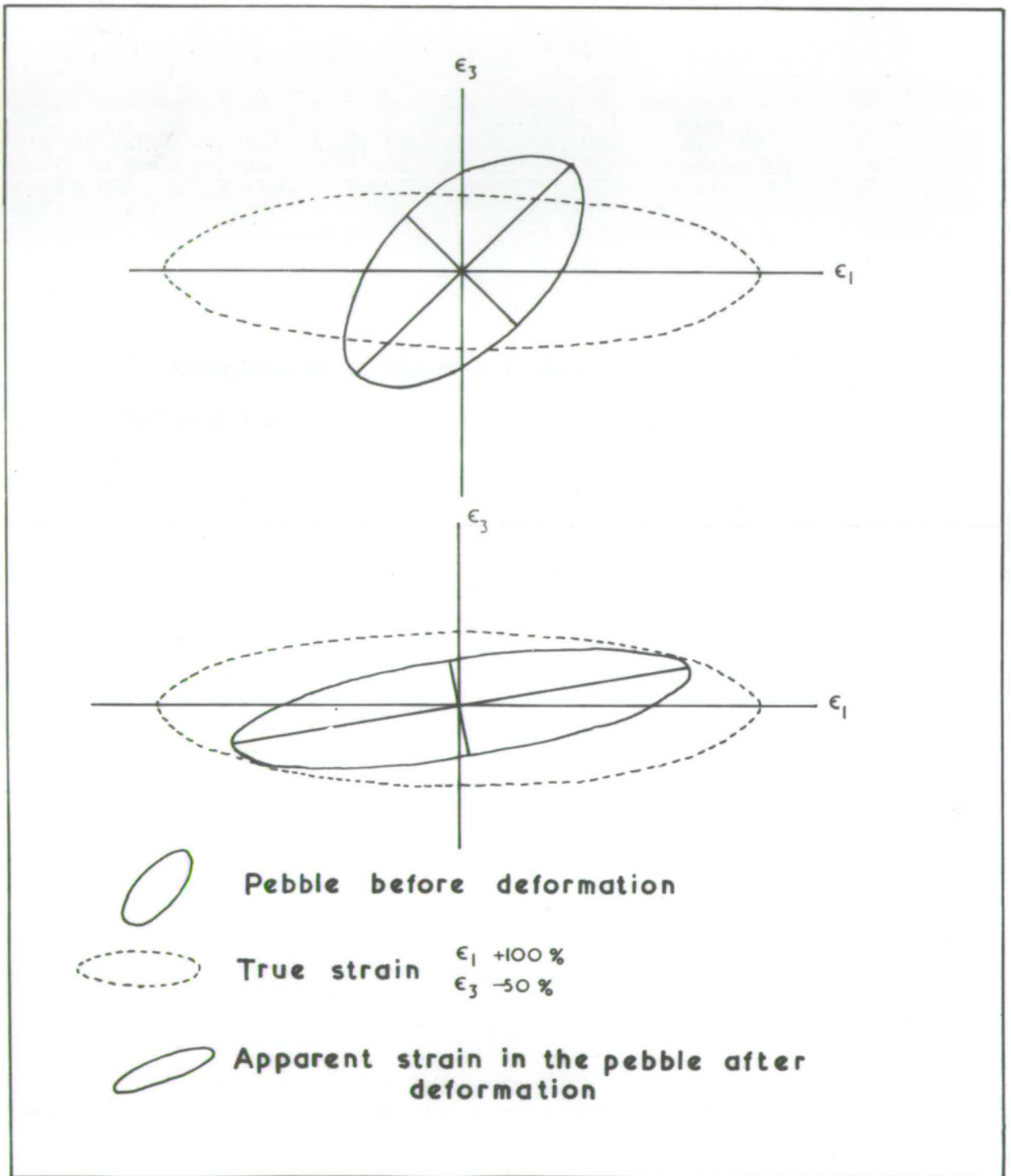
joint planes at a station. In order to determine whether 30 measurements were sufficient to define the average axial ratio along any one joint plane, a comparison was made between the average calculated from 30 measurements and that calculated from over 1,200. The comparison was made on the X/Y ratio at station 20 and the error calculated at $\pm$ 1,8%. A sample of 30 measurements is thus sufficient to define quite accurately the average axial ratio of the ellipsoid sections on the joint planes.

However, an error might result if the sections through the pebbles on the joint planes are not parallel to the principal planes of the pebble ellipsoids. Such deviations could be caused either by variations in the orientation of the joint planes or by an independent variation in the orien- :tation of the pebbles. This error is probably quite small at Bygdin because most of the pebble axes are parallel to one another and joint planes can be found within 5° of the principal planes of the pebbles. However, in some YZ sections at Olefjell, the long axes of the pebbles have a large variation in orientation about the Bl lineation (Fig.27). This is a result of the super- :position of a tectonic strain ellipsoid upon a pre-deformation sedimentary ellipsoid shape where the two ellipsoids are not parallel (Fig. 28). The resultant post-deformational ellipsoid is parallel to neither the initial sedimentary ellipsoid shape or the true strain ellipsoid. Thus a tectonic strain superposed on initial sedimentary ellipsoid pebbles which have no preferred orientation of axes, will result in a variation in orientation of the axes of the deformed pebble ellipsoids. Very large deformations will be required to bring initially disorientated axes into parallelism. The pebbles at Olefjell may have had a random (or near random) orientation of predeformation Z-axes in the YZ tectonic plane.

In order to reduce possible errors, measurements at Olefjell were taken in the YZ plane where possible, irrespective of the orientation of the Z-axes. However, measurements in the other plane (e.g.) XY will be in error because many of the ellipsoid sections are not parallel to the principal planes. The amount of this error is unknown because of the lack of pebble orientation data in any one station.

(b) Variation of pebble composition

Compositional variation between pebbles will cause the viscosity to vary between pebbles during the deformation. Viscosity differences probably give rise to varying strain rates and thus pebbles of differing compositions may not have the same shape at the end of deformation even if they were part of the same stress field. This is not an important problem at Bygdin because over 95% of the pebbles are almost pure quartzite and only quartzite pebbles were measured. During the pebble deformation, most of the pebbles probably had the same viscosity.

(c) Variation of original pebble shape and orientation.

This factor probably gives the largest errors encountered in measuring deformed pebbles. The writer's strain calculations are based on the assumption that the original pebble shape was a perfect sphere. However, the pebbles of most undeformed conglomerates do not have spherical shapes but are ellipsoids. This error is much larger than has been supposed in the past (Higgins, 1964). In addition, the orientation of the principal axes of the undeformed pebble ellipsoids with respect to the stress axes

Fig. 29.   Fields of error of strain measurement in deformed

pebbles calculated by Higgins (1960, Fig. 101)

replotted on the strain plane.

The fields are derived by superposing a single state

of strain on an initial ellipsoid shape of 4/3/2.   The

strain can be superposed in 6 different orientations so

that the strain axes are parallel to the initial shape

axes.   This provides 6 different final shapes which

define the field of error.   3 separate two-dimensional

strains corresponding to elongations of 50%, 66,6% and

75%, are superposed.

Fig 29
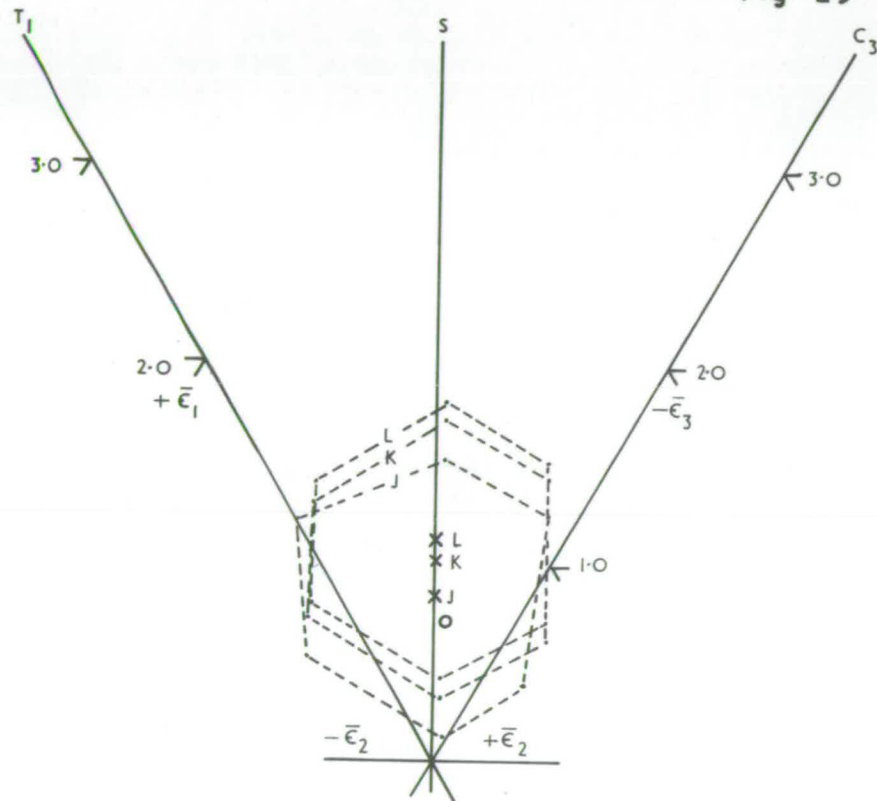
o Initial pebble shape
$X/Y/Z = 4/3/2$

× Superposed two dimensional strain

J 50% ELONGATION
K 66·6% ELONGATION
L 75% ELONGATION

Field within which final shape
may lie

Fig. 30.   Fields of error of strain measurement in deformed

pebbles calculated by Higgins (1964, Fig. 103)

replotted on the strain plane.

The fields of error are derived by superposing three-

dimensional strains on an initial pebble shape of 4/3/2.

The strains are -

	$\bar{\epsilon}_1$	$\bar{\epsilon}_2$	$\bar{\epsilon}_3$
1)	+1,39	−0,69	−0,69
2)	+1,1	−0,41	−0,69
3)	+0,41	+0,23	−0,61

Fig 30
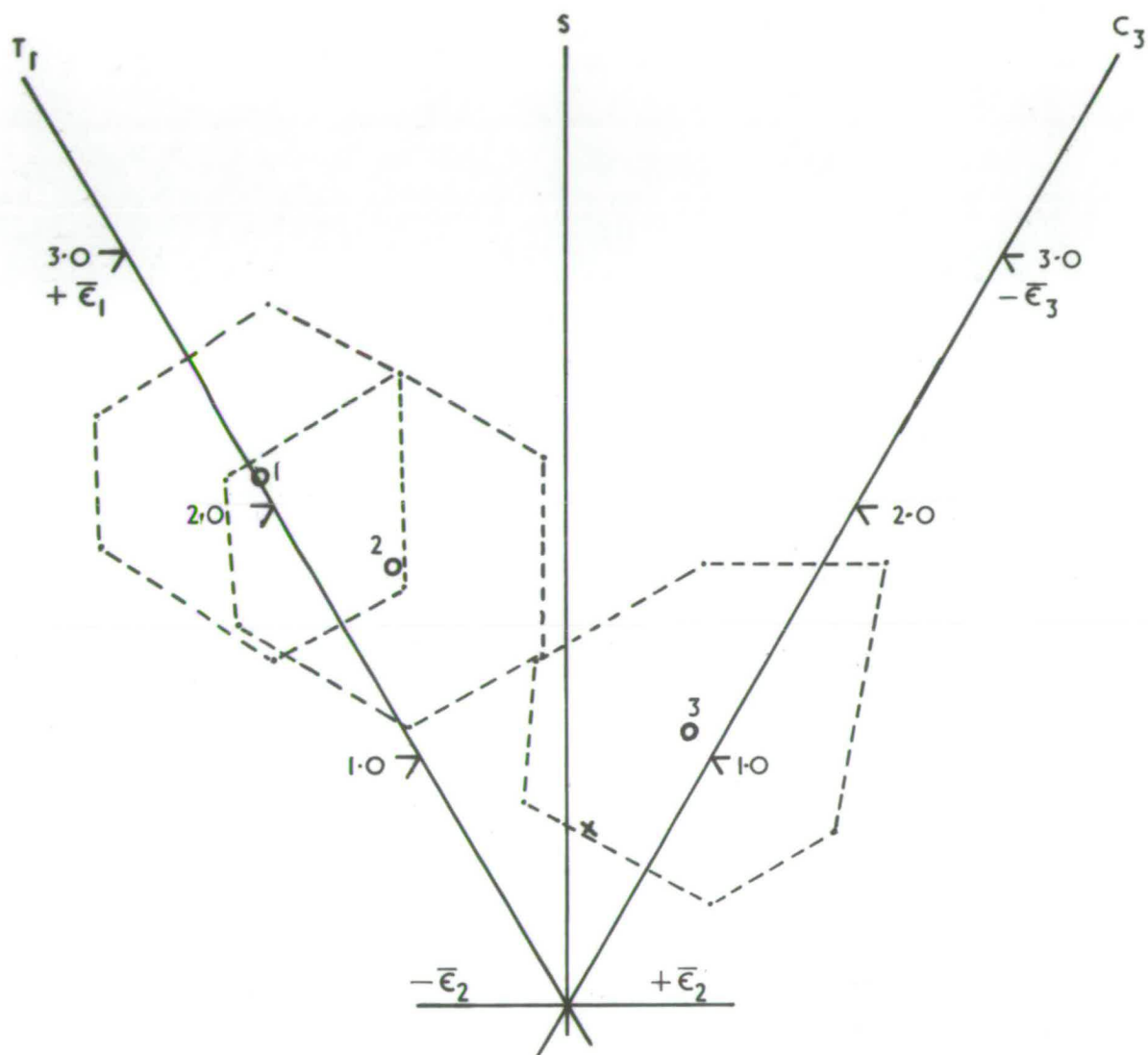
○ Superposed three dimensional strain

× Initial pebble shape
  X/Y/Z = 4/3/2

⬡ Field within which final pebble shape may lie

Fig. 31.   Possible fields of error in the strain calculations

of the Bygdin conglomerate.

An initial shape factor of $X/Y/Z = 1,0/1,52/2,17$

has been subtracted from two pebble stations

representing the highest and lowest states of

strain in the Bygdin area. The subtraction has

been carried out for the 6 different orientations

of the shape factor with respect to the axes of

the measured strain. The 6 shapes which are

calculated for each station define the field of

error.

Fig 31
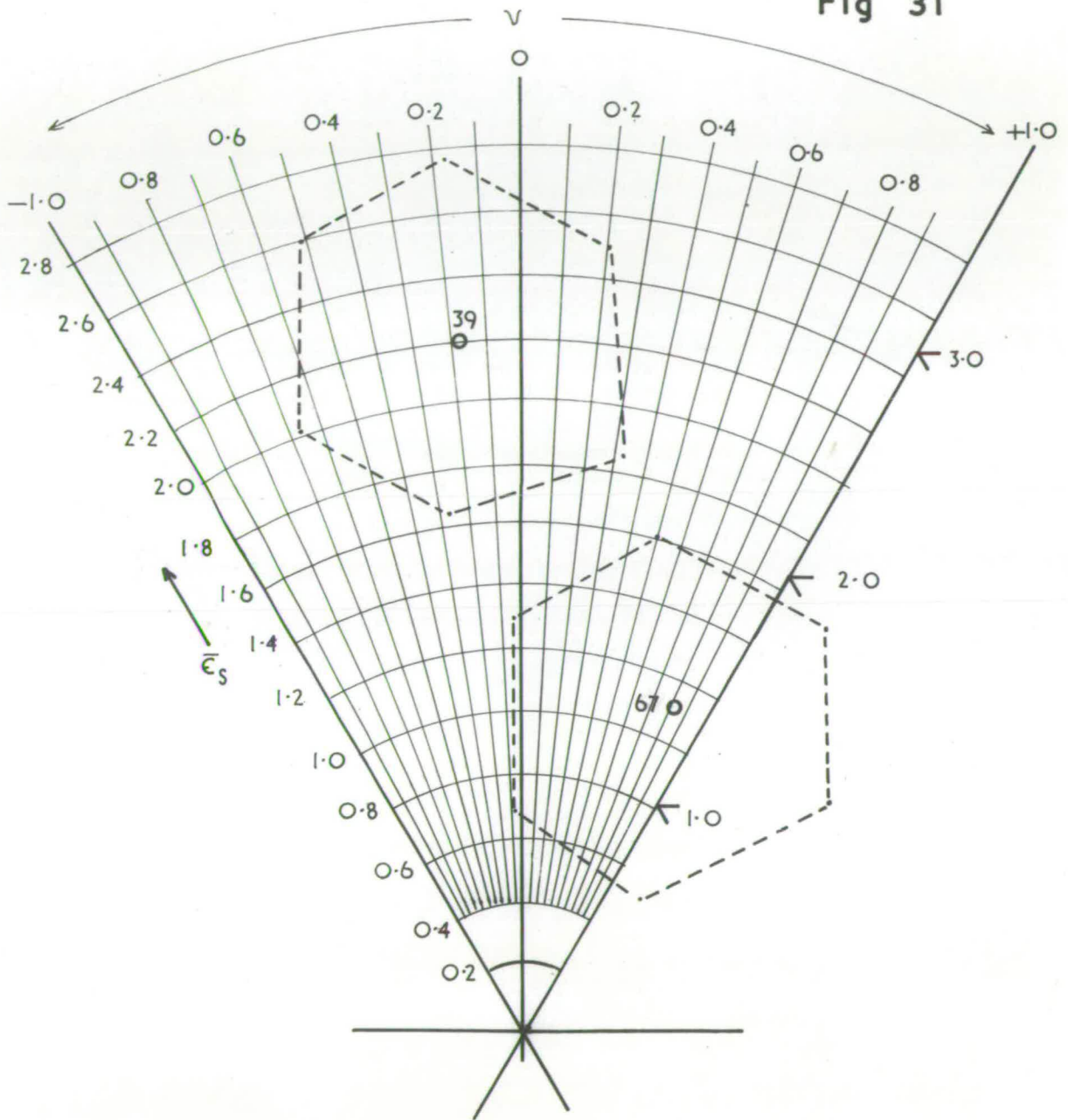
o Strain measured at stations
39 and 67

Possible field of error in strain
measurement

is important in determining the final shape of the pebbles. This problem has been studied by Ramsay and Higgins (Higgins, 1964), who have defined fields within which a pebble shape may fall at the end of a deformation, given any initial shape and orientation with respect to the stress axes, and a given strain. The fields are defined by the 6 possible orientations of the initial ellipsoid shape with respect to the stress axes so that the stress axes are parallel to the pebble axes. Pebble orientations which are not parallel to the stress axes lie within the field. Some of the fields given by Higgins are recalculated and plotted on the strain plane (Figs. 29 and 30). The error induced by this initial shape factor with regard to the amount and symmetry of strain may be up to 100% or more. However, the larger the deformation, the smaller the error.

In order to calculate the possible error at Bygdin, an initial shape factor has been subtracted from the measured pebble shapes of two stations representing the highest and lowest amount of deformation (Fig. 31). The shape factor chosen was one with X:Y:Z = 1,0:1,52:2,17 as this is near the average of shapes of undeformed sandstone and quartzite pebbles (given in Carrol, 1951; Flinn, 1956; Wentworth, 1925). Because natural strain units can be simply added or subtracted to provide addition or subtraction of strain, the initial shape factor was converted to natural strain units ($\overline{\varepsilon}_1^* = +0.33$, $\overline{\varepsilon}_2^* = +0.02$, $\overline{\varepsilon}_3^* = -0.40$) and then subtracted from the measured strain to provide the possible error involved by neglect of the shape factor in the strain calculations. Like the calculations of Higgins, 6 different subtractions were carried out for each station, representing the 6 possible orientations of the pre-deformation shape to the measured post-deformation shape, so

that the axes of both shapes are parallel. The field defined after the sub-
:traction of an initial shape factor represents the possible error in strain
measurements (Fig. 31). The true strain may lie anywhere within the hexagon
about the measured pebble shape (provided the pre-deformation shape at Bygdin
was close to that averaged from the literature).

The error in the measurement of the amount of strain ($\overline{\epsilon}_s$) is up
to $\pm$ 25% for the high deformation, and $\pm$ 50% for the low. The error in
symmetry ($\underline{v}$) is up to $\pm$ 0,45 $\underline{v}$-units for the high deformation and $\pm$ 0,90
$\underline{v}$-units for the low deformation. This last error with respect to the total
range of symmetry is one of $\pm$ 50%.

(d) Volume loss

Any volume loss during deformation (such as material carried away
in solution) will affect the accuracy of the strain calculations because
these calculations assume that the volume loss during deformation is zero.
Estimation of possible volume loss at Bygdin is impossible because of the
absence of undeformed pebbles. The difficulty of trying to add on any
possible volume loss is deciding whether the volume loss has an **isotropic**
symmetry or a symmetry similar to the deformation ellipsoid. Calculations
by Ramsay (unpublished data) indicate that a volume loss (up to 20%) can
alter the shape of the final ellipsoid and place it in the flattening field
even although the deformation was not one of flattening. All stations at
Bygdin in the flattening field might have only undergone two dimensional
deformation with the "flattening" purely a result of volume loss.

(e) Repeated deformation.

This is an important problem at Bygdin.because the area has under-
:gone three separate strains (B1, B2, B3) all of a plastic nature.   The two
later strains have probably modified the actual values of the first strain,
but more important, they may have modified the symmetry.

The minor structural evidence indicates that, despite modification
by the second and third movements, the cake pebbles are clearly seen to have
formed prior to the B2 and B3 movements, because the cake pebbles are
folded about B2 and B3 folds.

Similarly, the rod pebbles can be shown to pre-date the third
movement phase because they are folded by the B3 folds.   However, the rods
cannot be dated with respect to the B2 phase because of the absence of B2
minor folds in the areas of the rods.   The rods either pre-date B2 or were
formed from cake pebbles during the B2 phase.

Now any hypothesis of rod conglomerate forming from cake conglomerate
during the second movement phase, must explain the restricted distribution
of the rod conglomerates in contrast to the widespread distribution of the
B2 strains (i.e. folds).   The restricted distribution of the rods could
result of -

i)   variations in the symmetry of the B2 strain throughout
     the area.

ii) the B2 strain being superposed on cake pebbles which
     vary in orientation as a result of the B1
     deformation.

iii)   the B2 strain being superposed on cake pebbles which vary
in orientation as a result of the B2 deformation.

i)   Variations in the symmetry of the B2 strain are difficult to
discuss because arguments used to support this hypothesis could also be
used to support a hypothesis of cakes and rods forming during the B1
deformation.   This latter hypothesis is obviously more attractive than the
former.

ii)   The final shape of a pebble at the end of deformation is dependent,
not only on the initial shape, but also on the orientation of the pebble axes
with respect to the stress axes (Higgins, 1964).   Hence a constant strain
superposed on pebbles with varying initial orientations will produce different
shapes at the end of the deformation.   Rods could quite conceivably form
from cakes given initial variations in orientation of the principal axes
of the cakes.   Such variations in orientation have been produced by the
writer in experiments carried out on "silly putty" (pp. 69-70).   Now the
postulated variations could have been similar to those in the putty
experiments and could have formed during the B1 deformation. Superposition
of the B2 strain might then have produced rods, like the hypothetical
deformation discussed on pp. 71-72.

iii)   The variations in orientation of the cake pebbles formed prior
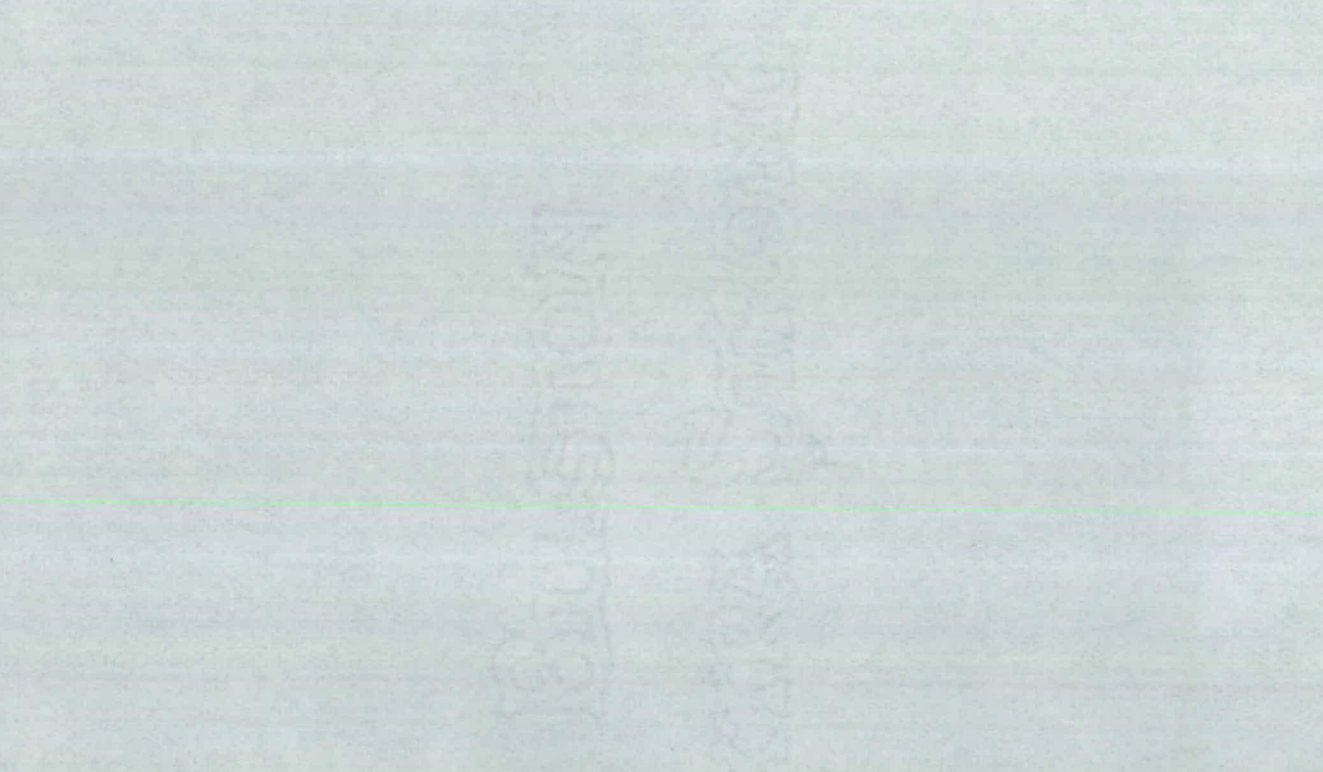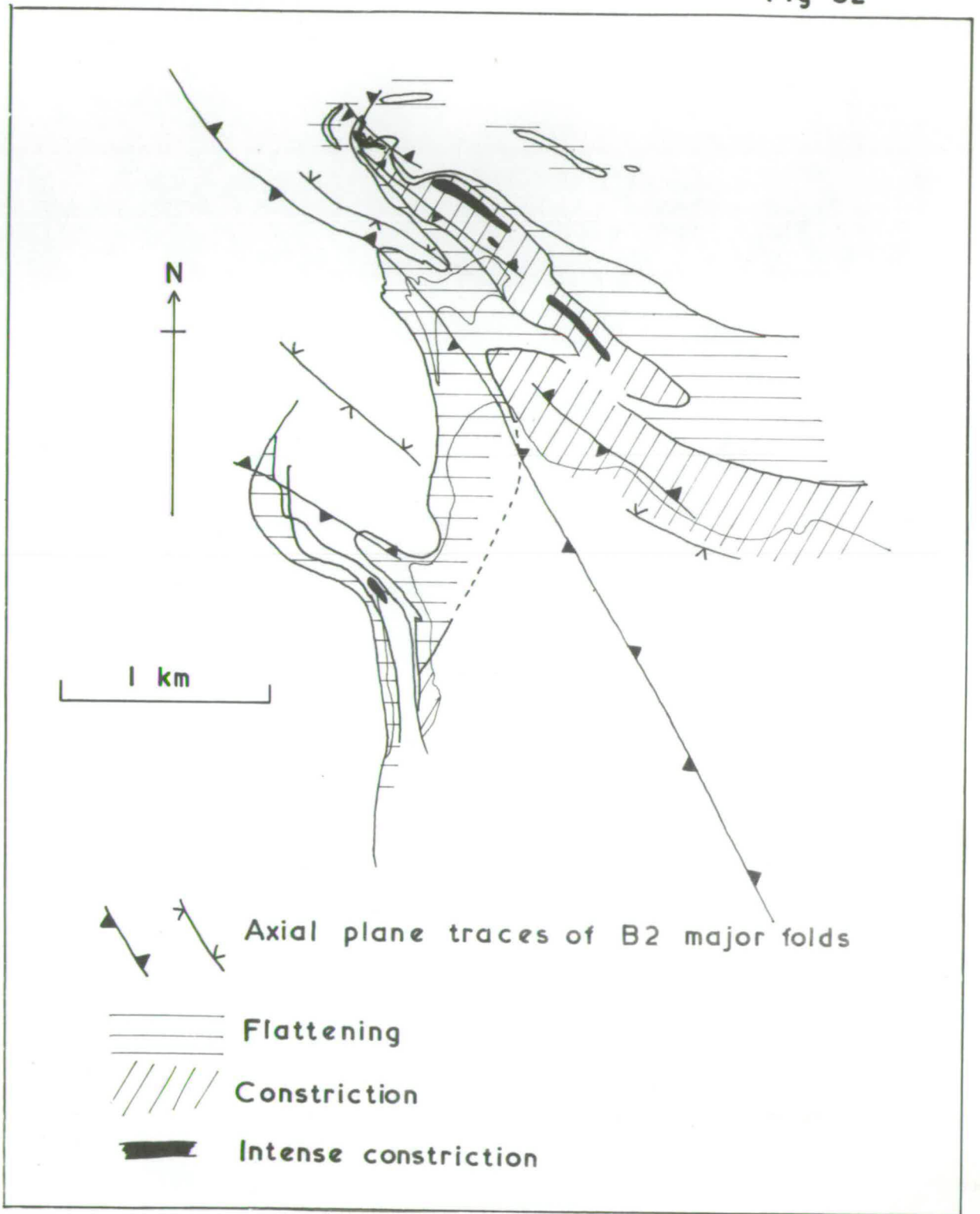to the B2 plastic strain could also have been produced by B2 concentric

Fig. 32.   Map of the distribution of the rod-conglomerates and
the major Second Fold traces.

Fig 32

Axial plane traces of B2 major folds

Flattening

Constriction

Intense constriction

1 km

folding. After folding, the orientation of the pebble axes could change systematically around the fold hinge. The superposition of a B2 plastic strain on the cakes could then form rods in the fold core and cakes on the limbs (or vice-versa).

If the hypotheses of rod conglomerates forming from cake conglomerates by the superposition of the B2 phase, are true, the B2 folds might then be expected to control the distribution of the rod conglomerates. A comparison of the distribution of the pebble shapes and major second fold traces (Fig. 32) indicates that the B2 folds might have controlled the rod formation as the areas of the rods lie in line with the fold traces. However, rods are absent in the largest fold of the area (the Bygdin Antiform) and the rods of antiform-a lie outside the fold trace. This last mentioned rod area lies at a tectonic level where the dihedral angle of antiform-a is only 150°-170°. The postulated difference in orientation of pebble axes of the shapes on the limb and in the fold core is only 10°-15° and this does not seem sufficient to cause much divergence in shape during a second deformation.

The correlation between rods and second fold traces is probably the converse of the above hypothesis. The rod conglomerates may have been areas of weakness during the second deformation which controlled the position of the major second fold traces.

The writer believes that the rods and cakes were the result of a single deformation (B1). There is a complete continuity in the field between the rods and cakes (i.e. intermediate shapes between rods and

cakes) with the intermediate shapes being folded by B2 minor folds proving that they are pre-B2. The variations in symmetry of the conglomerate deformation are largely unaffected by the later strains.

(5) DISTRIBUTION OF PEBBLE SHAPES

In spite of the probable errors in the strain measurements, the areal patterns of the two strain parameters ($\overline{\epsilon}_S$ and $\underline{v}$) seem to the writer to be highly significant (Figs. 33, 34 and 35). They show well defined maxima and minima that do not appear to be the result of the random distribution. As such, the patterns give a clue to the distribution of the symmetry and amount of strain.

(a) Amount of strain ($\overline{\epsilon}_S$)

The general pattern of $\overline{\epsilon}_S$ at Bygdin and Olefjell indicates that the amount of distortional strain is generally highest at the thrust plane and decreases downwards towards a minimum (Fig.33). The only exception to this downward decrease in $\overline{\epsilon}_S$ is in the conglomerate wedge on the southwest limb of antiform-a where the amount in fact increases downwards.

Two minima are present, one on the northeast limb of the Bygdin Antiform and the other at Olefjell. These minima seem to be almost completely surrounded by areas of higher distortional strain and may be the result of a lower strain rate in the minima than in the surrounding areas. The minimum at Olefjell has a lower value ($\overline{\epsilon}_S = +1.0$) than the minimum at Bygdin ($\overline{\epsilon}_S = +2.0$).

Map of the distribution of $\overline{\epsilon}_s$-values at Bygdin and Olefjell

Fig 33

Fig 34

N

+0.7

-0.3

+0.6
-0.3
+0.1
+0.1
+0.7
+0.9

+0.4 +0.3
+0.2
+0.1

+0.1 +0.1
-0.1

+0.7
-0.1

-0.1
-0.2
-0.3

+0.6
+0.1

-0.1 -0.2 -0.3

O   1   2
km

⟍⟍ L tectonites of the Jotun Nappe

▮ v values greater than −0·5 (i.e. RODS)

O— +0·9 **Areas of flattening**

O— −0·5 **Areas of constriction**

Map of the distribution of v-values at Bygdin

LAKE VINSTRI

0·4

0·6

0·4
0·3

0·2

0·2 0·3
0·1

N

0·3

0·3

0·3

0·2

0·4

0·4 0·7 0·7 0·4
0·8

0·1

0·2
0·3 0·4 0·7 0·4 0·3

0·2

ALL VALUES POSITIVE

0 1 2
km

0·1
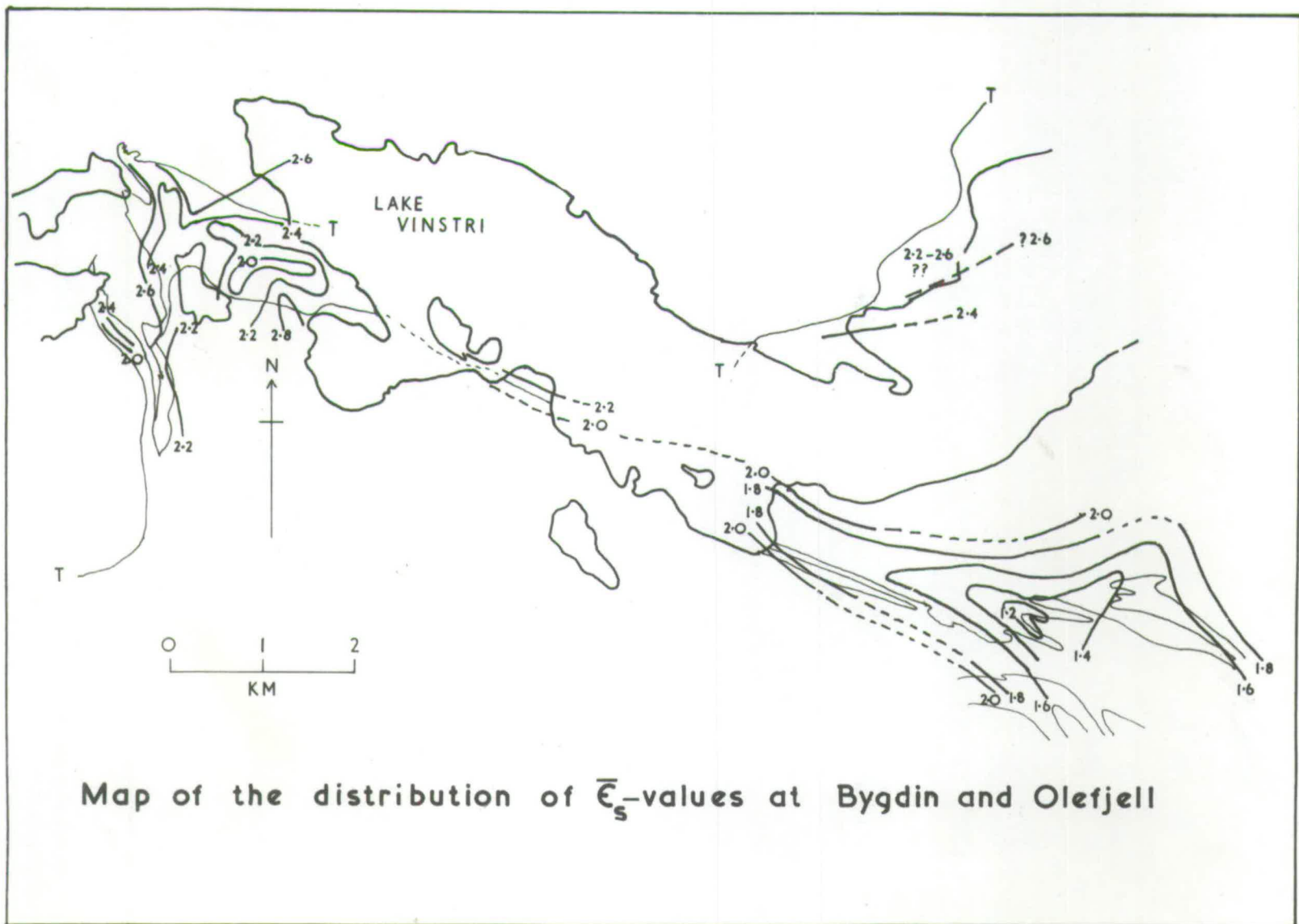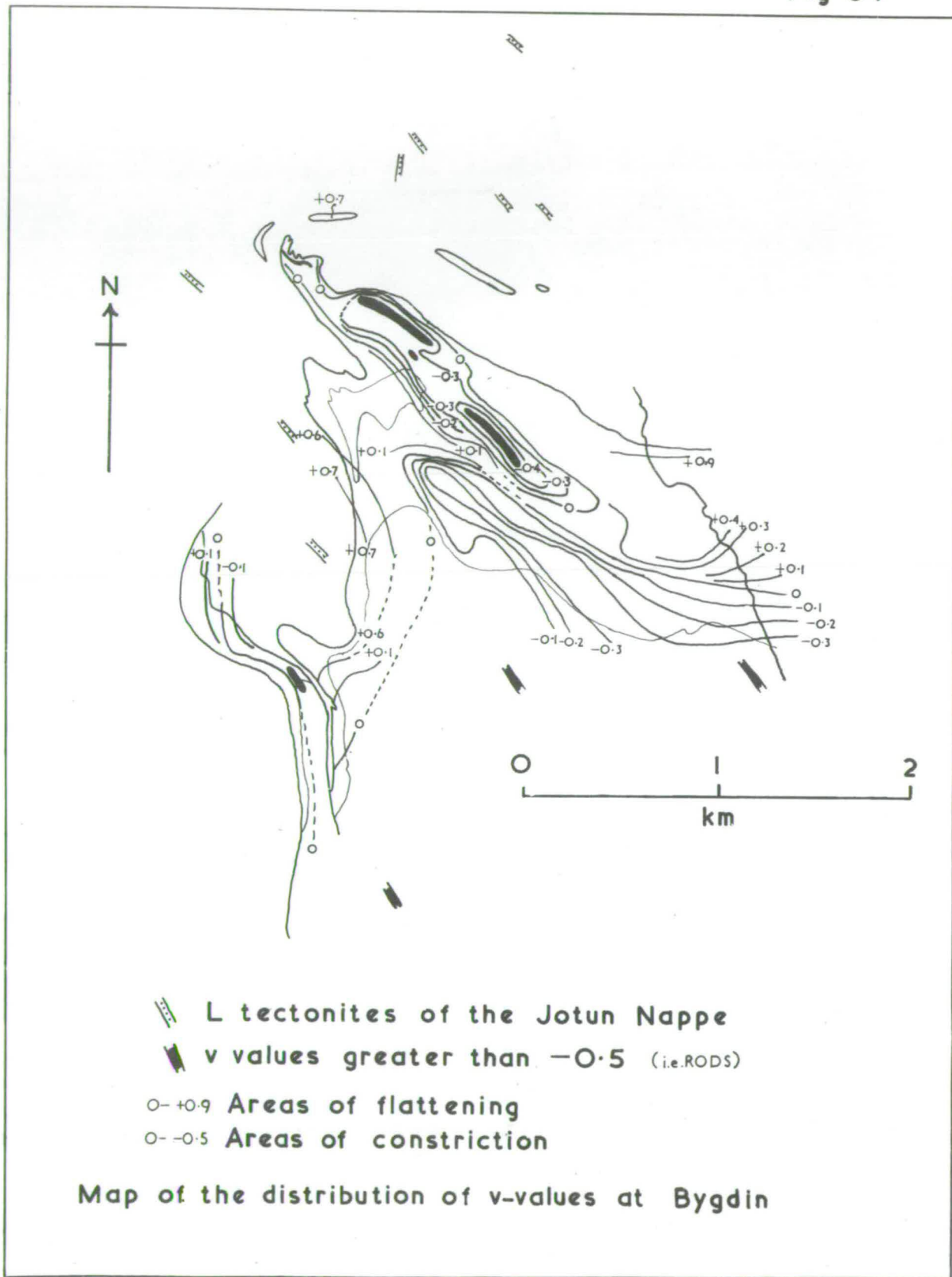0

OLEVATN

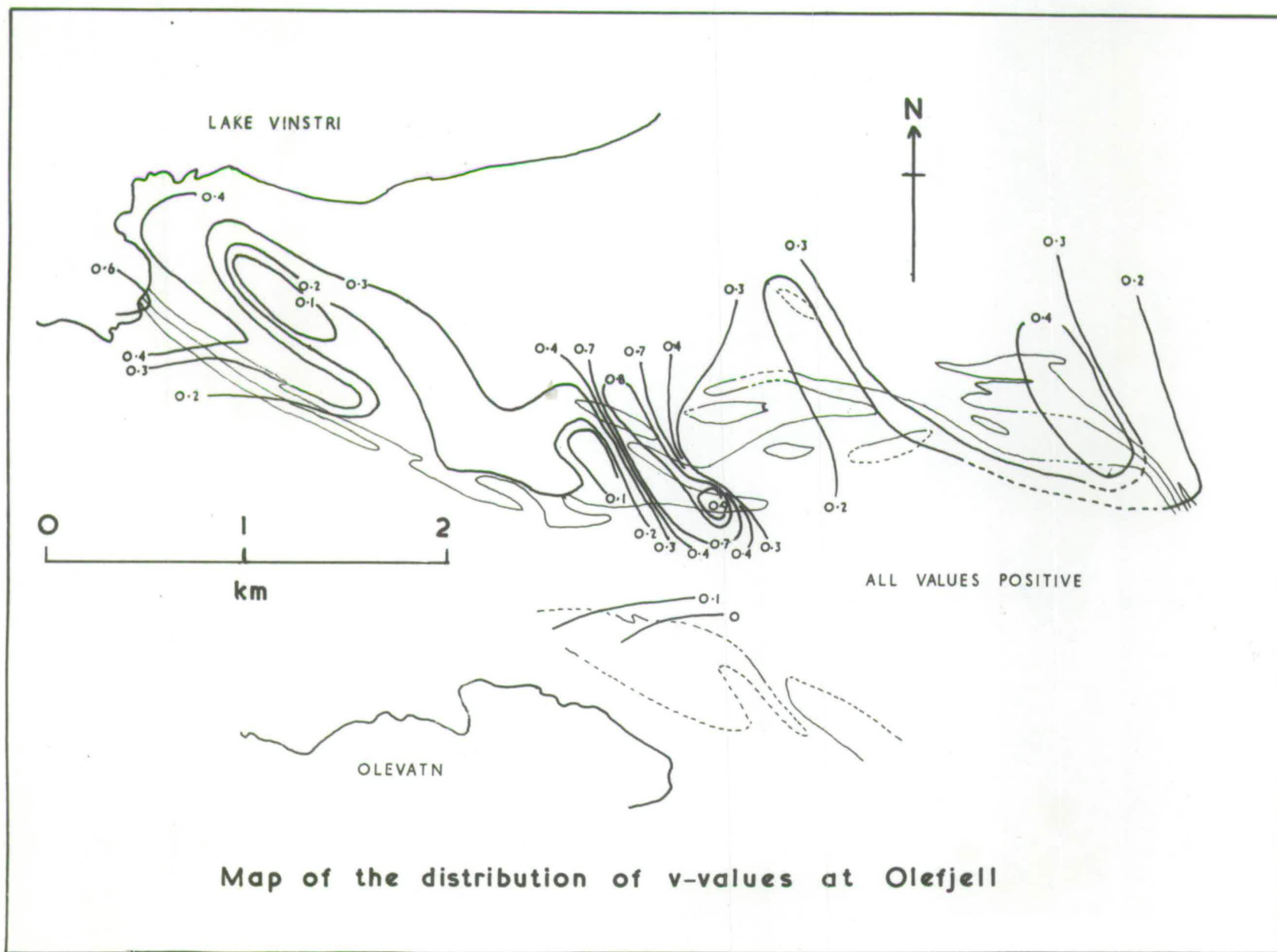Map of the distribution of v-values at Olefjell

Fig 35

(b) Symmetry of strain (ʊ)

The distribution of the symmetry coefficients of strain is similar
in the Bygdin and Olefjell areas (Figs. 34 and 35).   Throughout the whole
area the dominant symmetry of strain was one of flattening (defined by ʊ-values
of 0 to + 1,0).   Only one station could be measured on the north side of
Vinstrivatn (Station No.50), but a visual comparison of the conglomerate
here with that of Bygdin and Olefjell suggests that the dominant deformation
here was one of flattening.   (Visual estimation also suggests that the
amount of strain here was higher than that of Olefjell, but almost equal to
that of Bygdin, c.f. Fig.33).

The presence of cake conglomerate in thrust slices up to 300 metres
above the basal thrust plane north of Bygdin, suggests in addition that much
of the Jotun Nappe may also have undergone flattening.

The rod conglomerates at Bygdin (v ∠ -0,5) which have a constrictional
symmetry, are restricted to northwest trending plug-like areas (Fig. 34).   The
plugs are elongated parallel to the rod elongation with a lenticular cross-
section, and are completely surrounded by conglomerate which has undergone
flattening.

The plugs lie en-echelon on the northeast limb of the Bygdin
Antiform so that each successive plug to the southeast lies at a lower
structural level with respect to the thrust plane.   A plug-like area of
rod conglomerate is also situated on the southwest limb of antiform-a.

Flinn (1965) suggested that the symmetries of deformation discussed
above can also be recognised in non-conglomeratic rocks. For example,

schists which have undergone a flattening deformation can be expected on symmetry arguments, to have a foliation but no lineation (S-tectonites). Similarly rocks which have undergone constriction might be expected to have a lineation fabric but no foliation (L-tectonites). However, these fabrics might be difficult to recognise in areas which have undergone more than one deformation. For instance a later lineation could be superposed on an S-tectonite to produce a fabric which Flinn would call an L S-tectonite (i.e. one with a symmetry close to that of pure or simple shear). In this case the symmetry is a result of two deformations and does not give any guide to the symmetries of the two deformations producing the tectonic fabric.

L-tectonites were mapped by the author in the granitic rocks of the Upper Jotun Nappe (Fig.34) and consist of granitic rocks without a foliation but with a strong lineation of elongate felspars or hornblendes. Because of the apparent absence of minor structures of post-B1 deformations throughout most of the nappe, the above objection to Flinn's hypothesis does not apply and the writer accepts Flinn's view (Flinn, 1965) that these L-tectonites have a symmetry equivalent to the rod conglomerate.

The presence of L-tectonites and cake conglomerate slices within the Jotun Nappe suggests that the distribution of the symmetry of strain is similar in the nappe to that of the conglomerate near Bygdin. Mapping of these variations in the nappe however cannot be done in such detail as that of the conglomerate.

Despite the fact that the whole of the conglomerate at Olefjell has undergone flattening (Fig. 35), the distribution of the locii of equal y-values is similar to that at Bygdin. Areas of approximate two

dimensional deformation (y-values $\simeq 0$) lie in two northwest trending tongues similar to the plugs of rods at Bygdin. In contrast to Bygdin, the tongues are only surrounded by areas of flattening on three sides. The absence of strong flattening on the fourth side (at the lowest structural level) however may only be a result of the absence of strain data from the sparagmite below the conglomerate.

The movement pictures put forward by the writer to describe the deformation in the conglomerate at Olefjell and Bygdin are completely analogous and will be described in the conclusions.
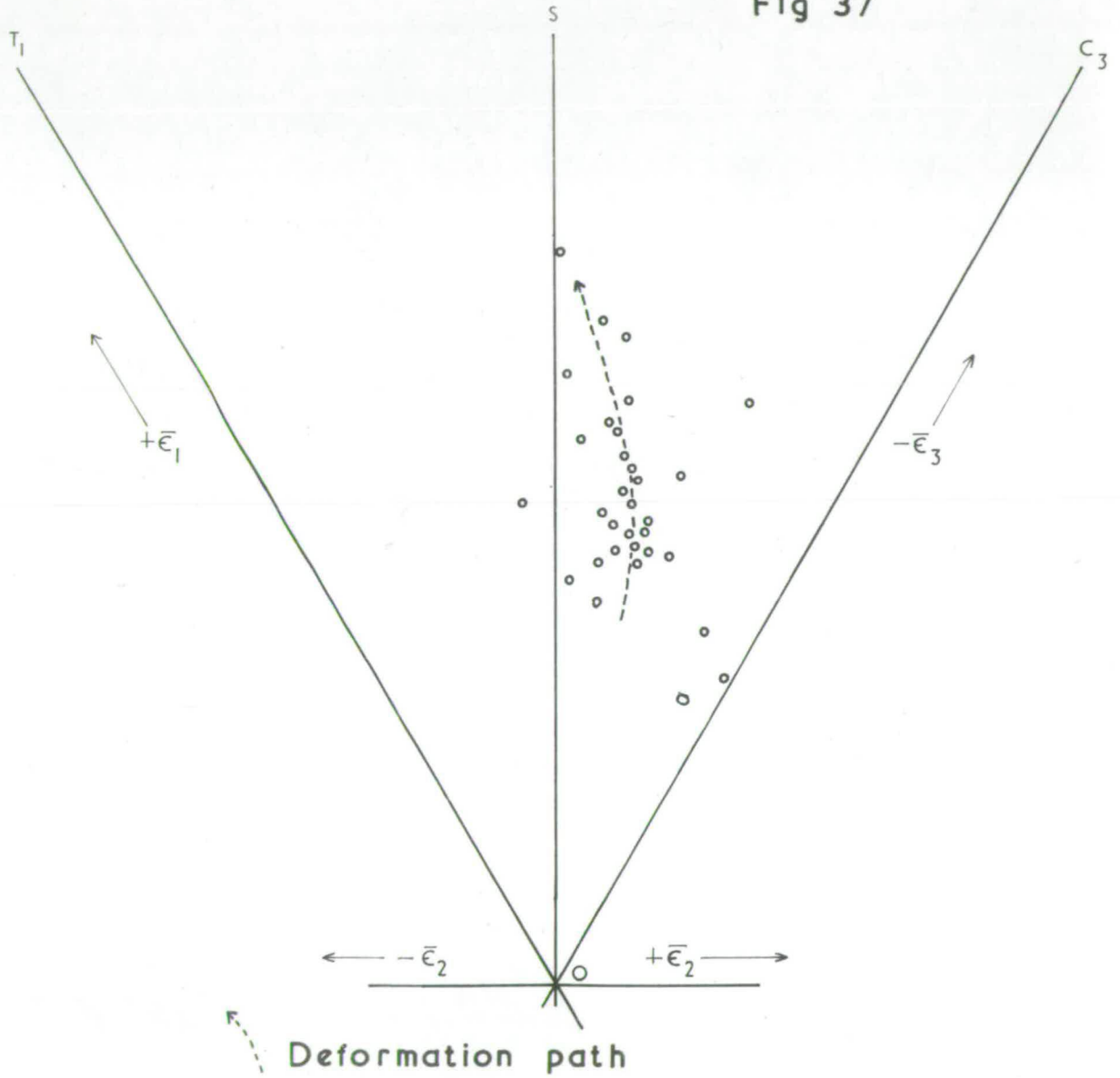
6. DEFORMATION PATHS

Recognition of deformation paths and the shape of these paths is extremely important in the understanding of the physics of rock deformation. Any determined geological deformation path would record the stages taken by the rock during its deformation and must influence any ideas of the possible movement picture of that rock.

Ramsay (1964) has determined that the simplest deformation path (i.e. one in which the stresses remain constant in value and orientation during the deformation and involves the application of the minimum amount of work) has the form $a = b^{\log a_1/\log b_1}$ and plots as a straight line on a logarithmic deformation plot (or on the strain plane). This is implicit in the engineering view that the minimum amount of work is applied in the deformation (i.e. the flow is unrestricted) when the increments of strain have a constant ratio during deformation (i.e. $d\bar{\varepsilon}_1/d\bar{\varepsilon}_3$ and $d\bar{\varepsilon}_2/d\bar{\varepsilon}_3$ remain constant) (Nadai, 1963 pp. 73-74). If the ratios of increments are constant, the deformation path on the strain plane must be a straight line.
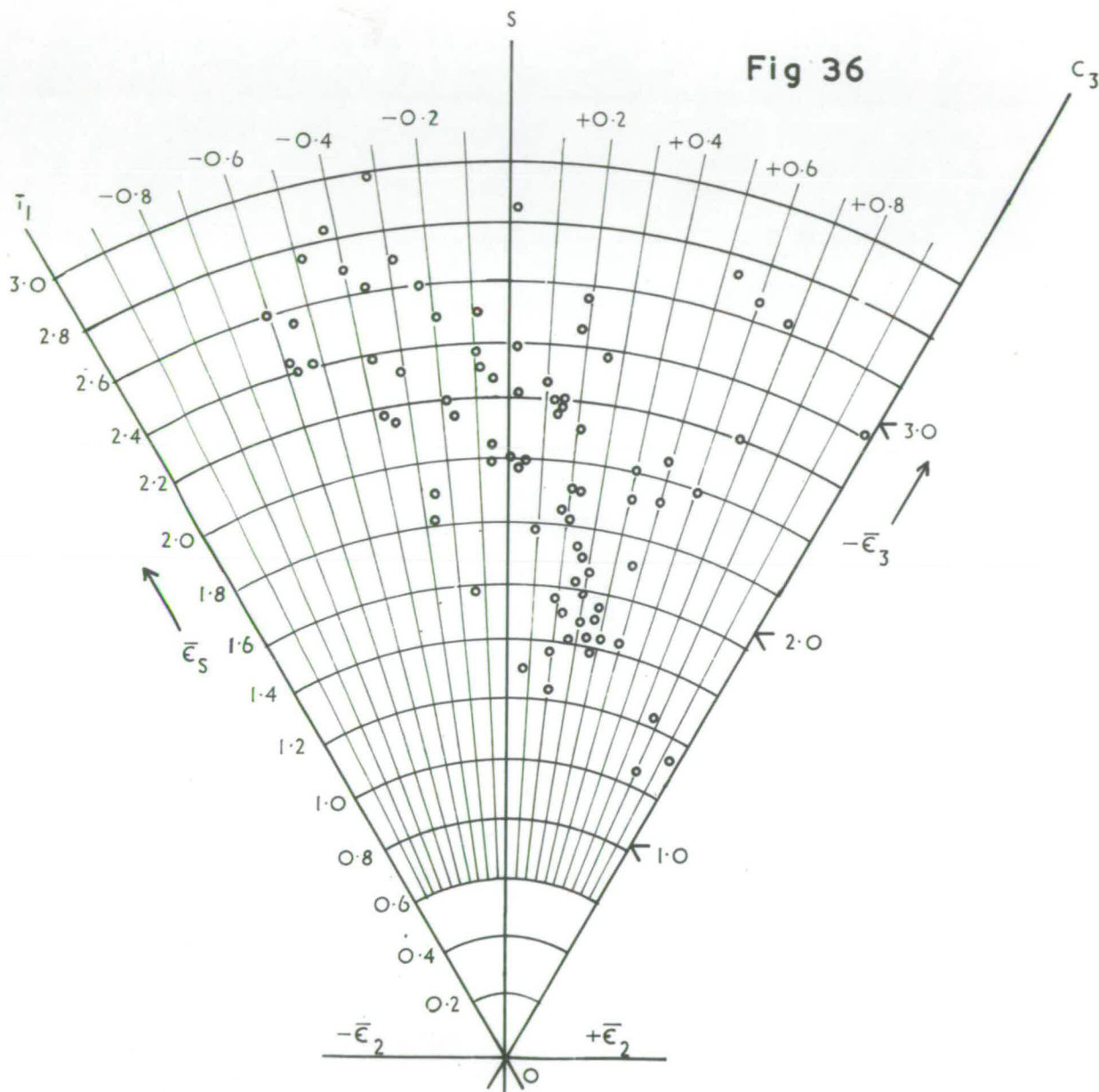
Strain plane plot of deformed pebbles from
Bygdin and Olefjell

Fig 37

Possible deformation path at Olefjell

If the deformation is more complex than that described above (i.e. the values or orientation of the stresses change during deformation) the deformation path on a logarithmic plot will become curved.

Recognition of these deformation paths, however, will probably be extremely difficult in geological strains. The strain measured in deformed oolites or pebbles represents the final stage in straining and gives no clue to the path taken to reach this final stage. Theoretically, any path can be taken to reach the final point.

In any one area, however, a collection of strain data might combine rock strains which have had the same symmetry of strain but differing strain rates. Therefore some parts will undergo less deformation than others and the spread of points which would result might then reveal a deformation path.

The combined plot of strains from Bygdin and Olefjell (Fig. 36) does not reveal any easily defined deformation paths. Each point on the plot may have been reached by a unique deformation path. However, the strains of Olefjell reveal a possible deformation path (Fig. 37). The majority of points define a curved line which may be a deformation path.

If this indeed represents a deformation path, the value and/or the orientation of the B1 stresses would appear to have changed during the first deformation (i.e. constrained flow; Nadai, 1950, pp. 426-429).

VI.   CONCLUSIONS

1.   INTRODUCTION

Reconstructions of the movement pictures of the three main deform-
:ations are attempted using the strain data from the pebbles and the symmetry
of the minor structures.   Problems which affect these reconstructions include
the discrepancy between the symmetry of the deformed pebbles and the symmetry
of thrusting;   the mechanical problem of the movement of a large thrust block
of the scale of the Upper Jotun Nappe;   the significance of fold axes and
lineations and the possibility of determining stress axes from the geometry
of folds.

Possible stress fields which caused the movements are tentatively
derived from the movement pictures.

2.   MOVEMENT PICTURE OF THE FIRST DEFORMATION

(a)   Comparison of the symmetries of pebble deformation and thrusting.

The symmetry of the pebble deformation cannot be directly related
to the symmetry of thrusting.   The kinematics of thrusting would be expected
to have a monoclinic simple shear symmetry which would induce monoclinic
fabrics in the rocks.

In such a simple shear, the pebbles would deform by shear along
planes parallel to the thrust plane (Fig. 33a) and the long axes of the pebbles
would be oblique to the thrust plane.   In addition, the plane of pebble
flattening (equivalent to S1 at Bygdin) would be truncated by the thrust
plane.   As a simple shear has a two dimensional symmetry, the intermediate
axes of the pebble should not be strained.

Fig. 38.   Sections of the hypothetical and actual pebble

deformation in the Bygdin area.

a)   Orientation of deformed pebbles in a postulated

monoclinic simple shear deformation.

b)   Actual orientation of the deformed pebbles with

respect to the thrust plane.

c)   Structural section through the Olefjell area

showing the three areas of flattening (F) which

are separated by the two areas of near two-
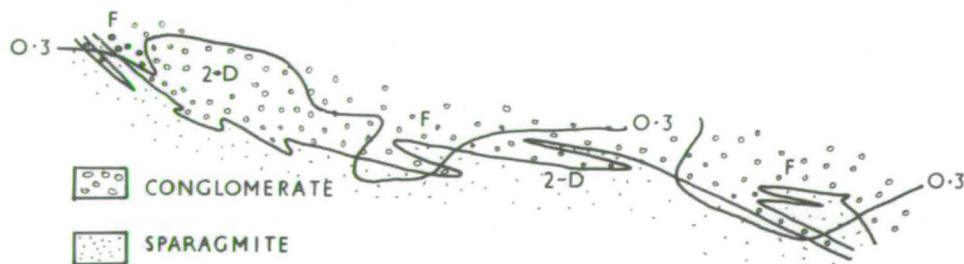
dimensional deformation (2-D).

The areas are separated by the line of

$v = 0,3$.

Fig 38

a

b

CONGLOMERATE

SPARAGMITE
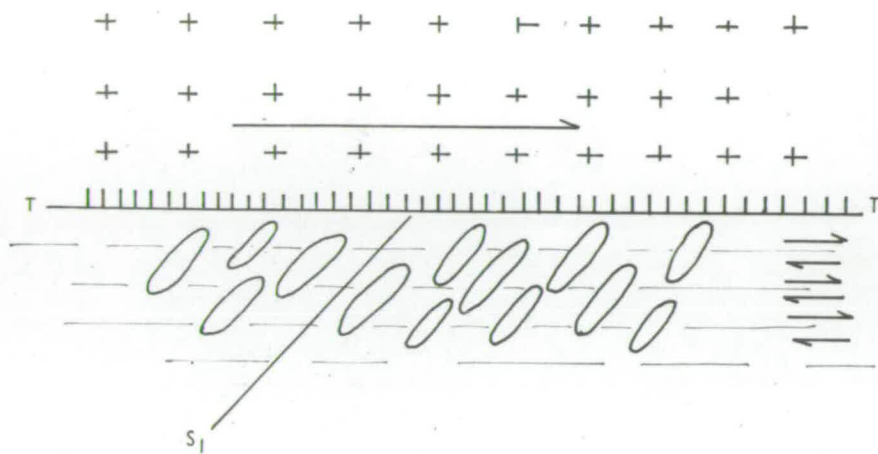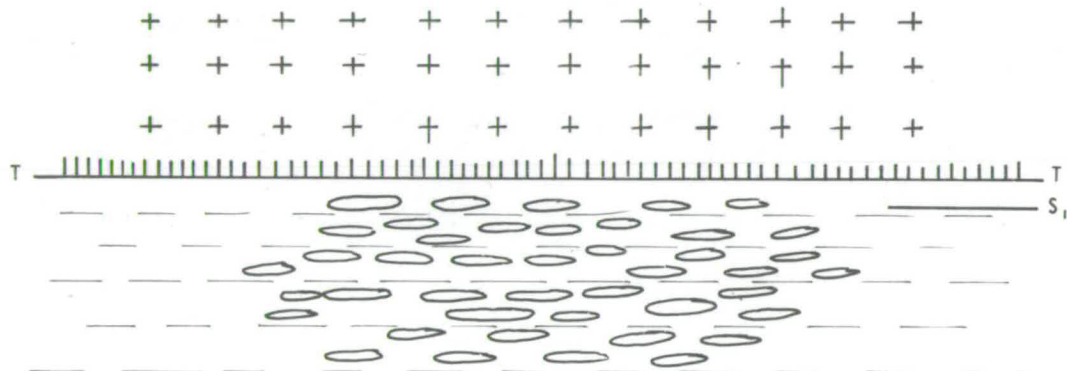
c

In fact the actual pebble deformation is of a high symmetry
(orthorhombic to near-axial) and the plane of pebble flattening (S1) and
the long axes of the pebbles are parallel to the thrust plane (Fig. 38 b).
The high symmetry of the pebbles (which is a result of strain along the
intermediate axial direction) and the parallelism of the pebbles to the
thrust plane, suggests that if the pebble deformation is to be correlated with
the thrust plane, the movement picture must contain a component in addition to
that of simple shear.

The deformation might include a rotational component which was
sufficient to rotate the pebbles into parallelism with the thrust plane. Two
types of possible rotation are -

   i) Rotation of axes accompanying a simple shear component
      of the deformation.

   ii) An independent external rotation which is a result of
       inhomogeneous flow. Pebbles would rotate as a result
       of the flow of the conglomerate matrix.

i) The high symmetry of the deformation suggests that any simple shear
component of the deformation must be minor. Infinite simple shear would be
required to align the long axes of the pebbles with the thrust plane. This
alignment must be due to some process other than that of simple shear.

ii) An independent external rotation seems unlikely because the amount
of matrix in many parts of the conglomerate is now small. At least towards
the final stages of the deformation, the pebbles could not rotate

independently of each other; they were probably locked together and deformed as a unit.

However, the pebble deformation may not be directly related to the thrusting because structural evidence indicates that pebble deformation may actually post-date thrusting. Cataclasis and phyllonite formation, which were probably synchronous with the actual thrusting of the nappe, may pre-date S1 formation (i.e. plane of pebble flattening) because phyllonite bands in the nappe are folded about S1 (p. 20).

The writer tentatively suggests that the pebble deformation post-dates at least some of the thrust movements. It is possible that the initial stages of the B1 deformation were produced by the thrust movements and had a monoclinic symmetry which was later effaced by a ?non-rotational high symmetry deformation. However, the high symmetry of pebble deformation demands that the postulated initial monoclinic pebble deformation must have been slight.

There is really no discrepancy between the symmetries of pebble deformation and thrust movements if a post-thrusting, high symmetry deformation took place.

(b) Pebble microfabrics

A few quartz-fabrics were measured by the writer, but are not reproduced here. These fabrics are identical to those published by Strand (1945) and thus the discussion of the pebble microfabrics will be based solely on Strand's results.

The quartz-microfabrics have near-orthorhombic girdles with the girdle axis parallel to the pebble elongation direction. Thus the orthorhombic symmetry of the microfabrics is essentially parallel to the orthorhombic symmetry of the deformed pebbles.

The writer, however, does not agree with Strand's suggestion that the quartz girdles formed simultaneously with the pebble deformation. The writer believes that these girdles post-date the pebble deformation and are actually of B2 age. The reason for this interpretation is that Strand's diagrams show the girdles and girdle maxima to have a constant geographic orientation throughout the whole area, irrespective of the strike and dip of the Sl foliation (which is plotted on all of Strand's diagrams). If the girdles were of Bl age, they might be expected to have some symmetrical orientation with respect to Sl, like the symmetry of the deformed pebbles. The B2 major folding should then have rotated the microfabrics so that the orientation of the fabric maxima would vary over the B2 major folds.

In fact, the girdle maxima have a constant geographic orientation throughout the Bygdin Antiform, and the girdle axes are also parallel to the B2 fold axes. This suggests that the quartz girdles could also be inter-:preted as a penetrative microfabric of B2 age.

Even if the writer's interpretation of the quartz fabrics is in error, at least the symmetry of the girdles is consistent with the symmetry of the pebble deformation.

(c) Variation of strain symmetry

The dominant pebble deformation at Bygdin and Olefjell was one of flattening normal to the nappe (p. 61). This is indicated by positive v-values between 0 and +1,0. However, the movement was not a pure flattening with equal extension to the northeast and northwest. All the v-values are less than +1,0, thus the symmetry is not axial but orthorhombic.

The greatest extension took place in a northwest-southeast direction, parallel to the assumed direction of thrust movement.

Experiments were carried out to try and reproduce the other symmetries of deformation (e.g. rods) using flattening as a motive force. The area which first suggested a possible mechanism was that of Olefjell. At Olefjell two areas of near two dimensional deformation ($v \rightleftharpoons 0$) lie between three areas of flattening (Fig. 33 c). These areas of flattening may have squeezed the two dimensional areas in a vice-like grip which did not allow them to extend in the intermediate direction (i.e. Einengung flow, Sander, 1948) but relief could only take place in a northwest-southeast direction.

Some qualitative experiments were carried out using "silly putty" to see if two areas of flattening can constrict the area which lies between them. The experiments were set up so that the putty was allowed to flatten under it's own weight. Flattening was the only motive force in the deformation, but a rotation of stress axes was produced by the geometry of the experiments.

Three blocks of putty were set up such that a shorter block was sandwiched between two larger blocks (Plate 12 a and b). Because the outside blocks were higher than the internal block, the axial force of gravity which causes the putty to deform, was greater on the outside blocks than in the internal block. Circles were impressed on the surface of the putty at the start of the deformation to determine the symmetries of the strains throughout the model. As all the blocks deformed, these circles deformed into ellipses and the areas of these deformed circles increased and decreased as a result of the three dimensional deformation. The middle block in all

the experiments underwent constriction in a horizontal direction with this direction decreasing in length.

These experiments show that pressure gradients can cause a rotation of stress axes. The outside blocks have a larger vertical stress and deform at a faster rate than the internal block. This restricts the space within which the internal block can deform and so causes constriction in a horizontal direction. With large pressure gradients, the internal block is actively squeezed in the horizontal direction so that it decreases in length.

This constriction causes the internal putty block to elongate outwards and upwards (Plate 13 a and b), thus the deformation in this block is in effect a flattening deformation which is normal to the flattening in the outside blocks. The author's experiments are not strictly analogous to the deformation in the rod conglomerate as the rods have undergone shortening in the horizontal and vertical directions.

Flinn (1961) carried out some experiments to try and reproduce the deformation of the Bygdin conglomerate, using a model nappe with a deep groove in the base. This deep groove represented the Bygdin "Invagination" (Map III) which was thought by Flinn to have been present in the base of the nappe during thrusting. Strains equivalent to the rod and cake conglomerate could only be produced by Flinn (ibid) when the deformation was a static flattening. Elongation in the model rod conglomerate took place parallel to the groove (equivalent to the northwest elongation at Bygdin) but in addition, elongation structures were also formed normal to the groove (equivalent to a northeast direction at Bygdin). Flinn suggested that the flattening and constrictional fabrics in his model were the result of pressure gradients, but because northeast elongations were absent

at Bygdin, he suggested that the "Invagination" did not cause the constriction in the rod conglomerate at Bygdin, but in fact the constriction may have formed the "Invagination". The present work (pp. 41-42, and Map III) has shown that this "Invagination" is post-pebble flattening and is a B2 major antiform. Thus the "Invagination" in the base of the nappe was not present during thrusting. Neither Flinn's nor the writer's experiments are really analogous to the pebble deformation, but they at least show that pressure gradients can cause rotation of stress axes and can reproduce constrictional and flattening fabrics.

The writer tentatively suggests two mechanisms to produce rod and cake fabrics in a general flattening field.

i) Rod and cake fabrics can be produced in a model similar to the putty experiments if the deformation has two phases. In the first phase (a) fabrics like those in the putty model would form with a flattening in a horizontal position on the outside and another flattening normal to this in the middle (Fig. 39a). The strains represented by these two types of deformation would plot on the complete strain plane as in Fig. 39 c.
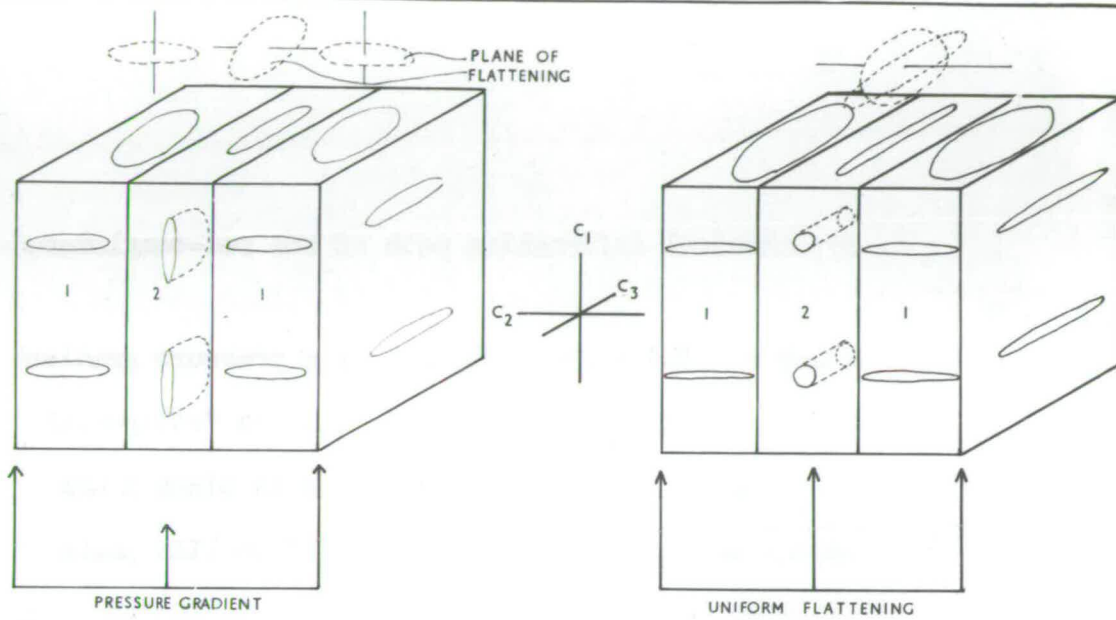
Now if the pressure gradients which cause this rotation of stress axes were to decrease so that there was a uniform flattening in the rocks parallel to the general flattening of the first stage, the outside areas would continue to flatten into cakes but the internal areas would redeform in such a way as to produce rods (Fig. 39 c, phase b). The deformation paths taken by the external and internal deformations are different. During the first phase, the external deformation path would move along one ray of pure flattening and the internal deformation along another. In the second phase (b), the external path would continue along the flattening ray

Fig. 39. Hypothetical deformation path of the rod-conglomerate.

Phase a) Under the influence of a pressure gradient, the conglomerate could deform like the "silly-putty" experiments so that the flattening in block 1 was normal to that of block 2. The deformation paths taken by blocks 1 and 2 are depicted on the complete strain plane.

Phase b) Under the influence of a uniform flattening normal to axis C1, the deformation path of block 1 would continue along the C1 axis. The path of block 2 would change direction and move parallel to the C1 axis. This change could move the deformation of block 2 into a field of constriction. However, the amount of strain in 2 would only be about half that of 1 at the end of deformation.

Fig 39

PLANE OF FLATTENING

1   2   1

PRESSURE GRADIENT

Phase a

C_1

C_2 — C_3

1   2   1

UNIFORM FLATTENING

Phase b

T_1

S   S

C_2 C_3

FLATTENING

2

a

b

CONSTRICTION

2

$\overline{\epsilon}_S 2$ a 1

S   S

CONSTRICTION

T_3 T_2

b

$\overline{\epsilon}_S 1$ 1

FLATTENING

S   S

C_1
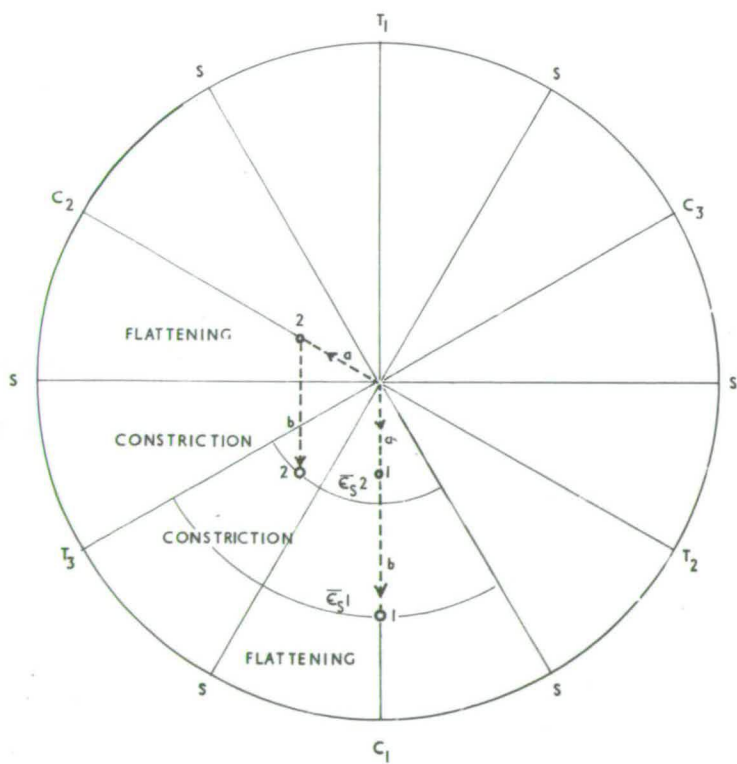
Fig. 40 Cross-section through the rod and cake conglomerates
with the postulated stress trajectories.

a)   Schematic cross-section through a plug of rod
conglomerate. The symmetry of strain in the
rods suggests that the plug has been constricted
by the surrounding cake conglomerate.

b)   Postulated stress trajectories which would account
for the constriction.

Fig 40

a

20 – 100 m

b

CAKES

RODS

σ_{MIN}

σ_{MAX}
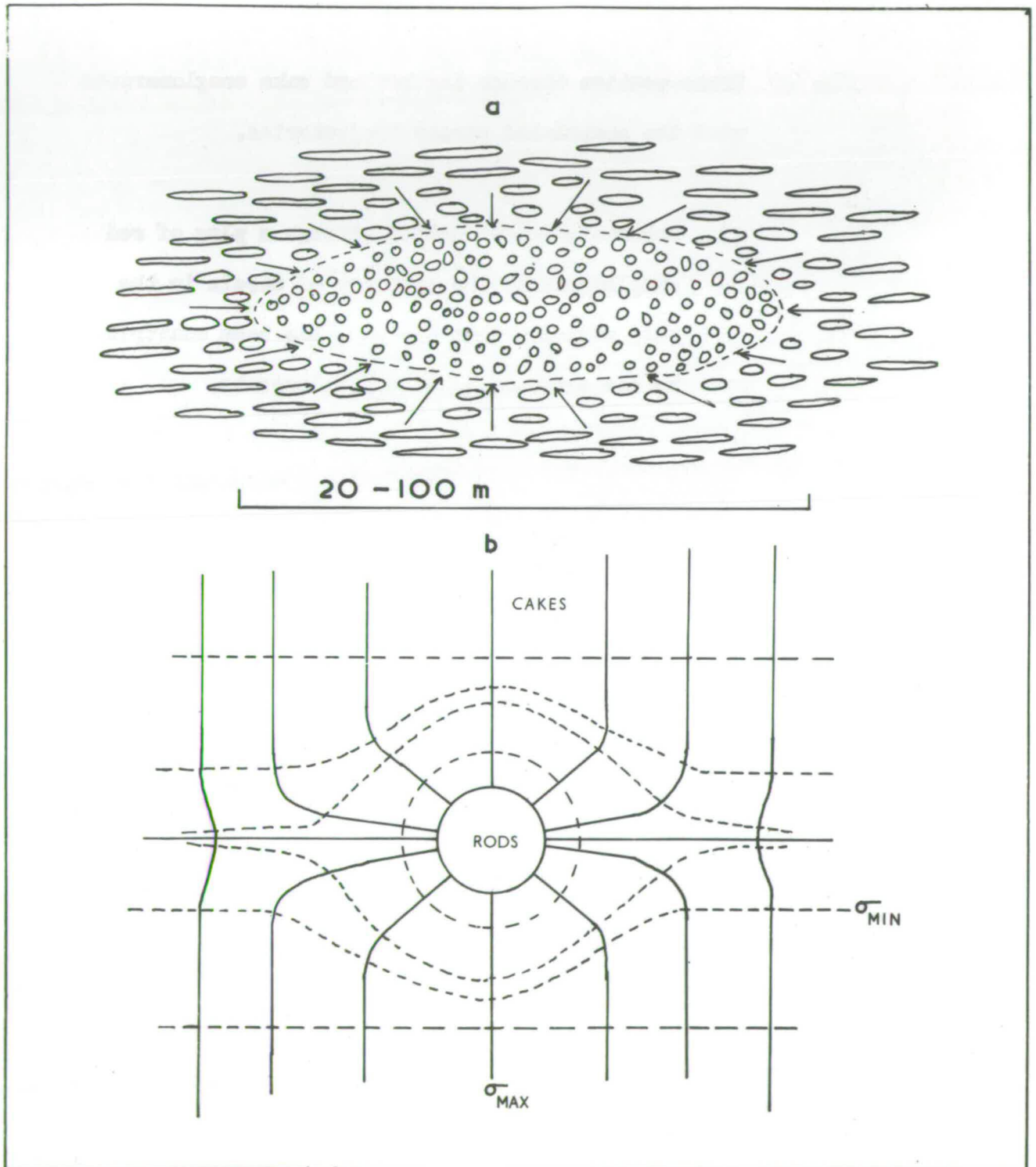
and remain cake-like in form.

However, the deformation path of the internal deformation would change direction during the second phase and move in the same direction as phase b of the external deformation. This would move the internal fabric towards a field of constriction and the fabric would become rod-like. The change in direction of the deformation path is purely a result of the dying out of the pressure gradients.

However, one strong objection to this theory is that at the end of this hypothetical deformation, the apparent amount of distortional strain ($\mathcal{E}_s$) in the rods would only be half that in the cakes whereas in fact (Fig.36) the apparent amount of strain in the rods and cakes are equal.

ii) The rods and cakes may also have formed in a deformation which did not have two phases like i) above. Complex pressure gradients like those developed in Flinn's model may have produced rotations of stress axes so that the areas of rods were compressed in a radial vice-like grip (Fig. 40 a). This radial compression could have caused two of the pebble axes to decrease at the same time rather than one decreasing and then the other as in hypothesis i).

The distribution of the stress trajectories required for this type of deformation are given in Fig. 40b, but the cause of the complex nature of these trajectories remains unknown. Flinn (1961) suggested that pressure gradients were produced by depressions and elevations in the base of the nappe. However, these depressions were not recognised by the writer in the field.

(d) <u>Significance of B1 linear structures.</u>

The B1 linear structures of the Bygdin area may have one of two possible origins. The rod conglomerate has a symmetry which suggests that it has been elongated in a northwest-southeast direction to produce the rod lineation. This lineation is equivalent to the "stretching lineation" of many structural geologists (c.f. Clough, in Gunn et al., 1897, pp.76-82). Similarly the L-tectonites of the nappe rocks (p. 60) seem to indicate a similar origin.

Most of the linear fabrics of the conglomerate lie in a northwest-southeast direction parallel to the rod lineation and the strain data indicates that this direction was one of maximum elongation. The writer tentatively suggests that most of the northwest B1 lineations in the nappe and the sediments are "elongation" or "stretching" lineations, which were produced by elongation of minerals and pebbles in the direction of maximum elongation and were formed at the same time as the pebble deformation.

However, the B1 fold axes are difficult to explain using this "elongation" hypothesis. Most of the B1 folds have northwest axes parallel to the principal elongation direction. Applying the symmetry principle, these folds could have formed by a shortening in a northeast-southwest direction. However, the strain data of the conglomerate indicates that this direction was generally one of elongation. The folding of the sparagmite bedding (p.22), the phyllonite bands in the nappe (p. 20), and the B1 folds in the pebbles (p.22) seem difficult to produce in a general field of flattening. Most of these folded elements were probably initially nearly horizontal, parallel to the base of the nappe and in a field of flattening (which was also parallel to the base of the nappe) and

would tend to boudinage rather than fold (i.e. the planar elements lie between the lines of no finite deformation in the boudinage field. Flinn, 1962, p.408). The Bl boudinage structures (p. 23) give evidence of this boudinage field.

The writer tentatively suggests that these Bl folds were not formed by the flattening deformation, but were in fact earlier. These folds could have formed during the thrusting phase, being produced by the shearing forces of thrusting. All the ?Bl folds in the sparagmite at Olefjell have a sense of movement consistent with a thrust movement from the northwest to the southeast.

Structural evidence for the detailed dating of the Bl folds is lacking. They can be shown to post-date much of the cataclasis (p. 20) but they cannot be separated from Sl and pebble deformation. If, however, the Bl folds pre-dated the flattening deformation, the folds would be modified by the flattening deformation making a separation difficult. This postulated modification could account for the northwest trend of some of the Bl folds. The shearing hypothesis suggests that folds would form with a northeast axial trend. There is in fact some evidence of the northeast trending Bl folds (Fig.4). The modification by the flattening would cause some of the fold axes to rotate (Flinn, 1962, p.394). The variation in symmetry of deformation would tend to cause complex patterns in the orientation of the rotated Bl folds at the end of deformation. As the maximum extension was in a northwest-southeast direction, the majority of fold axes would tend to rotate towards this direction. Thus the present northwest trend of the majority of these folds might be a result of later modification.

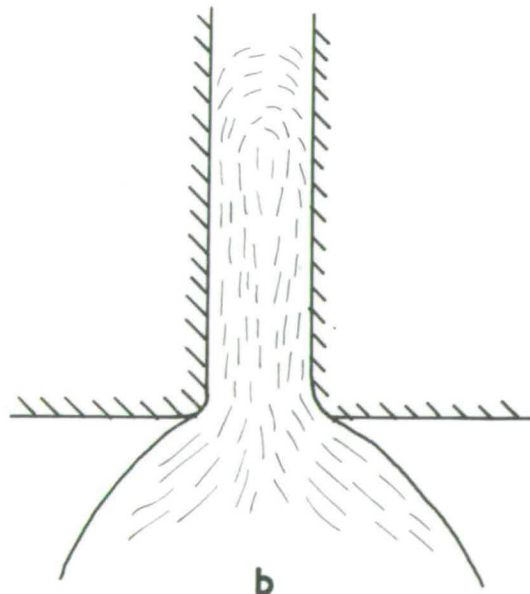Fig.41   Constrained flow in the extrusion experiments of
          Reidel.

          a) Directions of the maximum and minimum stress
              axes which develop in the extruded clay.

          b) Postulated lineation in the extruded clay.

Fig 41
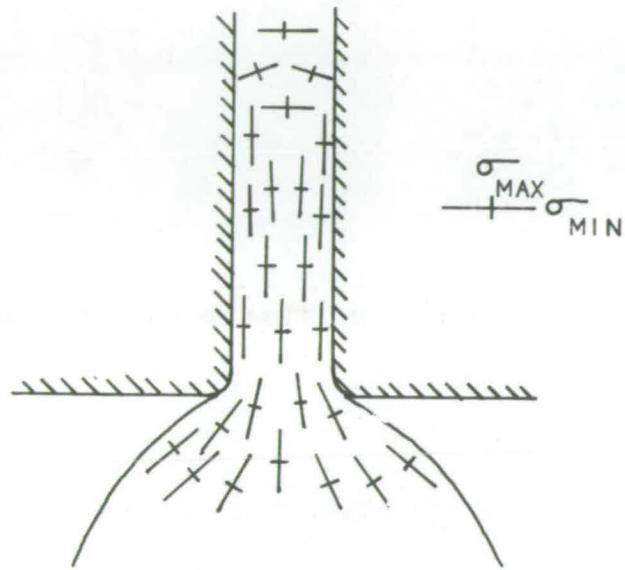
Constrained flow in the extrusion experiments of Riedel

The writer therefore suggests that the B1 linear fabrics are of two types.

    i) B1 fold axes were produced by the shear forces of thrusting and were modified by the later flattening deformation.

    ii) B1 "stretching" lineations which were formed in the direction of maximum elongation during the flattening deformation (c.f. p.27).

(e) <u>The effect of the variation of strain symmetry on the orientation of the B1 lineations.</u>

The variations in the symmetry of pebble deformation are similar to, but not as regular as, the strain perturbations of Turner and Weiss (1963, pp. 366-378). Now such perturbations must induce "constrained flow" in the rocks as there is a space problem in the areas between the perturbations. The deforming material there must adjust itself to the two different deformations on either side. This adjustment is termed "constrained flow" (Nadai, 1950, pp.426-428), and necessitates a rotational deformation where the stress axes must change in orientation from point to point within the material. This type of flow is illustrated by the extrusion experiments of Riedel (1929) where the stress axes can vary through 90° (Fig. 41a). If lineations were produced in Riedel's experiments, they would have the directions depicted in Fig. 41b.

Fig. 42.   Cross-sections through the rod and cake conglomerates

showing the postulated swing in the trend of the Bl

lineations.

a) Section parallel to the Sl foliation.

b) Section normal to the Sl foliation and parallel

    to the rod elongation.

Fig 42

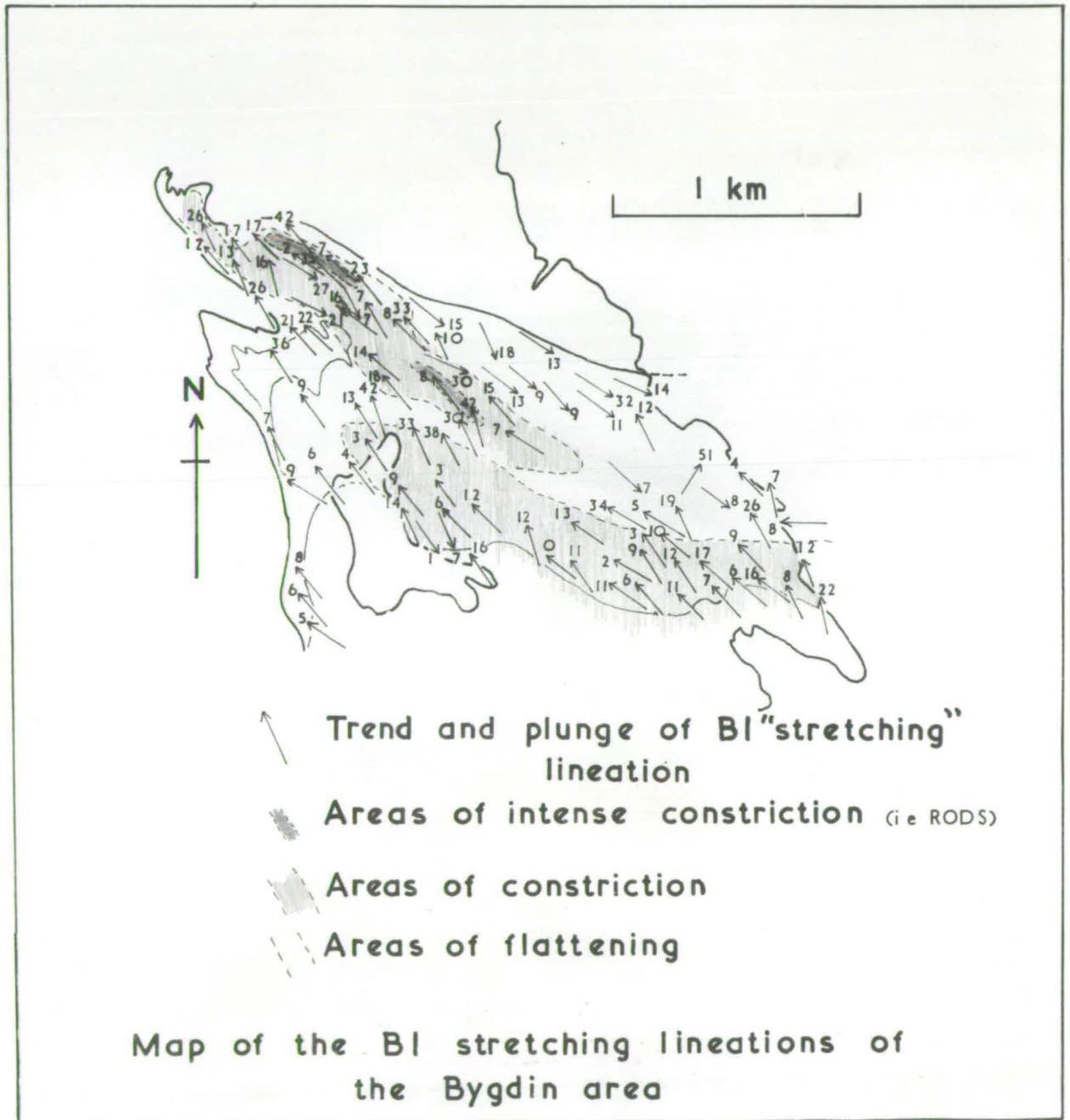
a

b
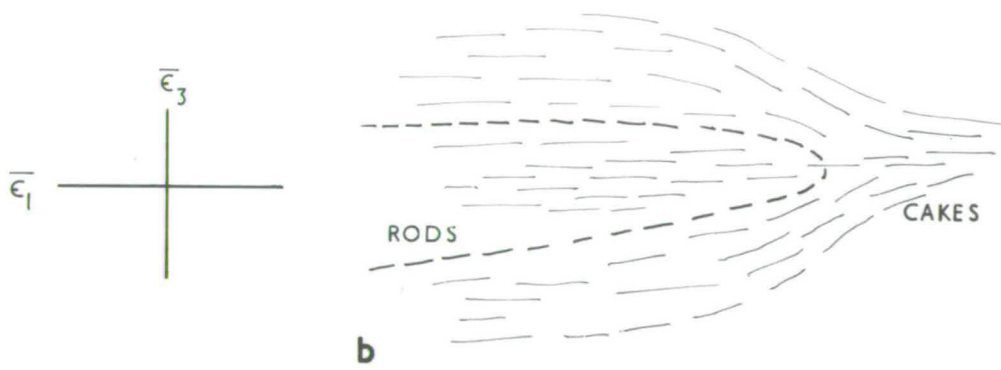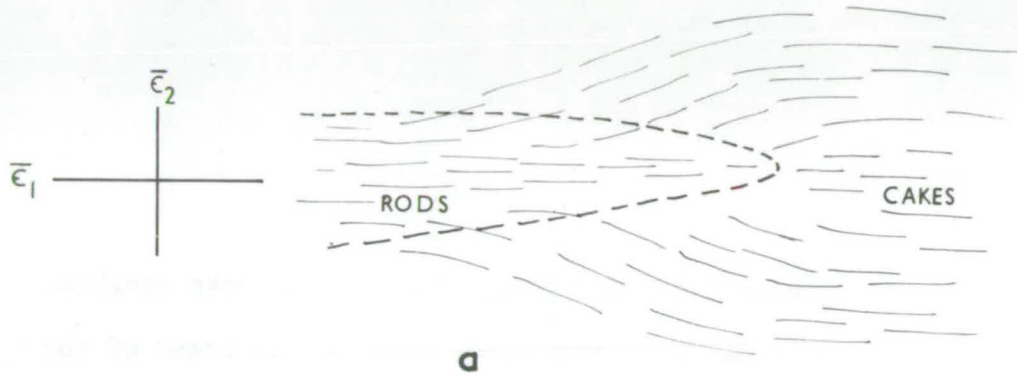
Outline of the plug like area of rods

Bl "stretching" lineation

Fig 43

Trend and plunge of Bl "stretching"
lineation

Areas of intense constriction (i e RODS)

Areas of constriction

Areas of flattening

Map of the Bl stretching lineations of
the Bygdin area

Now extending the constrained flow theory to the rod and cake conglomerates, the northwest Bl lineations which form during the pebble deformation, should change in orientation from the cakes into the rods. The expected swings are depicted in two diagrammatic sections through a plug of rod conglomerate. One section (Fig.42 a) is orientated parallel to Sl and the other (Fig. 42 b) normal to Sl and parallel to the pebble rodding. The two types of swing of the Bl lineation direction are a result of constrained flow which must take place between the rods and the cakes. However, these swings are not evident on a map of the Bl lineations (Fig.43). In fact, the variation in orientation is as great within the cake conglomerate as in the area between the cake and rod conglomerates. However, possible swings might have been destroyed by later refolding.

The only evidence of swings in the trend of the Bl lineation which may be a result of constrained flow are those at Barnesodden (Map II) and Synberg (Fig. 17). At Barnesodden, the Bl "stretching" lineation is roughly east-west and may swing into the regional northwest trend in Lake Vinstri. At Synberg, the Bl lineation is east-west in the lower Cambro-Ordovician sediments but swings into a northwest trend in the Mellsenn Division and continues in the northwest trend up into the Valdres Sparagmite.

However, these swings at Barnesodden and Synberg could also have been produced by rotation of an early Bl lineation by the flattening deformation.

(f) Mechanics of thrusting

The mechanical paradox of large overthrusts has been described
by Hubbert and Rubey (1959, pt. 1, pp. 122-129). They showed that frictional
resistance to thrusting restricts the size of a thrust block that can be
moved. Theoretically, a thrust block of the same thickness as the Upper
Jotun Nappe could only be moved if it were 18 $\frac{1}{2}$ km. wide. (Present day
width, 90 km.). Even if the nappe was moved by gravity gliding down a slope,
the inclination of the slope required would be about 30°.

Hubbert and Rubey (1959, pt. 1, pp. 129-162) have shown, however,
that frictional resistance can be overcome by high pore fluid pressures
in the rocks at the base of the nappe or in the rocks below the nappe.
High pore fluid pressures have a buoyancy effect similar to the "hover-
:craft" principle in which much of the weight of the nappe can be supported
by the fluid pressures and thus effectively reduce the frictional resistance.
With fluid/overburden pressure ratios of about 0,90, thrust blocks of the
scale of the Jotun Nappe can be moved (Present day dimensions - 180 km. by
90 km. by 5 km.).

If these high fluid pressures developed in the Jotunheim, they
probably existed in the sediments below the nappe rather than in the nappe
itself. The rocks of the Upper Jotun Nappe consist mainly of basic gneisses
and gabbros which appear to be almost completely impermeable.

The Valdres Sparagmite and conglomerate were probably still
unconsolidated when they were overthrust by the nappe (p.22). The over-
:thrusting of a thick impermeable gneiss and gabbro nappe would tend to cause
high fluid pressures in unconsolidated ?water-saturated sediments. If the

fluid/overburden pressure ratio reached 0,90, the Upper Jotun Nappe could have been moved quite easily.

(g) Conclusions

The first movement picture is conceived as starting with large scale thrusting of the Upper Jotun Nappe towards the southeast. The origin of this nappe is unknown because rocks of the Bergen-Jotun kindred have not been found in situ. The metamorphic facies of the Jotun Nappe suggests that the nappe was once part of a basement complex and may have been brought from an area at present in the sea off the west coast of Norway.

The mechanical paradox of thrusting cannot be solved for the initial stages of thrusting because the state of the rocks over which the nappe moved is unknown, but once the nappe reached the Sparagmite region, it was probably supported by high fluid pressures developed in the Sparagmite.

The thrusting developed extensive cataclasis and phyllonitization in the basal nappe rocks and may have caused folding of the phyllonites and sparagmite.

Because evidence of a rotational deformation is absent in the conglomerate, the general flattening deformation is ascribed to a post-thrusting phase when the nappe was essentially "dead". This flattening took place in part of the nappe (p. 60) and the sediments below the nappe.

It is suggested that the variations in symmetry of this deformation were caused by complex pressure gradients which induced plug-like areas of constictional flow to develop in the L-tectonites of the nappe (p. 62) , the two dimensional deformation areas at Olefjell, and in the

in the rod conglomerates. The dominant flow direction of the flattened and
constricted areas was towards the southeast and may have caused the sediments
to flow out underneath the front of the nappe. This dominant flow towards the
southeast induced extensive northwest-southeast "stretching" lineations in
the nappe rocks and the sediments. The cause of the pressure gradients is
unknown.

The swings in trend of B1 lineations at Barnesodden and Synberg
are either a result of constrained flow or they were pre-flattening
lineations which were rotated by the flattening deformation (pp. 73-74).

The amount of distortional strain decreases downwards from the
thrust plane towards a minimum (Fig. 33) and then at lower structural
levels increases again. Two minima are present, one at Bygdin and the other
at Olefjell. The swing of B1 at Barnesodden could be caused by the constrained
flow which would exist between the minimum at Olefjell and the maxium to the
northeast of Barnesodden.

If the principal stresses were parallel to the principal strains
of the B1 flattening, the maximum compression direction seems to have been
normal to the thrust plane with the minimum stress direction in a northwest-
southeast direction (provided the flattening was largely non-rotational: this
is a reasonable assumption). A possible force causing this deformation may
have been the weight of the overlying nappe.

The nappe was probably moved into its present position either by
gravity gliding or under the influence of a force acting on the back face of
the thrust block. The force of friction was probably reduced by high pore
fluid pressures in the sediments. The nappe may have then reached a static

GRANITE

GABBRO

CONGLOMERATE

SPARAGMITE

THRUST PLANE

AXIAL PLANE TRACE
OF B2 MAJOR FOLDS

1 KM
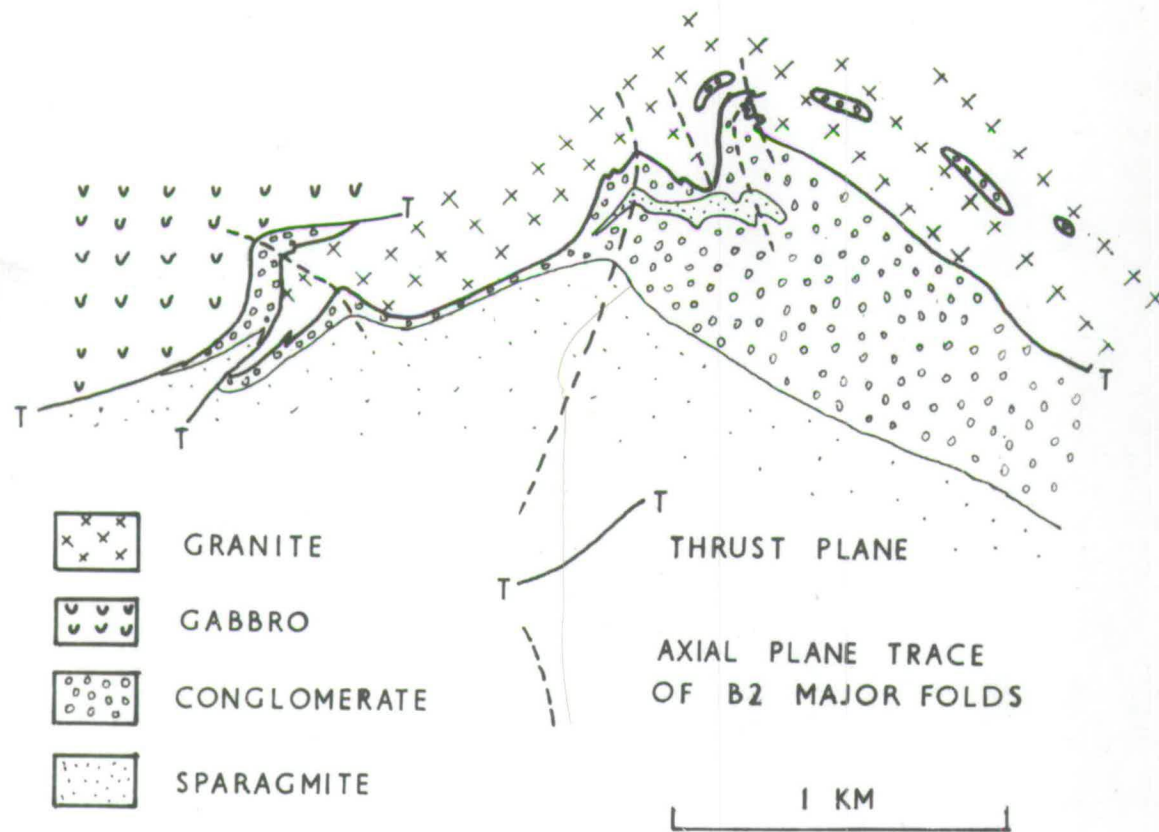
Structural section of the Bygdin
Antiform

Fig 44

phase where it was supported by these high pore fluid pressures. However, this fluid pressure would tend to decrease if the fluids were allowed to escape, (perhaps out underneath the nappe block). With decreasing fluid pressure, the block would gradually settle down on top of the sediments until the weight of the nappe was sufficient to flatten the sediments. With zero fluid pressure, the vertical pressure acting on the sediments would be approximately $1\frac{1}{2}$ kilobars (equivalent to the weight of the overlying nappe). Provided the sediments were unrestricted in directions parallel to the thrust plane, so that they could flow out underneath the nappe, this $1\frac{1}{2}$ kilobars would probably be sufficient to cause the late phase B1 deformation.

3. MOVEMENT PICTURE OF THE SECOND DEFORMATION

Quantitative strain measurements are not available for the B2 structures. However, arguments based on the symmetry and orientation of the second folds might suggest that the maxium compressive stress of the second deformation was normal to the second axial planes (Turner and Weiss, 1963, p. 524). The fact that many of the second fold axes are axes of buckling (p.25) suggests that at least some shortening took place in this direction with a partial movement upwards. A structural section of the Bygdin Antiform (Fig. 44) seems to indicate that the main movement of the antiform was upwards into the nappe. Some movement, however, could also have taken place parallel to the B2 axes.

The writer tentatively suggests that the maximum compressive stress during the second movement phase was near horizontal in a northeast-southwest direction normal to the second axial planes.

4. MOVEMENT PICTURE OF THE THIRD DEFORMATION

The minor B3 structures indicate that the movement picture of the third deformation may have been a complex mixture of concentric buckling (c.f. "brittle" conjugate folds, p.29) and plastic flow (c.f. pure "similar" folds, pp.28-29).

The analysis of the symmetry of the third structures indicates that the third deformation may have had a three dimensional symmetry (p.32) and the stress axes were orientated such that the maximum compression was almost vertical with the minimum stress axis north-south near the horizontal, and the intermediate stress direction east-west.

The vertical maximum compression, like that of the B1 deformation, suggests that gravity may have been the motive force of the third deformation. Active horizontal compression during the second movement phase may have caused the Bygdin Antiform to rise vertically into the nappe. As the B2 forces declined, the weight of the nappe may have exerted an increasing restraint upon the uprising antiform, and thereby induced the development of B3 structures.

5. ORIGIN OF THE "FALTUNGSGRABEN"

The origin of the large synclinal depression or "Faltungsgraben" (Goldschmidt, 1912) is unknown. This depression now causes the B1 and B2 linear structures to plunge at $20^{\circ}-30^{\circ}$ towards the northwest. However, without detailed structural investigations from the whole of the Jotunheim area, the age of the depression cannot be determined. The "Faltungsgraben" could be a primary structure forming at the same time as thrusting, or it could be later.

VII. ACKNOWLEDGEMENTS

VIII. BIBLIOGRAPHY

ANDERSON, E.M., 1948.   On Lineation and Petrofabric Structure, and the Shearing Movement by which they have been produced. *Quart.J. geol. Soc. Lond.*, 104, 99-132.

BATTEY, M.H., 1960.   Observations on the Peridotites and Pyroxenites of the Jotunheim Complex in Norway. *Int. geol. Congr.*, 21, Copenhagen, 1960, pt. 13, 198-207.

BJØRLYKKE, K.O., 1902.   Fra Hardangervidda, III. *Norg. geol. Unders.*, Nr. 34, 51.

BJØRLYKKE, K.O., 1905.   Det centrale Norges fjellbygning. *Norg. geol. Unders.*, Nr. 39.

BRØGGER, W.C., 1893.   Lagfølgen på Hardangervidda og den såkaldte "Høifjellskvarts". *Norg. geol. Unders.*, Nr. II.

CARROL, D., 1951.   Pebbles from a Pothole: a Study in Shape and Roundness. *J. sedim. Petrol.*, 21, 205-212.

CHRISTIE, J.M., 1963.   The Moine Thrust Zone in the Assynt Region, Northwest Scotland. *Univ. Calif. Publs geol. Sci.*, 40, 345-440

FLEUTY, M.J., 1964.   The Description of Folds. *Proc. Geol. Assoc.*, 75, 461-492.

FLINN, D., 1956.   On the Deformation of the Funzie Conglomerate, Fetlar, Shetland. *J. Geol.*, 64, 480-505.

FLINN, D., 1959.   On certain geological similarities between Northeast Shetland and the Jotunheim area of Norway. *Geol. Mag.*, 96 473-481.

FLINN, D., 1961.   On Deformation at Thrust Planes in Shetland and the
Jotunheim Area of Norway.   Geol. Mag., 98, 245-256.

FLINN, D., 1962.   On Folding during Three-Dimensional progressive
Deformation. Quart. J. geol. Soc. Lond., 118, 385-428.

FLINN, D., 1965.   On the Symmetry Principle and the Deformation
Ellipsoid. Geol. Mag., 102, 36-45.

GOLDSCHMIDT, V.M., 1912.   Die Kaledonische Deformation der Südnorwegischen
Urgebirgstafel. Skr. VidenskSelsk. Christiania Mat.-naturv.Kl.
2, Nr. 19.

GOLDSCHMIDT, V.M., 1916a.   Konglomeraterne inden Høifjellskvartsen.
Norg. geol. Unders., Nr. 77.

GOLDSCHMIDT, V.M., 1916b.   Übersicht der Eruptivegesteine im kaledonischen
Gebirge zwischen Stavanger und Trondhjem. Skr. VidenskSelsk.
Christiania Mat.-naturv. Kl., 2, 1916.

GREENWOOD, H.J., 1963.   The Synthesis and Stability of Anthophyllite.
J. Petrol., 4, 317-351.

GUNN, W. et al, 1897.   The Geology of Cowal. Mem. geol. Surv. Scotland.

HIGGINS, A.K., 1964.   The Structural and Metamorphic Geology of the Area
between Nufenpass and Basodino Tessin, S. Switzerland. Unpublished
Ph.D. Thesis, Imperial College, Univ. of London.

HOLTEDAHL, O., 1936.   Trekk av det skandinaviska fjelljedestrøks historie.
Skand.Naturfors. Møde, 19, Helsingfors, 129.

HOLTEDAHL, O., 1960. Geology of Norway. Norg. geol. Unders., Nr. 208.

HUBBERT, M.K. and RUBEY, W.W., 1959. Role of Fluid Pressure in Mechanics
of Overthrust Faulting. Bull. geol. Soc. Am., 70, 115-205.

JOHNSON, M.R.W., 1956. Conjugate Fold Systems in the Moine Thrust Zone
in the Lochcarron and Coulin Areas. Geol. Mag., 93, 345-350.

JOHNSON, M.R.W., 1964. Conjugate Folds, Kinks, and Drag. Geol. Mag.
101, 466-467.

JOHNSON, M.R.W., and STEWART, F.H., 1963. The British Caledonides.
Oliver and Boyd, Edinburgh, 269 pp.

KNOPF, E.B., 1931. Retrogressive Metamorphism and Phyllonitization. Pt.1.
Am. J. Sci., 21, 1-27.

KULLING, O., 1961. On the Age and Tectonic Position of the Valdres
Sparagmite. Geol. För. Stockh. Förh., 83, 210-214.

KVALE, A., 1953. Linear Structures and their Relation to Movement in the
Caledonides of Scandinavia and Scotland. Quart. J. geol. Soc. Lond.
109, 51-74.

LAPWORTH, C., 1885. The Highland Controversy in British Geology. Nature,
Lond., 32, 558-559.

LODE, W., 1926. Versuche über den Einfluss der mittleren Hauptspannung
auf das Fliessen des Metalle Eisen, Kupfer und Nickel. Z.Phys.
36, 913-939.

LOUDEN, T.V., 1963. The Sedimentation and Structure in the Macduff
District of North Banffshire and Aberdeenshire. Unpublished
Ph.D. Thesis, University of Edinburgh.

MURET, G., 1960. Partie S.E. de la Culmination du Romsdal, Chaine
Caledonienne, Norvege. Int.geol. Congr., 21, Copenhagen. 1960,
Pt. 19, 23-32.

NADAI, A., 1950. Theory of Flow and Fracture of Solids: Engineering
Societies Monographs, McGraw-Hill, New York. Vol. I, 572 pp.

NADAI, A., 1963. Theory of Flow and Fracture in Solids: Engineering
Societies Monographs, McGraw Hill, New York, Vol. 2, 705 pp.

OFTEDAHL, C., 1961. On the Genesis of the gabbroic rock Bodies of the
Norwegian Caledonides. Bull. geol. Instn Univ. Upsala, 40,
87-94.

RAMBERG, H., 1959. Evolution of Ptygmatic Folding. Norsk geol. Tidsskr.,
39, 99-152.

RAMSAY, J.G., 1957a. Superimposed Folding at Loch Monar, Inverness-
shire and Ross-shire. Quart. J. geol. Soc. Lond., 113,
271-307.

RAMSAY, J.G., 1957b. Moine-Lewisian Relations at Glenelg, Inverness-
shire. Quart. J. geol. Soc. Lond., 113, 487-523.

RAMSAY, J.G., 1960. The deformation of early linear Structures in Areas
of repeated Folding. J. Geol., 68, 75-93.

RAMSAY, J.G., 1962a. The Geometry and Mechanics of Formation of
"similar" type Folds. J.Geol., 70, 309-327.

RAMSAY, J.G., 1962b. The Geometry of conjugate Fold Systems. Geol. Mag.,
99, 516-526.

RAMSAY, J.G., 1964. Progressive Deformation in tectonic Processes. Trans. Am. geophys. Un., 45, No. 1. (Abstract of 45th Annual Meeting).

RAST, N., 1956. The Origin and Significance of Boudinage. Geol. Mag., 93, 401-408.

RIEDEL, W., 1929. Das aufquellen geologisches Schmelzmassen als plastischer Formänderungsvorgang. Neues Jb. Miner. Geol. Paläont. BeilBd., 62b, 151-170.

SANDER, B., 1948. Einführung in die Gefügekunde der Geologischen Körper. Pt.I, Springer-Verlag, Vienna, 215 pp.

SMITHSON, S.B., 1964. Forløpige resultater av tryngdemalinger over Jotundekkene. Tidsskr. Kjemi Bergv. Metall., 5, 97-101.

de SITTER, L.U., 1958. Boudins and Parasitic Folds in relation to Cleavage and Folding. Geologie Mijnb., 20, 277-286.

STRAND, T., 1945. Structural Petrology of the Bygdin Conglomerate. Norsk geol. Tidsskr., 24, 14-31.

STRAND, T., 1951. Slidre Memoir. Norg. geol. Unders., Nr. 180. (English Summary).

STRAND, T., 1958. Valdres Sparagmittens stratigrafiske stilling. Norg. geol. Unders., Nr. 205, 184-198.

STRAND, T., 1961. The Scandinavian Caledonides: A Review. Am. J. Sci., 259, 161-172.

STRAND, T., 1962. On the Age and Tectonic Position of the Valdres Sparagmite. Geol. För. Stockh. Förh., 84, 230-231.

TURNER, F.J. and WEISS, L.E., 1963. Structural Analysis of Metamorphic Tectonites. McGraw-Hill, New York, 545 pp.

WENTWORTH, C.K., 1925. Chink-faceting: A new Process of Pebble Shaping. J.Geol., 33, 260-267.

WYNNE-EDWARDS, H.R., 1963. Flow Folding. Am. J. Sci., 261, 793-814.

APPENDIX A.

Station No. and No. of measurements	X/Y/Z	$\bar{\epsilon}_1$	$\bar{\epsilon}_2$	$\bar{\epsilon}_3$	$\bar{\epsilon}_s$	υ
1 xy-30 xz-30	1,0/11,1/18,3	1,14	0,64	-1,78	2,21	0,66
2 xy-30 xz-30	1,0/4,2/32,0	1,83	-0,20	-1,64	2,47	-0,17
3 xy-30 xz-30	1,0/2,3/30,0	1,99	-0,58	-1,41	2,52	-0,51
4 xy-30 xz-30	1,0/4,0/16,6	1,41	-0,01	-1,40	2,00	-0,01
5 xy-30 xz-30	1,0/7,5/54,3	1,99	0,01	-2,00	2,84	0,01
6 xy-30 xz-30	1,0/7,4/30,2	1,61	0,20	-1,80	2,43	0,17
7 xy-30 xz-30	1,0/2,1/32,0	2,06	-0,65	-1,41	2,59	-0,57
8 xy-30 xz-30	1,0/15,8/39,9	1,54	0,61	-2,15	2,74	0,50
9 xy-30 xz-30	1,0/3,4/35,9	1,98	-0,38	-1,60	2,58	-0,32
10 xy-30 xz-30	1,0/4,8/14,0	1,24	0,17	-1,40	1,83	0,19
11 xy-30 xz-30	1,0/4,2/36,3	1,92	-0,24	-1,68	2,56	-0,20
12 xy-30 xz-30	1,0/8,2/34,5	1,66	0,23	-1,89	2,53	0,19
13 xy-30 xz-30	1,0/4,5/23,6	1,61	-0,05	-1,56	2,24	-0,05
14 xy-30 xz-30	1,0/3,2/38,8	2,05	-0,45	-1,61	2,66	-0,36
15 xy-30 yz-30	1,0/2,5/36,9	2,10	-0,59	-1,51	2,67	-0,38

Station No. and No. of measurements	X/Y/Z	$\bar{\epsilon}_1$	$\bar{\epsilon}_2$	$\bar{\epsilon}_3$	$\bar{\epsilon}_S$	υ
16 xy-30 xz-19 yz-11	1,0/2,1/25,0	1,90	-0,58	-1,32	2,40	-0,54
17 xy-30 xz-30	1,0/2,1/24,3	1,88	-0,57	-1,31	2,37	-0,54
18 xy-30 xz-30	1,0/2,6/12,2	1,35	-0,20	-1,15	1,79	-0,24
19 xy-30 xz-30	1,0/5,7/21,3	1,46	0,14	-1,60	2,18	0,14
20 xy-30 yz-25	1,0/2,9/26,0	1,82	-0,39	-1,44	2,37	-0,36
21 xy-30 xz-30	1,0/2,3/25,0	1,87	-0,52	-1,35	2,37	-0,48
22 xy-30 xz-30	1,0/5,9/22,0	1,47	0,15	-1,62	2,20	0,15
23 xy-8 xz-15	1,0/18,1/18,9	0,99	0,95	-1,95	2,40	0,97
24 xy-30 xz-30	1,0/2,9/19,8	1,64	-0,30	-1,34	2,08	-0,30
25 xy-30 xz-30	1,0/4,4/16,2	1,36	0,07	-1,42	1,98	0,07
26 xy-30 xz-30	1,0/4,9/22,2	1,54	0,03	-1,57	2,20	0,03
27 xy-30 xz-30	1,0/3,0/15,4	1,45	-0,17	-1,28	1,95	-0,19
28 xy-30 xz-30	1,0/4,4/27,0	1,71	-0,11	-1,59	2,35	-0,10
29 xy-30 xz-30	1,0/3,8/16,4	1,42	-0,04	-1,38	1,98	-0,04

Station No. and No. of measurements		X/Y/Z	$\bar{\epsilon}_1$	$\bar{\epsilon}_2$	$\bar{\epsilon}_3$	$\bar{\epsilon}_S$	υ
30	xy-30 xz-30	1,0/2,7/20,1	1,67	-0,34	-1,33	2,17	-0,34
31	xy-30 yz-30	1,0/3,3/47,3	2,17	-0,49	-1,69	2,81	-0,38
32	xy-30 xz-30	1,0/3,5/21,7	1,63	-0,18	-1,45	2,20	-0,18
33	xy-30 xz-30	1,0/6,1/13,7	1,14	0,33	-1,47	1,90	9,33
34	xy-30 xz-30	1,0/6,9/13,7	1,10	0,41	-1,51	1,92	0,47
35	xy-30 xz-30	1,0/7,8/26,7	1,51	0,27	-1,78	2,36	0,25
36	xy-30 xz-30	1,0/4,0/17,7	1,46	-0,04	-1,42	2.05	-0,04
37	xy-30 yz-30	1,0/4,0/41,0	2,01	-0,31	-1,70	2,66	-0,25
38	xy-30 yz-30	1,0/4,4/60,9	2,25	-0,39	-1,86	2,96	-0,29
39	xy-30 xz-30	1,0/3,6/20,6	1,59	-0,16	-1,43	2,15	-0,16
40	xy-30 xz-17 yz-13	1,0/3,2/24,7	1,75	-0,29	-1,46	2,31	-0,27
41	xy-30 xz-30	1,0/16,4/34,4	1,43	0,68	-2,11	2,65	0,58
42	xy-30 xz-30	1,0/13,6/21,6	1,18	0,72	-1,90	2,35	0,70
43	xy-30 xz-10	1,0/17,6/32,4	1,36	0,75	-2,11	2,64	0,65
44	xy-30 xz-30	1,0/5,7/21,4	1,47	0,13	-1,60	2,18	0,13

Station No. and No. of measurements	X/Y/Z	$\bar{\epsilon}_1$	$\bar{\epsilon}_2$	$\bar{\epsilon}_3$	$\bar{\epsilon}_s$	υ
45 xy-30 xz-30	1,0/4,5/25,1	1,65	-0,08	-1,57	2,29	-0,07
46 xy-30 xz-30	1,0/6,6/15,2	1,18	0,35	-1,54	1,98	0,39
47 xy-30 xz-30	1,0/4,9/32,2	1,79	-0,10	-1,68	2,47	-0,09
48 xy-30 xz-30	1,0/5,8/23,9	1,53	0,11	-1,64	2,26	0,10
49 xy-30 xz-30	1,0/7,7/16,0	1,17	0,44	-1,61	2,04	0,47
50 xy-30 yz-30	1,0/5,4/28,1	1,66	0,01	-1,68	2,37	0,01
51 xy-30 xz-30	1,0/5,6/20,8	1,45	0,14	-1,59	2.17	0,14
52 xy-30 xz-30	1,0/2,9/8,8	1,10	-0,01	-1,09	1,55	0,02
53 xy-30 xz-30	1,0/4,0/4,1	0,47	0,46	-0,94	1,15	0,99
54 xy-30 xz-30	1,0/4,2/5,1	0,61	0,42	-1,02	1,27	0,77
55 xy-30 yz-30	1,0/3,5/7,1	0,89	0,17	-1,07	1,40	0,27
56 xy-30 yz-30	1,0/3,08/6,31	0,85	0,14	-0,99	1,32	0,23
57 xy-30 yz-30	1,0/2,8/5,8	0,82	0,11	-0,94	1,26	0,19
58 xy-30 yz-30	1,0/3,8/7,7	0,92	0,21	-1,13	1,48	0,31

Station No. and No. of measurements		X/Y/Z	$\bar{\epsilon}_1$	$\bar{\epsilon}_2$	$\bar{\epsilon}_3$	$\bar{\epsilon}_S$	υ
59	xy-30 yz-30	1,0/4,0/9,4	1,03	0,17	-1,20	1,60	0,23
60	xy-10 xz-6	1,0/5,9/18,5	1,36	0,21	-1,56	2,08	0,21
61	xy-30 xz-30	1,0/3,6/6,8	0,85	0,22	-1,06	1,39	0,35
62	xy-30 yz-30	1,0/3,9/7,1	0,85	0,26	-1,11	1,43	0,39
63	xy-30 yz-30	1,0/4,5/10,6	1,07	0,21	-1,29	1,69	0,27
64	xy-30 yz-30	1,0/4,0/8,0	0,92	0,23	-1,16	1,50	0,33
65	xy-30 yz-30	1,0/4,2/7,2	0,84	0,30	-1,13	1,45	0,45
66	xy-30 xz-30	1,0/4,0/9,9	1,07	0,20	-1,24	1,65	0,21
67	xy-30 xz-30	1,0/3,5/4,0	0,51	0,37	-0,88	1,09	0,80
68	xy-30 xz-30	1,0/2,7/6,4	0,91	0,04	-0,95	1,32	0,07
69	xy-30 yz-30	1,0/3,6/8,2	0,97	0,15	-1,13	1,50	0,22
70	xy-30 yz-30	1,0/4,3/10,9	1,10	0,18	-1,29	1,71	0,23
71	xy-30 yz-30	1,0/3,8/7,7	0,92	0,20	-1,12	1,47	0,30
72	xy-30 xz-30	1,0/4,1/9,4	1,02	0,20	-1,22	1,61	0,26
73	xy-30 xz-30	1,0/3,6/8,5	1,00	0,13	-1,14	1,53	0,18

Station No. and No. of measurements		X/Y/Z	$\overline{\epsilon}_1$	$\overline{\epsilon}_2$	$\overline{\epsilon}_3$	$\overline{\epsilon}_S$	υ
74	xy-30 xz-30	1,0/4,2/8,5	0,94	0,24	-1,19	1,54	0,34
75	xy-30 yz-30	1,0/4,6/12,8	1,19	0,17	-1,36	1,82	0,20
76	xy-30 xz-30	1,0/3,9/12,6	1,23	0,07	-1,30	1,80	0,08
77	xy-10 xz-10	1,0/4,5/13,5	1,23	0,14	-1,37	1,86	0,16
78	xy-10 xz-10	1,0/5,2/14,3	1,23	0,21	-1,44	1,91	0,24
79	xy-30 xz-30	1,0/4,2/16,2	1,38	0,02	-1,41	1,98	0,03
80	xy-30 xz-30	1,0/8,4/14,2	1,06	0,54	-1,59	2,00	0,61
81	xy-30 xz-30	1,0/5,1/10,1	1,00	0,32	-1,32	1,69	0,41

PLATE 1

Phyllonite bands in the Jotun Nappe
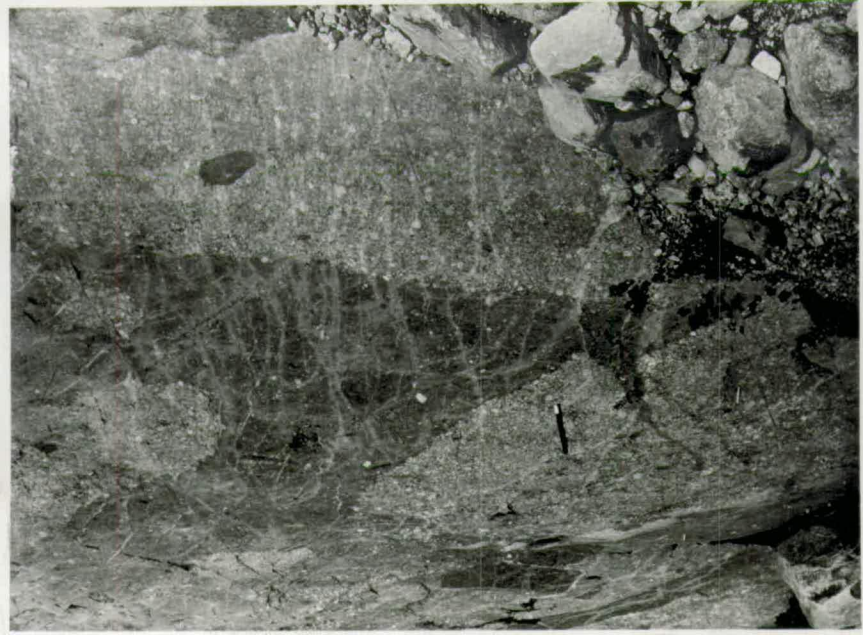
PLATE 2

a)   Deformed pebbles flattened in S1.

b)   Deformed pebbles (and S1) folded by B2 minor folds.
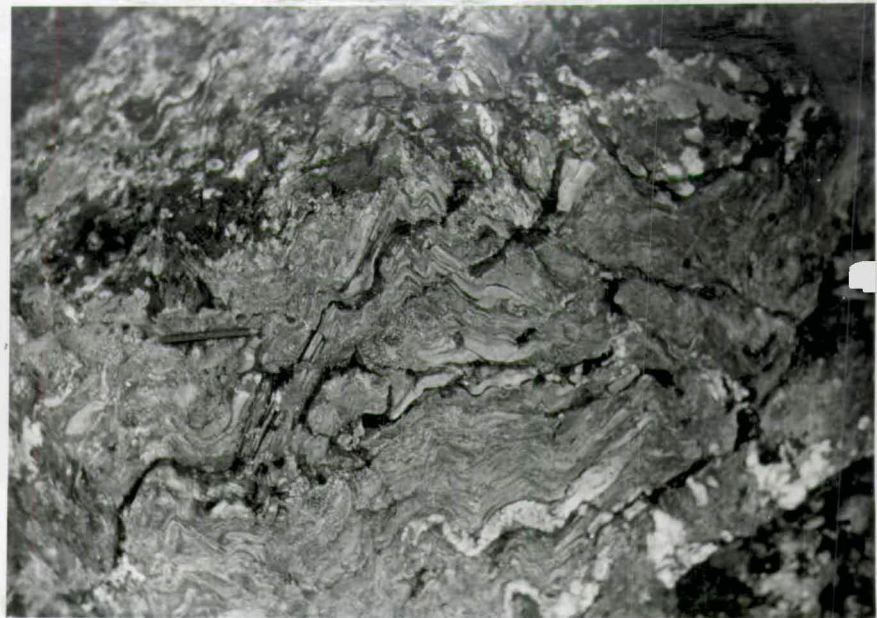
PLATE 4

a)   Large ?B1 folds in the Valdres Sparagmite.

b)   Inverted current bedding in the Valdres Sparagmite.
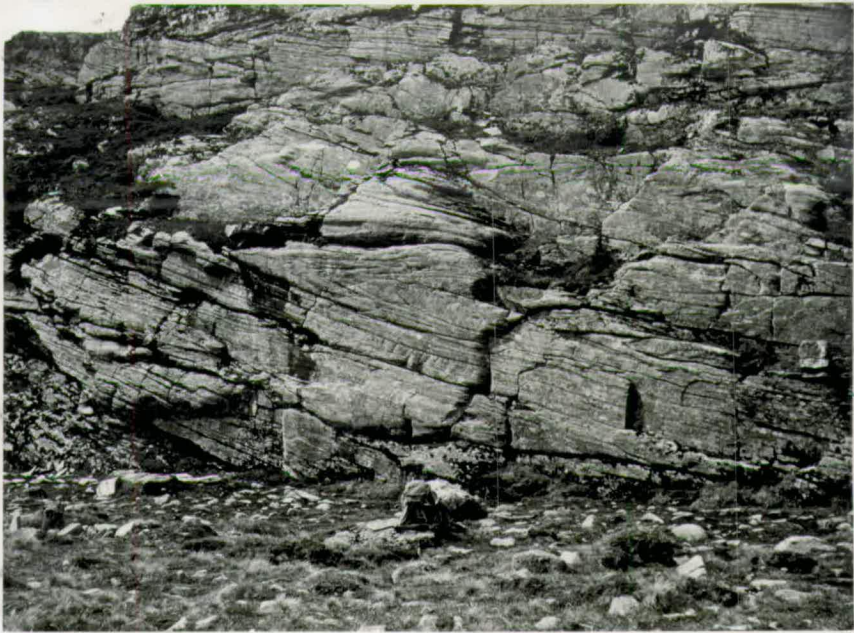
PLATE 5.

a)   Rhomboid boudins in a phyllonite band of the Jotun Nappe
      (locality 2, Fig. 6).   Tension and compression axes have
      been derived by bisecting the angle between the rhomboid
      planes.

b)   Large B2 fold refolding a B1 fold in a pegmatite vein on
      the limb of antiform-f.
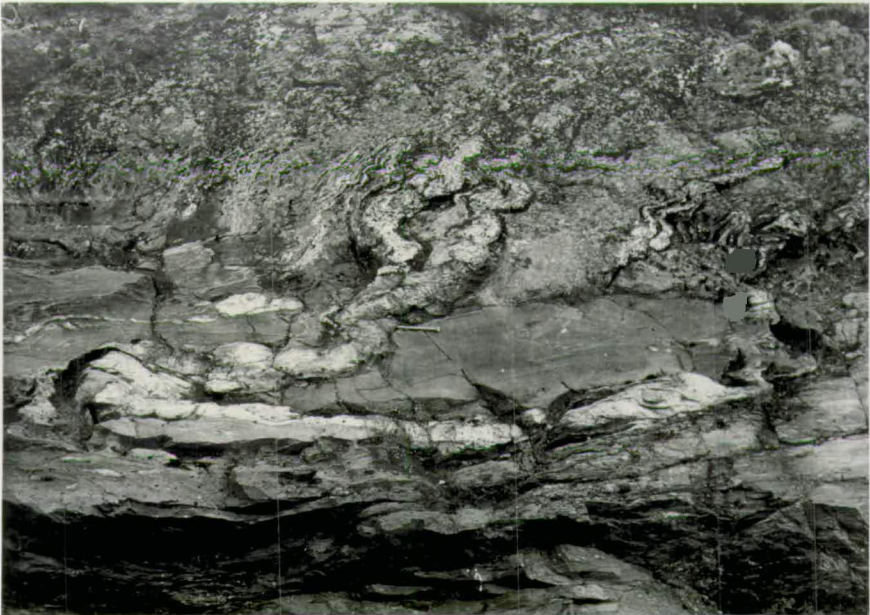
PLATE 6.

B2 minor folds in the conglomerate.
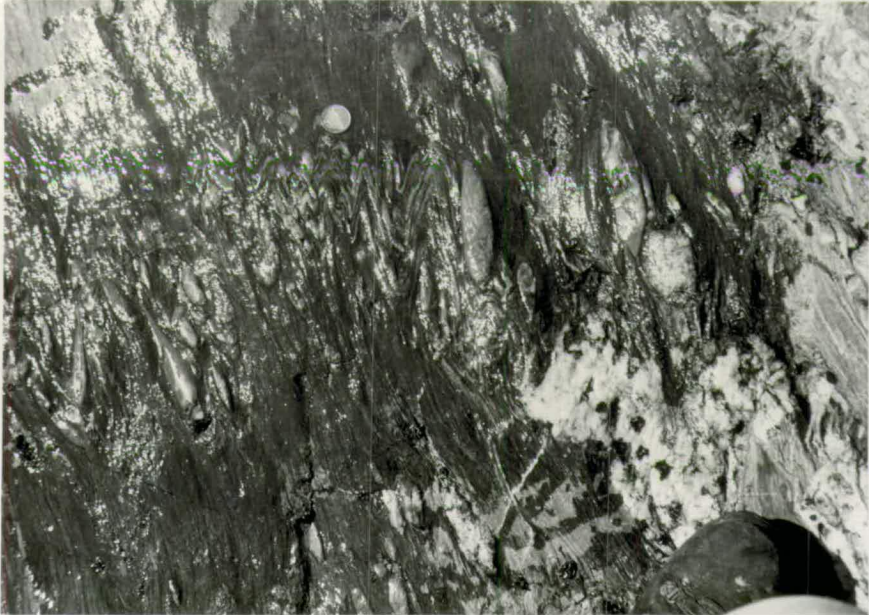
PLATE 7.

B3 minor folds.

a)   Rod conglomerate near the Bygdin Hotel.

b)   Valdres Sparagmite.
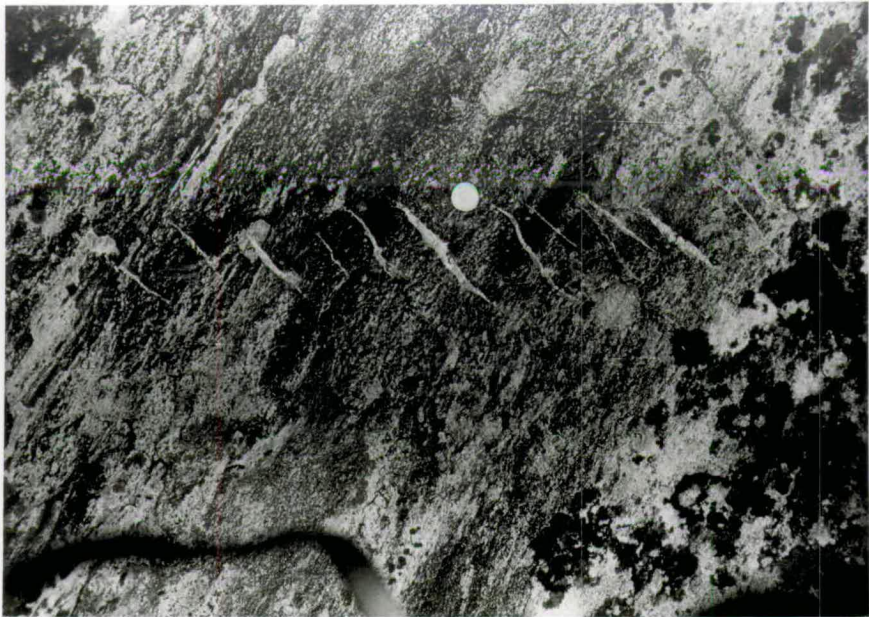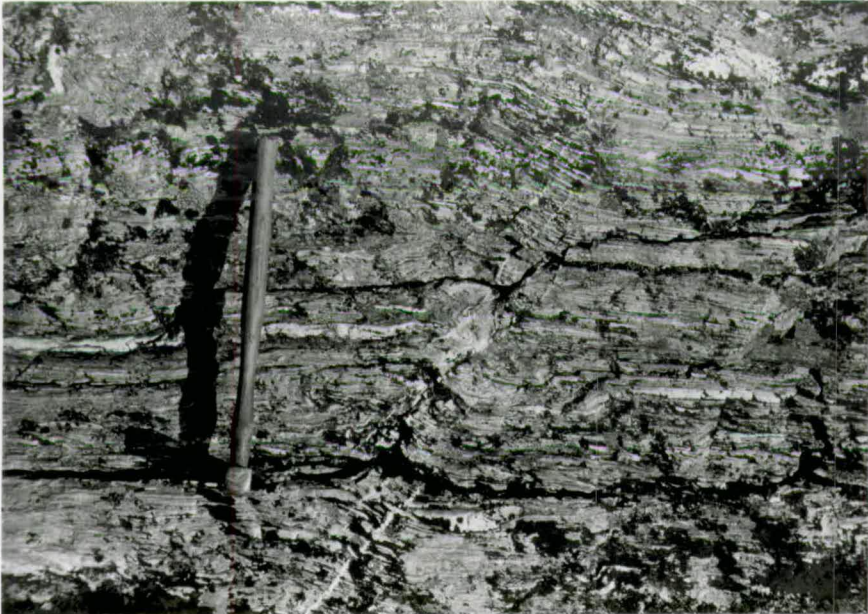
PLATE 8.

a)   Quartz-filled tension gashes.

b)   B4 minor fold with quartz-filled tension gashes which
      cut a B3 minor fold (centre of photograph).

PLATE 9.

a)   Photomicrograph of the S1 strain slip cleavage at
      Synberg.   Mellsenn Division.

b)   Photomicrograph of the S1 foliation in the Valdres
      Sparagmite showing the rounded relic ?clastic grains
      of quartz and felspar.
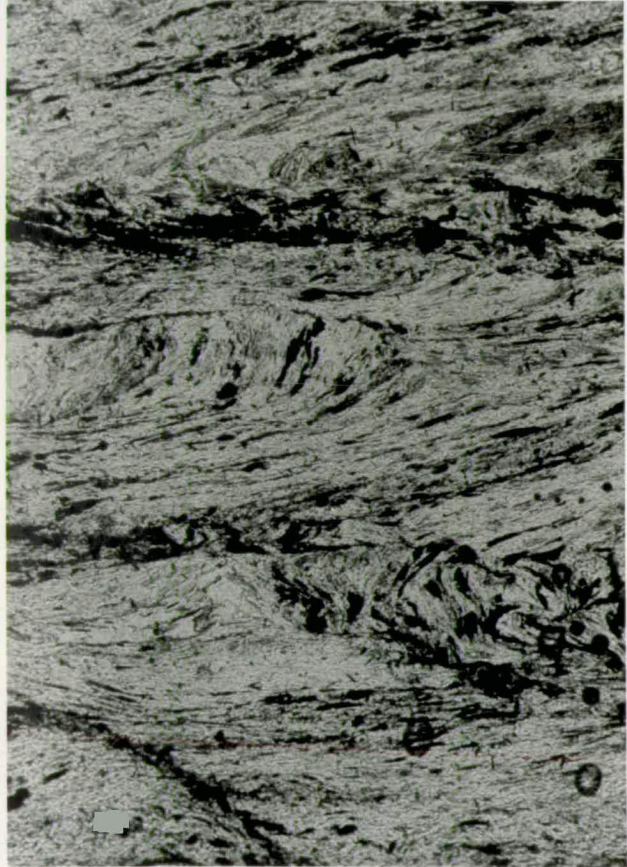
PLATE 10.

Intermixing of the conglomerate and igneous lithologies in the
thrust zone near the Bygdin Hotel.

a)   Deformed quartzite pebbles in a matrix of igneous
      phyllonite.   Limb of antiform-f.

b)   Layers of non-conglomeratic igneous phyllonite inter-
      :layered with deformed conglomerate.   Limb of antiform-f.
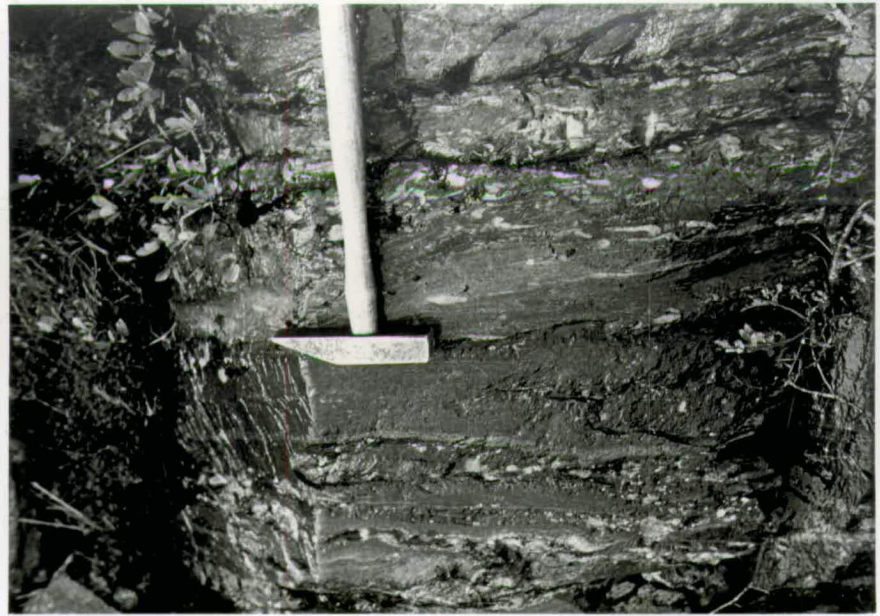
PLATE 11.

a)   Rhythmic layering in the Bitihorn gabbro.

b)   Intermediate igneous xenoliths in the granitic rocks
      of the Jotun Nappe.
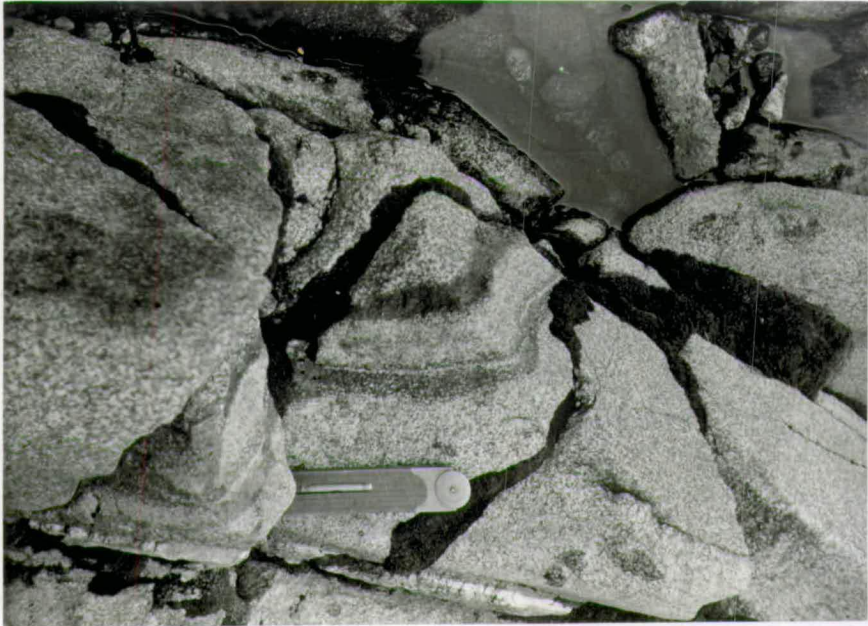
PLATE 12.

Undeformed putty model.
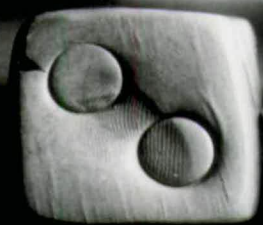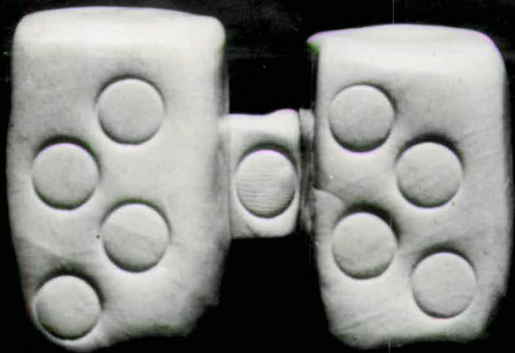
PLATE 12.

PLATE 13.

Deformed putty model.

PLATE 3
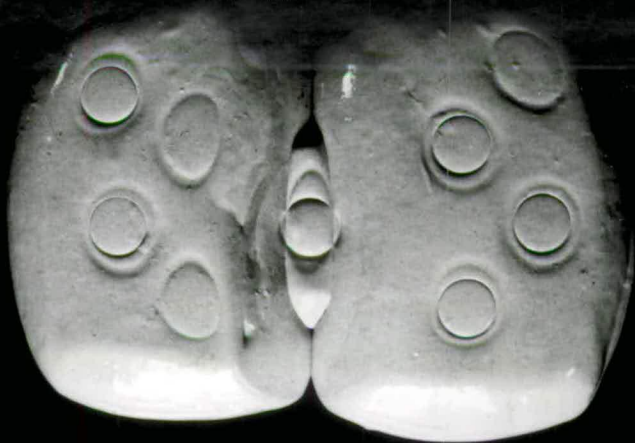
Minor folds in the Valdres Sparagmite.

The origin of these folds in unknown.   They may either be
tectonic or sedimentary slump folds.
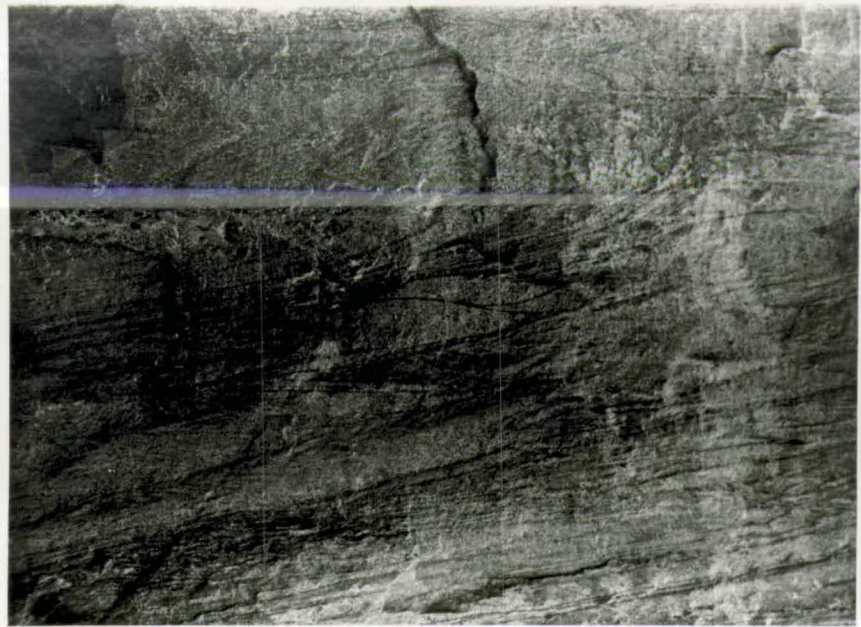
ABSTRACT OF THESIS

Name of Candidate .... John Robert HOSSACK.

Address .... 20 Hailstones Crescent, Armadale.

Degree .... Ph.D. .... *Date* ...... July, 1965.

Title of Thesis .... Structural Analysis of the Bygdin Area, Southern Norway.

Abstract

The area studied is situated at Bygdin on the southeast margin of the Upper Jotun Nappe, which is the highest nappe of the marginal thrust zone of the Norwegian Caledonides, and has been thrust over Cambro-Ordovician sediments (including the Bygdin conglomerate).

Detailed field studies have been carried out to determine the structural history of the area, and the deformation pattern of the Bygdin conglomerate which underlies the basal thrust plane of the Jotun Nappe.

Four sets of minor structures are recognized (B1, B2, B3 and B4) with the earliest set (B1) being produced by the overthrusting of the nappe. This B1 phase caused the deformation of the Bygdin conglomerate and formed cataclastic and mylonitic fabrics normally associated with nappe thrusting. Most of the B1 linear structures trend northwest-southeast parallel to the postulated direction of thrusting of the nappe.

The second movement phase formed folds and lineations (B2) with a northwest-trend exactly parallel to the B1 linear trend. In addition to the minor structures, ten major antiforms and synforms of B2 age are recognized. The largest B2 fold of the area (the Bygdin Antiform) folds the basal thrust plane of the Jotun Nappe.

The B3 folds occur only on the minor scale and have large variations in orientation of the fold axes and axial planes. This variation is thought to be due to the conjugate symmetry of the B3 structures.

The B4 structures are associated with joint formation and consist of joint-drag folds and quartz-or chlorite-filled tension gashes.

The deformed pebbles of the Bygdin conglomerate have been measured and engineering strain units have been used to define the amount and symmetry of the B1 strain.

These measurements show that the amount of distortional strain is generally highest at the thrust plane and decreases downwards towards two minima. Structurally below the position of these minima, the amount of strain increases again.

The symmetry measurements show that the dominant pebble deformation was a pancake-like flattening, normal to the thrust plane. The existence of flattened conglomerate slices within the Jotun Nappe is taken to indicate that the flattening deformation also took place in the nappe. B1 minor structures and symmetry arguments suggest that this flattening post-dated the thrusting and occurred when the nappe had stopped moving.

In addition to the pancake-like pebbles, rod shaped pebbles occur in northwest trending plug-like areas which are completely surrounded by the flattening fabrics. Rod-like fabrics also occur in the nappe rocks and are believed to have undergone a deformation similar to that of the rod conglomerate.

Use other side if necessary.

Experimental work by Flinn suggests that the constrictional symmetry of the rod fabrics can be produced in a general flattening deformation if complex pressure gradients exist. It is tentatively suggested that the flattening deformation was the result of a vertical flattening under the weight of the Upper Jotun Nappe and that complex pressure gradients caused the constrictional fabrics to flow like toothpaste from a tube. The northwest trending B1 lineations were formed in the direction of maximum elongation and are "stretching" fabrics.

The symmetry of the B2 folds indicate that they could have been formed by a northeast-southwest compression which caused the Bygdin Antiform to rise vertically into the Jotun Nappe.

The maximum stress direction has been determined from the conjugate symmetry of the B3 folds and like that of the B1 phase, appears to have been near-vertical. It is suggested that at the end of the B2 phase, the Bygdin Antiform became unstable because it was no longer supported by the B2 stresses and that readjustment took place during the B3 phase under the influence of the weight of the overlying nappe.

GEOLOGICAL MAP OF THE BYGDIN AREA

FAGERDALSTJERN

LAKE BYGDIN

GJISYNSHORN

BYGDIN

STAVTJERN

KOLBJØRNSØY

LAKE VINSTRI

SANDDALSTJERN

BARNESODDEN

BITIHORN

OLEFJELL

OLEVATN
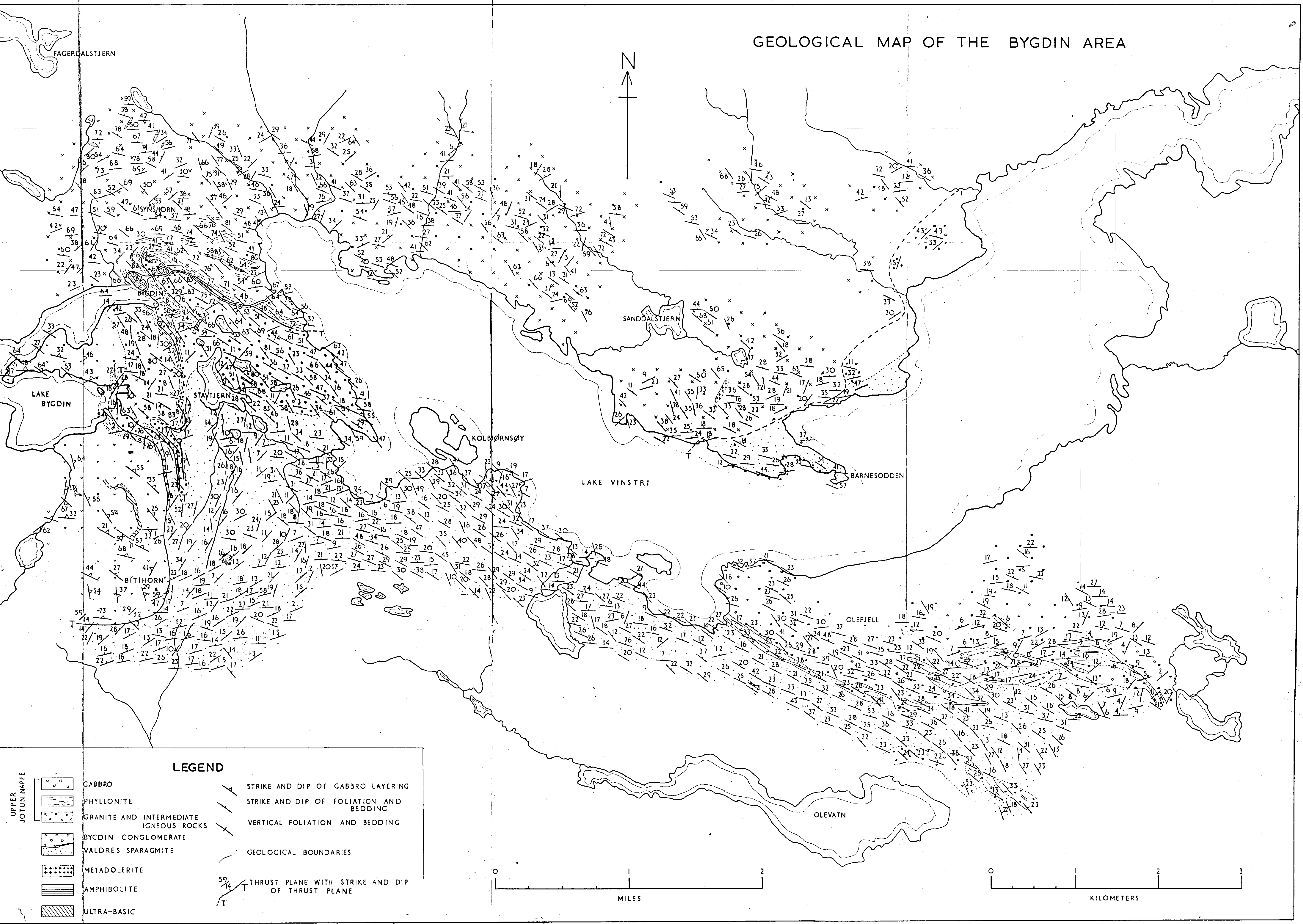
LEGEND

UPPER JOTUN NAPPE

	GABBRO		STRIKE AND DIP OF GABBRO LAYERING
	PHYLLONITE		STRIKE AND DIP OF FOLIATION AND BEDDING
	GRANITE AND INTERMEDIATE IGNEOUS ROCKS		VERTICAL FOLIATION AND BEDDING
	BYGDIN CONGLOMERATE		
	VALDRES SPARAGMITE		GEOLOGICAL BOUNDARIES
	METADOLERITE		
	AMPHIBOLITE		THRUST PLANE WITH STRIKE AND DIP OF THRUST PLANE
	ULTRA-BASIC		

MILES

0   1   2

KILOMETERS

0   1   2   3
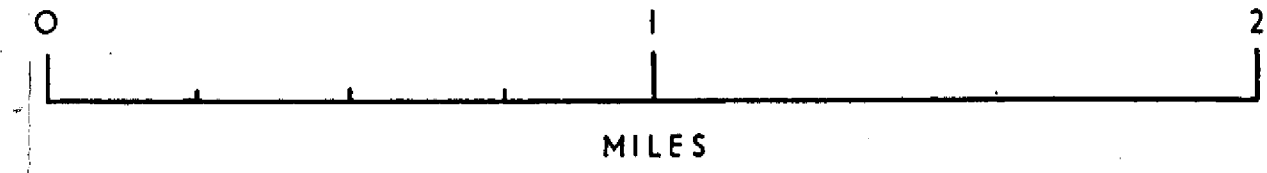
STRUCTURAL ANALYSIS

Fig. 2
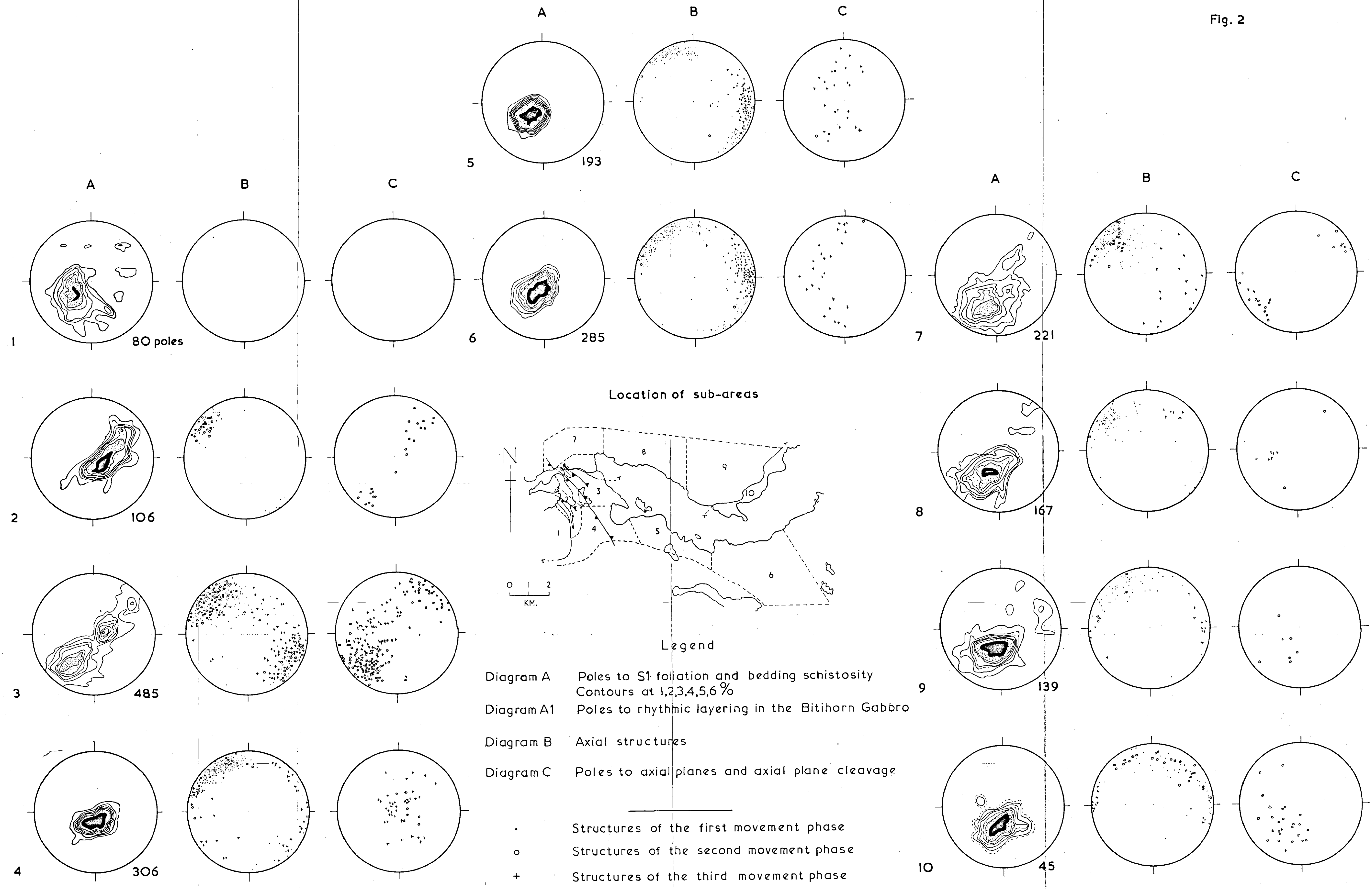
Location of sub-areas

Legend

Diagram A   Poles to S1 foliation and bedding schistosity
             Contours at 1,2,3,4,5,6 %

Diagram A1   Poles to rhythmic layering in the Bitihorn Gabbro

Diagram B   Axial structures
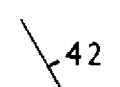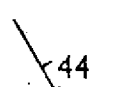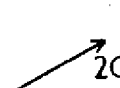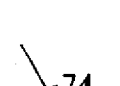
Diagram C   Poles to axial planes and axial plane cleavage

· Structures of the first movement phase

o Structures of the second movement phase

+ Structures of the third movement phase

STRUCTURAL MAP OF THE BYGDIN AREA

COMBINED GEOLOGICAL AND STRUCTURAL MAP OF THE BYGDIN INVAGINATION
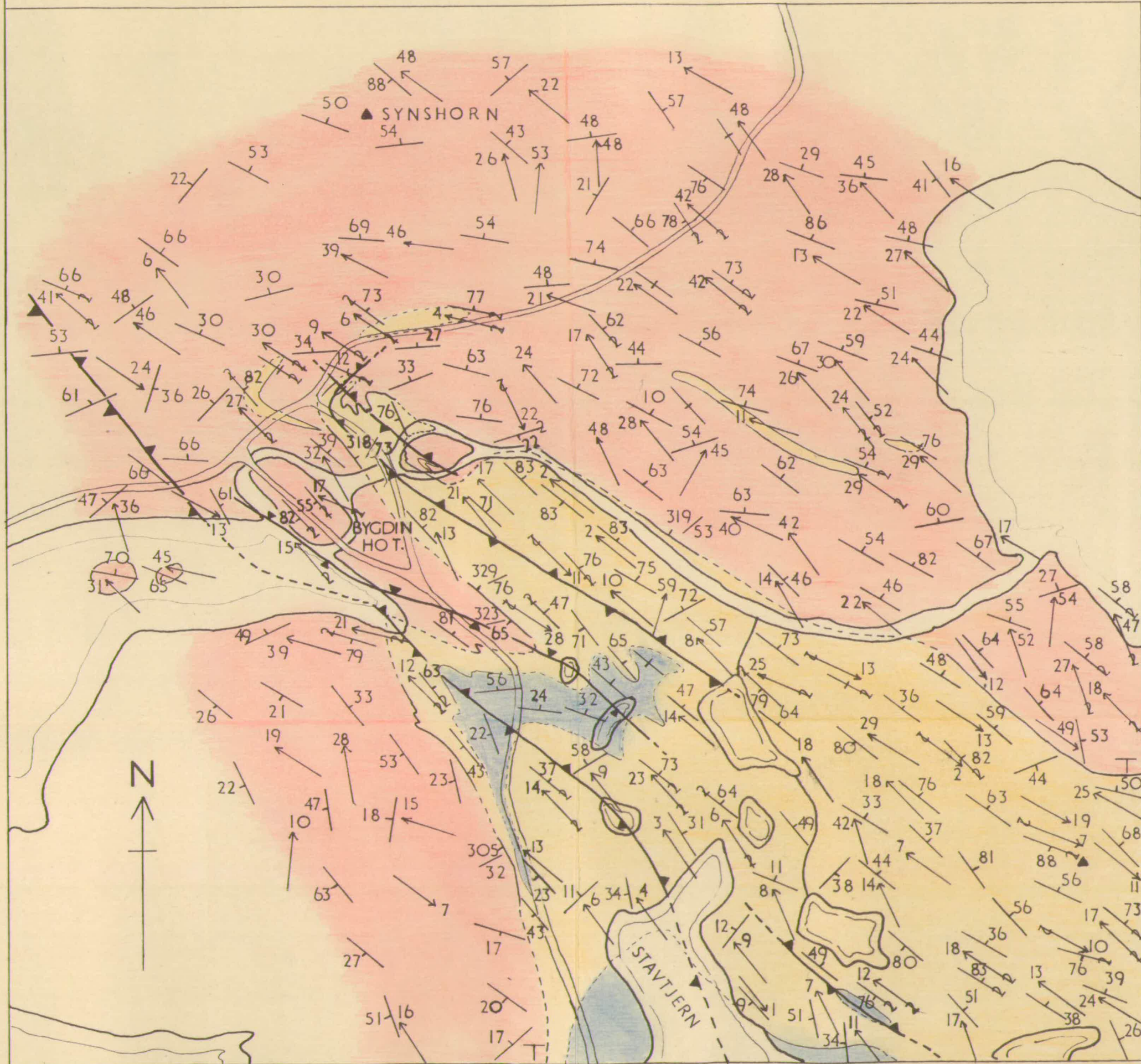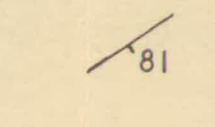
LEGEND

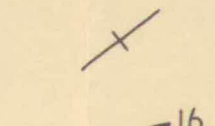JOTUN IGNEOUS ROCKS
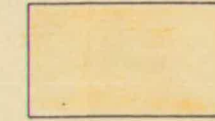
BYGDIN CONGLOMERATE

VALDRES SPARAGMITE
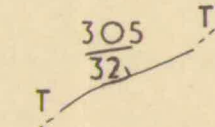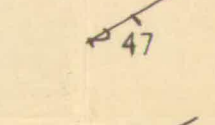
THRUST PLANE WITH STRIKE AND DIP OF THRUST PLANE

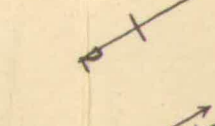STRIKE AND DIP OF FIRST AXIAL PLANES AND FOLIATION

VERTICAL FIRST AXIAL PLANES AND FOLIATION

PLUNGE OF FIRST LINEAR STRUCTURES

STRIKE AND DIP OF SECOND AXIAL PLANES AND FOLIATION

VERTICAL SECOND AXIAL PLANES AND FOLIATION

PLUNGE OF SECOND LINEAR STRUCTURES

AXIAL PLANE TRACE OF MAJOR SECOND ANTIFORM

AXIAL PLANE TRACE OF MAJOR SECOND SYNFORM

SCALE — 1:10,000